

ONTOGENY AND PHYLOGENY OF CATARRHINE CRANIA: AN ANALYSIS OF  
THE EVOLUTION OF ONTOGENETIC SHAPE CHANGE TRAJECTORIES  
USING 3D GEOMETRIC MORPHOMETRICS

by

EVAN A. SIMONS

A DISSERTATION

Presented to the Department of Anthropology  
and the Graduate School of the University of Oregon  
in partial fulfillment of the requirements  
for the degree of  
Doctor of Philosophy

June 2019

## DISSERTATION APPROVAL PAGE

Student: Evan A. Simons

Title: Ontogeny and Phylogeny of Catarrhine Crania: An Analysis of the Evolution of Ontogenetic Shape Change Trajectories Using 3D Geometric Morphometrics

This dissertation has been accepted and approved in partial fulfillment of the requirements for the Doctor of Philosophy degree in the Department of Anthropology by:

Stephen R. Frost	Chairperson
Frances White	Core Member
Nelson Ting	Core Member
Samantha Hopkins	Institutional Representative

and

Janet Woodruff-Borden	Vice Provost and Dean of the Graduate School
-----------------------	--

Original approval signatures are on file with the University of Oregon Graduate School.

Degree awarded June 2019

© 2019 Evan A. Simons

## DISSERTATION ABSTRACT

Evan A. Simons

Doctor of Philosophy

Department of Anthropology

June 2019

Title: Ontogeny and Phylogeny of Catarrhine Crania: An Analysis of the Evolution of Ontogenetic Shape Change Trajectories Using 3D Geometric Morphometrics

While there have been numerous previous investigations into catarrhine cranial ontogeny, these studies have often led to conflicting results, possibly due to the use of different methodologies. Furthermore, comparing the trajectories of many taxa simultaneously can be cumbersome, as this is often accomplished by examining large matrices of pairwise angles among them. Additionally, because relatively complete ontogenetic sequences of fossil materials are scarce to non-existent, most analyses of ontogenetic trajectories are limited to extant taxa, making it difficult to determine how trajectories have changed over time. Finally, there are several long-standing hypotheses about the role of size in the evolution of catarrhine cranial morphology that have yet to be tested using the sophisticated techniques of shape analysis that are currently available.

This dissertation addresses these issues by: 1) examining how the use of different methodologies influences the production of ontogenetic trajectories, 2) developing new methods for the analysis of extant and ancestral ontogenetic trajectories, and 3) using this information in conjunction with a comparative approach to more fully understand the role of size in the cranial evolution of catarrhines.

This dissertation includes previously published, co-authored material.

## CURRICULUM VITAE

NAME OF AUTHOR: Evan A. Simons

### GRADUATE AND UNDERGRADUATE SCHOOLS ATTENDED:

University of Oregon, Eugene  
New Mexico State University, Las Cruces  
University of Wisconsin, Milwaukee

### DEGREES AWARDED:

Doctor of Philosophy, Anthropology, 2019, University of Oregon  
Master of Arts, Anthropology, 2012, New Mexico State University  
Bachelor of Arts, 2010, University of Wisconsin, Milwaukee

### AREAS OF SPECIAL INTEREST:

Geometric Morphometrics

### PROFESSIONAL EXPERIENCE:

Graduate Teaching Fellow, University of Oregon, 2012 -Present  
Graduate Teaching Assistant, New Mexico State University, 2010-2012

### GRANTS, AWARDS, AND HONORS:

Graduate Teaching Fellowship, University of Oregon, 2012 -Present  
Doctoral Dissertation Improvement Grant, National Science Foundation, 2018  
Malcom McFee Paper Award, University of Oregon, 2015  
The Johnston Graduate Research Fellowship, University of Oregon, 2014  
Outstanding Graduate Assistant Award, New Mexico State University 2012  
*Summa cum Laude*, University of Oregon, Milwaukee, 2010

## PUBLICATIONS:

Evan A. Simons, S.R. Frost, and M. Singleton. 2018. Ontogeny and phylogeny of the cercopithecine cranium: a geometric morphometric approach to comparing shape change trajectories. *Journal of Human Evolution* 124, 40-51.

K. Turley, Evan A. Simons, and S.R. Frost. 2018. Trajectory analysis among African Hominoids can provide insights into genetic versus epigenetic influences during ontogeny. *American Journal of Physical Anthropology*, 167, 173-177.

Evan A. Simons and S.R. Frost. 2016. Constructing cranial ontogenetic trajectories: a comparison of growth, development, and chronological age proxies using a known-age sample of *Macaca mulatta*. *American Journal of Physical Anthropology*, 161, 296-308.

## ACKNOWLEDGMENTS

I would like to thank Drs. Jennifer Cramer and James Pampush, who saw that I was interested in anthropology as an undergraduate and helped me turn these interests into a graduate career. I truly wouldn't be doing this today if it wasn't for their mentorship, inspiration and friendship. Similarly, thank you to my Master's advisor Dr. Brenda Benefit, who taught me so much about primate evolution, particularly how interesting monkeys are, and helped to facilitate my continuing research into evolutionary anthropology. I am also extremely thankful to have had friends and family who provided support and encouragement along the way.

I wish to express sincere gratitude to my advisor Dr. Stephen Frost. Steve has been a consistent source of inspiration and support throughout my graduate career, and our conversations about primate evolution have always guided me to new and interesting avenues of research. He has provided me every opportunity to succeed in the pursuit of my interests, and his mentorship has been unwavering at every step of this process. I cannot imagine having a better advisor.

Thank you to Dr. Michelle Singleton for sharing her cercopithecine cranial landmark data for pilot projects, and for helping me to better understand cranial shape ontogeny. Thank you also to Kieran McNulty for sharing his human cranial landmark data, and for providing me with the opportunity to gain field experience in Kenya. Thank you to Dr. Scott W. Simpson for the opportunity to participate in paleontological fieldwork in Galili, Ethiopia. Many thanks also to M. Ponce de León and C. Zollikofer (Anthropology Institute and Museum, Zurich), E. Gilissen (Royal Museum for Central Africa, Tervuren), D. Lunde (National Museum of Natural History), M. Omura (MCZ,

Harvard), L. Jellema (Cleveland Museum of Natural History), and M. Surovy and S. Ketelsen (American Museum of Natural History) for their assistance and access to the skeletal materials in their care. These investigations were supported by a Doctoral Dissertation Improvement Grant from the National Science Foundation (BCS-1751885), and by the Department of Anthropology at the University of Oregon.

Finally, thank you to Lindsey Stafford, whose love, support, and willingness to relocate across the country several times so that I could pursue this goal has meant everything to me.



To Lindsey Stafford

## TABLE OF CONTENTS

Chapter	Page
I. INTRODUCTION .....	1
1.1 Background .....	2
1.1.1 Ontogeny and Evolution .....	2
1.1.2 Cranial Ontogeny in Primates .....	4
1.1.3 Ontogenetic Allometry and Ontogenetic Scaling .....	6
1.2 Investigational <i>Précis</i> .....	10
1.2.1 Ontogenetic Trajectories in <i>Macaca mulatta</i> .....	11
1.2.2 Comparing and Reconstructing Trajectories .....	12
1.2.3 Testing for Ontogenetic Scaling .....	12
II. CONSTRUCTING CRANIAL ONTOGENETIC TRAJECTORIES .....	14
2.1 Introduction.....	14
2.2 Materials and Methods.....	16
2.2.1 Sample.....	16
2.2.2 Analytical methods .....	18
2.2.2.1 Generalized Procrustes analysis.....	18
2.2.2.2 Procrustes Distance .....	18
2.2.2.3 Computing ontogenetic trajectories .....	19
2.2.2.4 Simulating adult morphologies .....	19
2.2.2.5 Assessment of simulated adult morphologies.....	20
2.2.2.6 Comparison of trajectories .....	20
2.2.2.7 Principal components analysis.....	21
2.2.2.8 Visualization .....	21
2.3 Results.....	21
2.3.1 Comparison of Trajectories.....	22
2.3.2 Comparison of Simulated Adults.....	22
2.3.3 Comparison of Interchanged Trajectories.....	24
2.4 Discussion .....	25

Chapter	Page
2.4.1 Properties of cranial shape trajectories .....	25
2.4.1.1 Ontogenetic proxies .....	25
2.4.1.2 Trajectories .....	29
2.4.1.3 Initial shape of specimens .....	30
2.4.2 The use of ontogenetic trajectories .....	31
2.4.3 Implication of Proxies for Heterochrony .....	33
2.5 Conclusion .....	35
 III. ONTOGENY AND PHYLOGENY OF THE CERCOPITHECINE	
CRANIUM.....	37
3.1 Introduction.....	37
3.2 Materials and Methods.....	39
3.2.1 Materials .....	39
3.2.1.1 Sample.....	39
3.2.1.2 Data Collection .....	39
3.2.2 Analytical Methods .....	40
3.2.2.1 Generalized Procrustes Analysis.....	40
3.2.2.2 Ontogenetic trajectories .....	40
3.2.2.3 Developmental shape change trajectory PCA ( $\delta$ PCA) .....	41
3.2.2.4 Comparison of cranial trajectories .....	42
3.2.2.5 Ontophylomorphospace .....	43
3.2.2.6 Phylogenetic signal .....	45
3.3 Results.....	46
3.3.1 $\delta$ PCA.....	46
3.3.2 Ontophylomorphospace .....	49
3.3.3 Phylogenetic signal .....	52
3.4 Discussion.....	52
3.4.1 Extant Ontogenetic Trajectories .....	52

Chapter	Page
3.4.2 Estimated Ancestral Trajectories .....	54
3.4.3 Phylogenetic Signal .....	56
3.4.4 Limitations .....	57
3.6 Conclusion .....	58
 IV. ONTOGENETIC ALLOMETRY AND SCALING IN CATARRHINE	
CRANIA .....	61
4.1 Introduction.....	61
4.2 Materials and Methods.....	64
4.2.1.1 Sample.....	64
4.2.1.1 Data collection .....	65
4.2.2 Analytical Methods.....	65
4.2.2.1 Allometric trajectories .....	66
4.2.2.2 Phenotypic trajectory analysis .....	67
4.3 Results.....	69
4.3.1 Allometric trajectories .....	69
4.3.2 Ontogenetic trajectories .....	74
4.4 Discussion .....	78
4.4.1.1 Colobinae .....	80
4.4.1.2 Cercopithecini .....	81
4.4.1.3 Papionini .....	81
4.4.1.4 Hominoidea.....	83
4.4.2 Size as a line of least evolutionary resistance .....	84
 V. CONCLUSION .....	87
 APPENDIX: TABLES FOR PROCRUSTES ANOVA RESULTS.....	90
 REFERENCES CITED.....	92

## LIST OF FIGURES

Figure	Page
1. Figure 1.1 Visual representation of ontogenetic scaling.....	8
2. Figure 2.1 <i>Macaca mulatta</i> adult male skull with landmarks collected .....	18
3. Figure 2.2 Principal components plot .....	27
4. Figure 2.3 Visualization of simulated adults .....	28
5. Figure 3.1 Molecular phylogenetic tree of the species in this investigation.....	44
6. Figure 3.2 $\delta$ PCA plot .....	48
7. Figure 3.3 Visualizations of shape change magnitudes associated with $\delta$ PC axes 1-3 .....	49
8. Figure 3.4 Ontophylomorphospace of cranial ontogenetic trajectories .....	50
9. Figure 4.1 Visual comparison of allometric trajectories.....	73
10. Figure 4.2 The first two PCs of trajectory space by clade .....	79

## LIST OF TABLES

Table	Page
1. Table 2.1 Study sample .....	17
2. Table 2.2 Angular differences (in degrees) of trajectories produced from the three ontogenetic proxies .....	22
3. Table 2.3 Procrustes distances between mean configurations of simulated and actual adults using the ontogenetic proxies by sex .....	23
4. Table 2.4 Procrustes distances from comparison of ontogenetic proxies for simulated adults .....	23
5. Table 2.5. Number of simulated adults that fell within 95% range of actual adult scatter around mean configurations.....	23
6. Table 2.6. Procrustes distances between mean configurations of simulated and actual adults .....	24
7. Table 3.1 Study sample by dental stage.....	39
8. Table 3.2 Angular differences and Euclidean distances .....	46
9. Table 4.1 Study sample by dental stage.....	65
10. Table 4.2 Angles among Colobinae allometric trajectories.....	69
11. Table 4.3 Magnitude comparison of Colobinae allometric trajectories.....	70
12. Table 4.4 Angles among Cercopithecini allometric trajectories.....	70
13. Table 4.5 Magnitude comparison of Cercopithecini allometric trajectories.....	70
14. Table 4.6 Angles among Papionini allometric trajectories.....	71
15. Table 4.7 Magnitude comparison of Papionini allometric trajectories.....	72
16. Table 4.8 Angles among Hominoidea allometric trajectories .....	72
17. Table 4.9 Magnitude comparison of Hominoidea allometric trajectories .....	73
18. Table 4.10 PTA: Colobinae trajectory angle comparison.....	74

Table	Page
19. Table 4.11 PTA: Colobinae trajectory shape and magnitude comparison.....	75
20. Table 4.12 PTA: Cercopithecini trajectory angle comparison.....	75
21. Table 4.13 PTA: Cercopithecini trajectory shape and magnitude comparison .....	76
22. Table 4.14 PTA: Papionini trajectory angle comparison.....	76
23. Table 4.15 PTA: Papionini trajectory shape and magnitude comparison.....	77
24. Table 4.16 PTA: Hominoidea trajectory angle comparison .....	77
25. Table 4.17 PTA: Hominoidea trajectory shape and magnitude comparison .....	78
26. Table 4.18 Path distances from phenotypic trajectory analyses, by clade.....	78

## CHAPTER I

### INTRODUCTION

To terms of magnitude, and of direction, must  
we refer all our conceptions of Form.  
D'Arcy Thompson (1917: 15)

There exists a causal relationship between ontogeny, the embryonic and postnatal life course of an individual, and phylogeny, the evolutionary history of a lineage. Just as adult morphology is largely the product of ontogenetic patterns, evolutionary history is mediated by changes to these developmental regimes (Garstang, 1922; de Beer, 1930; Gould, 1977). While adult specimens may demonstrate how morphology has changed over time, ontogenetic studies provide a means for determining how these differences are accomplished and can therefore provide insights into the processes responsible for observed changes (McNulty, 2012). For these reasons, an investigation of how ontogeny influences adult morphology, and how these ontogenetic patterns have changed over evolutionary time, is critical to our understanding of the evolution of humans and other catarrhines. The skull as the element of inquiry was chosen because it is an important evolutionary unit that provides many of the synapomorphies on which primate and catarrhine systematics are based. For these same reasons, fossil crania can often be assigned to a taxonomic group more reliably than postcranial remains. Additionally, crania, and importantly, juvenile crania, are often better represented in museum collections than postcranial material. Finally, the skull contains many repeatable and diagnosable landmarks ("Type 1" landmarks in the vocabulary of geometric morphometrics), which are valuable in landmark based morphometric methods (Bookstein, 1991).

While there have been numerous previous investigations into catarrhine cranial ontogeny, these studies have often led to conflicting results, possibly due to the use of different methodologies. Furthermore, comparing the ontogenetic trajectories of many taxa simultaneously can be cumbersome, as this is often accomplished by examining large matrices of pairwise angles among them. Additionally, because relatively complete ontogenetic sequences of fossil materials are scarce to non-existent, most analyses of



ontogenetic trajectories are limited to extant taxa, making it difficult to determine how trajectories have changed over time. Finally, there are several long-standing hypotheses about the role of size in the evolution of catarrhine cranial morphology that have yet to be tested using the sophisticated techniques of shape analysis that are currently available.

This dissertation addresses these issues by: 1) examining how the use of different methodologies influences the production of ontogenetic trajectories, 2) developing new methods for the analysis of extant and ancestral ontogenetic trajectories, and 3) using this information in conjunction with a comparative approach to more fully understand the role of size in the cranial evolution of catarrhines.

## **1.1 Background**

### *1.1.1 Ontogeny and Evolution*

Studies of ontogeny began in earnest with the early nineteenth century embryological investigations of Johann Meckel, Antoine Serres, and Karl Ernst von Baer (Lovtrup, 1978; Amundson, 2005). In what would later be referred to as the Meckel-Serres law, Meckel and Serres independently argued that the earliest stages of vertebrate embryos tend to resemble each other, and therefore during their development embryos pass through the adult stages of organisms situated lower on the *scala naturae*. This was soon thoroughly refuted by von Baer, who formulated his four laws of embryological development, which state that 1) the most general characters of a group arise earlier in the embryo than the special, 2) from general forms, less general forms arise until special forms are developed, 3) embryos, rather than passing through other forms during development, becomes separated from them, and 4) the embryos of 'higher forms' never resemble those of other forms, only their embryos (Hall, 1998; Amundson, 2005). Both the Meckel-Serres and von Baerian laws were temporally and philosophically pre-Darwinian; neither was discussing evolutionary relationships or how embryos might fit in to an evolutionary framework.

After the publication of the *Origin of Species* (in which Darwin argues for the importance of embryology to the understanding of evolutionary relationships), the German embryologist Ernst Haeckel, who was a staunch proponent of descent with modification, reanimated the Meckel-Serres law with the formulation of his 'biogenetic

law' (better known by the more mellifluous dictum 'ontogeny recapitulates phylogeny,' Haeckel coined both the words ontogeny and phylogeny perhaps for this very purpose...), substituting evolutionary stages for rungs in the *scala naturae* (Gould, 1977; Richtsmeier, 2018). Haeckel argued that embryos literally passed through the evolutionarily stages of *adult* ancestors, and therefore an organism's evolutionary history could be traced through its ontogenetic stages of development (Gould, 1977). Importantly, because the biogenetic law stated that embryos display the adult stages of ancestors over the course of development, recapitulation only allowed for the terminal addition of traits, with earlier stages having to be deleted to make room for them. This raised the hackles of many of Haeckel's contemporary embryologists, as it required nonsensical ancestral adult stages to explain observed embryonic stages (e.g., if all ontogenetic stages represent an adult stage of an ancestor, then there would need to be an adult mammal going through its adult life-stage attached to a placenta, to match the prenatal stage of placental mammals) (Amundson, 2005). While these and other observations eventually led to the downfall of the biogenetic law (Gould, 1977), Haeckel's response to these critiques was to develop numerous *ad hoc* caveats, which he placed under the aegis of heterochrony (another term coined by Haeckel). Heterochrony is defined as a change in the timing of developmental events in a descendant relative to an ancestor, which for Haeckel, allowed embryos to not adhere to the strict evolutionary stages of adult ancestors, as in some cases organisms would change the timing (onset/offset) or pace (rate) of their development (Gould, 1977). However, as heterochrony was seen as an aspect of the failing recapitulationist program, it fell out of favor with most researchers in the late 19th century (Gould, 1977). Heterochrony was later revitalized by de Beer (1947) and further by Gould (1977), and has played a large role in ontogenetic investigations ever since (see reviews in McKinney and McNamara, 1991; Klingenberg, 1998; Minugh-Purvis and McNamara, 2002; Mitteroecker et al., 2004, 2005).

Despite several prominent investigations of the role of ontogeny in evolution in the early to mid 20<sup>th</sup> century (e.g., Garstang 1922; Schultz, 1926; Huxley, 1932; Waddington, 1942), considerations of ontogeny were conspicuously absent from much of the Modern Synthesis (Amundson, 2005; Müller, 2007). However, a renaissance of developmental perspectives in evolution began in last quarter of the 20<sup>th</sup> century (Hall,

1998), and ontogeny has increasingly been invoked to explain a multitude of patterns of primate and human evolution ever since (Gould, 1977; Shea, 1981, 1983, 1989; McKinney and McNamara, 1991; Ravosa, 1992; Ravosa et al., 1993; Ravosa and Ross, 1994; Godfrey and Sutherland, 1996; Vrba, 1996; Lieberman et al., 2000; Leigh, 2001, 2007; Ponce de León and Zollikofer 2001; Minugh-Purvis and McNamara, 2002; Penin et al., 2002; Antón and Leigh, 2003; Leigh et al., 2003; Thompson et al., 2003; Berge and Penin, 2004; O'Higgins and Pan 2004; Ackermann, 2005; Gonzalez et al., 2011; Baab et al., 2012; Gunz, 2012; McNulty, 2012; Terhune et al., 2013; Singleton, 2015; Carlson et al., 2016).

### *1.1.2 Geometric morphometric studies of cranial ontogeny in Primates*

Landmark-based geometric morphometrics is a type of statistical analysis that investigates the shape variation of landmark coordinates after factors of non-shape variation (i.e., scale, orientation, and position) have been held constant, while also preserving the geometry of these coordinates (Bookstein, 1991; Rohlf and Marcus, 1993; Dryden and Mardia, 1998; Mitteroecker and Gunz, 2009; Baab et al., 2012). By far, the most commonly employed method for nullifying the effects of non-shape variation is the Least-Squares based Procrustes method (Marcus and Corti, 1996; Rohlf, 1999; Adams et al., 2013). This method overlays the landmark configurations through an optimization criterion (i.e., it minimizes the sum of squared distances between equivalent landmarks) and allows for the analysis of anatomical landmarks after the effects of non-shape variation have been mathematically held constant. When applied to more than two specimens, this procedure is iterative and referred to as a generalized Procrustes analysis (GPA). After collecting landmark data from a specimen, this procedure first translates specimen configurations to a common location by superimposing their centroids (geometric mean of landmark data), it then scales each configuration to unit centroid size (which is calculated as the square root of the sum of squared distances of each landmark to the centroid), and finally it rotates all configurations until corresponding landmarks across all specimens are as close together as possible (Rohlf, 1999). Although the specimens are scaled to unit centroid size, this information is actually just sequestered, and the centroid size of each specimen is most commonly used to measure size. The

variation that remains after a GPA represents the variation in shape (Marcus and Corti, 1996). Once a GPA has been executed, superimposed specimen configurations can be represented as a single point in a high-dimensional shape space (Baab et al., 2012). Because this variation concerns the relative displacement of landmarks to each other in multiple directions, it is important to use multivariate statistical methods to analyze these differences (Klingenburg, 2010). A major benefit of geometric morphometric analysis is the ability to visually represent statistical results as actual shapes, allowing for visual comparison of analytical results with actual specimens (Rohlf and Marcus, 1993; Baab et al., 2012; Adams et al., 2013). Additionally, it allows for a determination of the magnitude and pattern of shape differences between data sets. For these reasons, geometric morphometrics is especially suited to address questions regarding ontogeny (Collard and O'Higgins, 2001; Ponce de León and Zollikofer 2001; Penin et al., 2002; McNulty et al., 2004; Mitteroecker et al., 2004; O'Higgins and Pan, 2004; Cobb and O'Higgins, 2007; Singleton 2012), and allometry (Klingenberg, 1998, 2016; Singleton, 2002, 2012; Frost et al., 2003; Mitteroecker et al., 2004; Schaefer et al., 2004; Mitteroecker and Gunz, 2009; Gonzalez et al., 2011; Perez et al., 2011; Klingenberg and Maugan-Lobon, 2013; Mitteroecker et al., 2013).

Comparisons of ontogenetic shape trajectories are a standard approach in geometric morphometrics (Cheverud and Richtsmeier 1986; Leigh and Cheverud, 1991; O'Higgins and Jones, 1998; O'Higgins, 2000; Collard and O'Higgins, 2001; O'Higgins and Collard, 2002; Ackermann and Krovitz, 2002; Leigh et al., 2003; Cobb and O'Higgins, 2004; Leigh, 2006, 2007; McNulty et al., 2006; Singleton et al., 2010; McNulty, 2012). While there are a variety of methods to study ontogenetic trajectories using geometric morphometrics, the most common strategies are to use either the first principal component axis of an ontogenetic sample (which often serves as a proxy for size), as performed by Collard and O'Higgins (2001), O'Higgins and Collard (2002), and Mitteroecker et al. (2004), or the beta coefficients from a multivariate regression of Procrustes aligned shape coordinates against the covariate of developmental stage, as in McNulty et al. (2006) and Singleton et al. (2010). Comparisons among the vectors (using either method) are then made through the calculation of the angle between them, computed as the arccosine of their inner dot product (Collard & O'Higgins, 2001). A

small angle between vectors indicates similar patterns of shape change, while a larger angle indicates more divergent patterns (Cobb & O'Higgins, 2004).

However, conclusions drawn from these investigations are often equivocal. An eminently likely cause of these conflicting conclusions is the use of different ontogenetic proxies (e.g., size vs. developmental stage) to construct ontogenetic trajectories. For example, Collard and O'Higgins (2001) and O'Higgins and Collard (2002), who used size as an ontogenetic proxy in their investigations of cranial ontogenetic trajectories in papioins, argued that *Papio* and *Mandrillus*, and *Cercocebus* and *Lophocebus* all significantly differ in their ontogenetic trajectories. A different result was found by Leigh (2007), who argued that the ontogenetic trajectories of *Cercocebus*, *Lophocebus*, and *Mandrillus* are similar to each other, but differ from the ontogenetic trajectory of *Papio*. In contrast to these studies, Singleton et al. (2010), who used dental developmental stage to construct trajectories, concluded that papionins largely have a shared ontogenetic trajectory, or at least that differences between trajectories are not statistically significant given available sample sizes.

There is also a lack of consensus regarding the similarity of cranial ontogenetic trajectories in extant African apes, with some authors arguing that shape change among species follows roughly parallel trajectories, with the majority of morphological differences between species arising early in ontogeny (Ackermann and Krovitz, 2002; Berge and Penin, 2004; Lieberman, et al., 2007), while others argue that ontogenetic trajectories of cranial shape change, at least between some African ape species, are divergent (Cobb and O'Higgins, 2004, 2007; Mitteroecker et al., 2005; McNulty et al., 2006).

Therefore, a more thorough understanding of how trajectories are constructed and how the choice of ontogenetic proxy might influence interpretations is sorely needed. This information can then be used to inform the choice of investigators when addressing the specific questions of future studies.

### *1.1.3 Ontogenetic allometry and ontogenetic scaling*

Body size is an immensely influential aspect of most components of an organism, including morphology (Thompson, 1917; Huxley, 1932; Gould, 1966, 1971; Schmidt-

Nielsen, 1984). This association of size and shape is referred to as allometry, which can play a significant role in the evolution of morphological disparity and provide important insights into that morphological evolution. (Huxley, 1932; Jungers, 1985; Shea, 1985, 1995; Cheverud, 1982; Klingenberg, 1998, 2010, 2016; Gerber et al., 2008; Cardini and Polly, 2013). Researchers have differentiated between three levels of allometric inquiry: static allometry, which compares size-shape covariation among individuals within a population at a particular ontogenetic stage (e.g., adults within a species); evolutionary allometry, which compares size-shape covariation among ancestors and descendants; and ontogenetic allometry, where size-shape covariation is examined over the course of growth and development (Cock, 1966; Cheverud, 1982; Klingenberg, 1998).

In studies of ontogenetic allometry, ontogenetic scaling (*sensu* Gould, 1966; Shea, 1985; 1995) has often been invoked to explain cranial morphological differences between smaller and larger forms of closely related taxa (Freedman, 1962; Pilbeam and Gould, 1974; Jungers and Fleagle, 1980; Shea, 1981, 1983a, b, 1985, 1995; McKinney, 1986; Atchley and Hall, 1991; Ravosa et al., 1993). Ontogenetic scaling is the result of the extension/truncation of common growth allometries to new size ranges, i.e., ontogenies differ merely in the length of the compared trajectories while they maintain a similar relationship between size and shape, and these changes in shape occur in similar directions (see Figure 1.1; and Klingenberg, 1998). If the allometric trajectories differ in y-intercept transpositions (a parallel shift in the entire trajectory) and/or different slope coefficients (a change in the pattern of the trajectory) then ontogenetic scaling cannot explain shape differences among specimens (Figure 1.1). Strict ontogenetic scaling can produce scaled variants in shape, whereby a smaller organism is a proportionately scaled down version of a larger one (or vice versa). It is important to note that this does not necessarily mean that all proportions of the morphological element of interest are the same at both sizes. For example, due to the consequences of negative allometric scaling of neurocranial dimensions and positive allometric scaling of facial dimensions, smaller primates have relatively larger neurocrania and shorter faces than their larger counterparts (Gould, 1975; Singleton, 2013). Therefore, while it is not necessary for scaled variants to have identical shapes with one being large and the other small, the

commonality of the direction of the allometric trajectories is (with the only difference lying in trajectory magnitude).

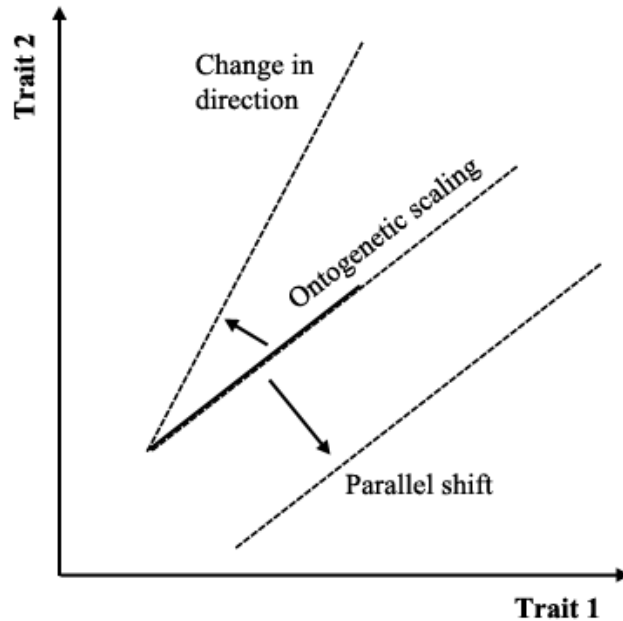


**Figure 1.1:** Redrawn from Klingenberg (1998). Visual representation of ontogenetic scaling. Ontogenetic scaling occurs when there is only a truncation or extension of a common allometric trajectory. A change in trajectory direction or a parallel shift in the entire trajectory cannot result in ontogenetic scaling. Solid line: ancestral trajectory; dashed lines: possible descendant trajectories.

There are several prominent examples of hypothesized ontogenetic scaling in comparisons of primate cranial morphology. Giles (1956) suggested that chimpanzees and gorillas were scaled variants of each other, with gorillas extending the chimpanzee cranial morphotype into a new size range (see also Shea, 1983, 1985). Shea (1992) argued that *Miopithecus talapoin* is a scaled variant of other, larger guenons, with differences in cranial shape arising from having a shared allometric trajectory of differing lengths. Pilbeam and Gould (1974) argued that robust and gracile australopithecine cranial morphologies were the result of scaled variations on a single theme. Freedman (1963) and later Leigh (2006) argued the same for members of genus *Papio*. It has also

been suggested that cranial similarities between the diphyletic large (i.e., *Papio* and *Mandrillus*) and small (i.e., *Lophocebus* and *Cercocebus*) African papionins are the result of homoplasy via allometric scaling, with *Papio* being a scaled-up version of its sister taxon *Lophocebus*, and *Mandrillus* being a scaled-up version of *Cercocebus* (Harris, 2000). There is however no consensus on the prevalence (or even existence of) ontogenetic scaling in catarrhine crania. Furthermore, several of these proposed examples of ontogenetic scaling are based on studies of bivariate generalizations of shape (e.g., Giles, 1956; Pilbeam and Gould, 1974; Shea, 1992). As shape (and indeed, an ontogenetic trajectory of shape change) is a multidimensional trait, it is important to evaluate if ontogenetic scaling is a common pattern in the evolution of catarrhine cranial shape using the advanced methods of multidimensional shape analysis.

Another important aspect of ontogenetic scaling is that size is the determining factor of shape and perhaps under the influence of selection, while the observed shapes are the byproduct of these size changes and possibly not the result of direct selection themselves. The comparison of ontogenetic trajectories in this way (ontogenetic scaling or not) has been termed a 'criterion of subtraction,' and has been argued to be a fruitful way of elucidating possible selective forces operating over evolutionary time, in that one can evaluate whether observed shapes are the product of selection for those shapes, or if they are the product of differential end points on a shared ontogenetic trajectory (Gould, 1966, 1975; Shea, 1985, 1995; Ravosa and Profant, 2000; Ravosa and Vinyard, 2002). Extending this to an evolutionary timescale, some have suggested that size is possibly a 'line of least evolutionary resistance' (Marroig and Cheverud, 2005, 2010; Ungar and Hlusko, 2016), and that size changes may be a first step in adaptation and diversification, with size responding more quickly than shape to environmental change (Elton et al., 2010). The finding of differential end points on a shared ontogenetic trajectory (i.e. ontogenetic scaling) among closely related taxa would indicate that size was a strongly influential evolutionary pressure on cranial shape and would provide support for the hypothesis of size as a path of least evolutionary resistance.

Supporting size as a line of least resistance, Marroig and Cheverud (2005, 2010) argued that body size evolution is the most significant factor in producing observed cranial morphologies in Platyrrhines, and that most taxa are scaled variants of each other.



Similarly, Cardini and Elton (2007) argued that size evolution has played a large role in the cranial morphological evolution of the Cercopithecini tribe. However, other researchers have questioned the influence of size on cranial morphological variation. For example, in their investigation of platyrrhine cranial evolution, Perez et al. (2011) found that size does not account for a large proportion of cranial shape variation once phylogenetic structure is taken into account. In their investigation of *Chlorocebus*, a geographically widespread genus of Cercopithecini, Elton et al. (2010) determined that forces other than size are instrumental in producing cranial morphological variation. Thus, it is currently uncertain if size can be considered as a line of least evolutionary resistance in the production of catarrhine cranial morphologies.

## **1.2 Investigational *Précis***

To investigate the evolution of catarrhine cranial ontogeny, three studies were conducted. Each of these analyses examines different aspects of ontogenetic trajectories, with each successive investigation expanding in taxonomic scope. An ontogenetic trajectory is the path taken by an organism through multivariate trait space and describes changes in form over the course of ontogeny (Alberch et al., 1979; Magwene, 2001). Ontogenetic trajectories are most often calculated as vectors composed of a direction (pattern of shape changes over ontogeny) and magnitude (amount of shape changes over ontogeny), and variation in either or both components can influence adult morphology (Zelditch et al., 2012). For example, two species can share a similar amount of shape change over the course of ontogeny, but if the directions (patterns) of these shape changes differ between them, the resulting adults will be dissimilar in shape because of variation in the way shapes are changing. It is important to note that the specimens measured in the subsequent studies are at the tail-end of their ontogenetic trajectories, i.e., the majority of shape changes occur from a fertilized egg to birth, prior to when the specimens were able to be measured. Despite this, important shape transformations that contribute to adult morphology still occur in these later ontogenetic stages (Collard and O'Higgins, 2001; Singleton, 2012; Zelditch et al., 2012).

While heterochrony has provided a conceptual framework for many ontogenetic studies (see reviews in Gould, 1977; McKinney and McNamara, 1991; Minugh-Purvis

and McNamara, 2002), and traditional heterochronic terminology could be used to describe differences among the developmental shape trajectories discussed herein (e.g., hypo-/hypermorphosis), these investigations will eschew the framework of heterochrony in the interpretation of results, due to the cogent concerns that have been raised regarding the application of traditionally bivariate analyses of heterochrony in a multivariate shape context (Mitteroecker et al., 2004; 2005; Gunz, 2012). Additionally, the ontogenetic hypotheses presented in these analyses are testable in a way that heterochronic hypotheses often are not (Klingenberg, 1998; Mitteroecker et al., 2004; 2005).

The first two chapters of this dissertation have been published with the coauthors Dr. Stephen R. Frost (Chapter I and II) and Dr. Michelle Singleton (Chapter II). Dr. Frost substantially helped with the editing and conceptual development of Chapters I and II, and Dr. Singleton provided cranial landmark data and editorial expertise for Chapter II. I was the primary contributor to both of these investigations. I designed the studies, performed the statistical analyses, produced the figures, and wrote the manuscripts.

### *1.2.1 Constructing cranial ontogenetic trajectories in *Macaca mulatta**

As noted above, recent morphometric research has generated opposing conclusions regarding the similarities of ontogenetic trajectories among catarrhine crania, possibly due to the different ontogenetic proxies that are used to calculate them (Collard and O'Higgins, 2001; O'Higgins and Collard, 2002; Cobb and O'Higgins, 2004, 2007; Mitteroecker et al., 2004; 2007; Leigh, 2007; Singleton et al., 2010). Additionally, some researchers have argued that the chronological age of the specimens is often necessary to adequately compare ontogenetic trajectories (Gould, 1977; Alberch et al., 1979). To address these issues, the investigation in Chapter II focuses on addressing two questions: first, of the three most common ontogenetic proxies that are used to investigate cranial growth and development (cranial size, molar eruption stage, and chronological age), which, if any, provide the most reliable linear approximations of cranial ontogenetic trajectories when using multivariate regression models?; second, of the parameters of initial specimen shape, the pattern of shape change, and the magnitude of shape change, which plays the largest role in the production of adult cranial morphologies?

Employing geometric morphometric methods and an ontogenetic sample of *Macaca mulatta* crania with associated ages at death, vectors of coefficients describing shape changes correlated with each of the three ontogenetic proxies were produced, and direct comparisons among these vectors were performed by quantifying the angle (in degrees) between them, calculated as the arccosine of their inner dot product. These trajectories were also used in developmental simulations to further evaluate the relative reliability of each of the proxies. The verisimilitude of the simulated adults was tested using permutation procedures, which compared simulated adult cranial shapes with those of actual adults. This investigation focuses on a single species of *Macaca mulatta* from the Cayo Santiago skeletal collection from the Laboratory of Primate Morphology and Genetics in Puerto Rico as information on chronological age is often absent in wild specimens but is reliably known in this population of macaques, and because this collection has an uncommonly large collection of juveniles which allowed for a large sample with which subtle differences among trajectories could be detected.

This investigation demonstrates that using dental developmental stage as a proxy for ontogeny in multivariate regression analyses produces highly reliable approximations of ontogenetic trajectories of cranial shape change. There are also other qualities which make dental stage a preferable proxy. For example, dental stage estimates the amount of shape change associated with knowable and discrete stages of development that are approximately equivalent across taxa and sexes, rather than those associated with a continuum of sizes that may differ. Dental stage has also been shown to explain substantially more shape variance than linear regressions with size as the covariate (Gunz and Bulygina, 2012). This is therefore the ontogenetic proxy used in the analyses in Chapter III. Additionally, of the parameters of initial specimen shape, the pattern of ontogenetic shape changes, and the magnitude of ontogenetic shape changes, the pattern of shape changes was found to have the strongest influence on the production of adult cranial morphology. This indicates that directly comparing patterns of development is a functional means of elucidating how adult shape differences are produced.

*1.2.2 Comparing a broad sample of ontogenetic trajectories simultaneously, and estimating ancestral trajectories of ontogenetic shape change in cercopithecines*

While the analysis of ontogenetic trajectories is common in geometric morphometrics, comparing the trajectories of many taxa simultaneously can be cumbersome and time-consuming as the number of pairwise comparisons increases as a factorial function ( $n-1!$ ) relative to the number of trajectories being evaluated, and is, in some cases, unable to make use of one of the main advantages of geometric morphometrics, visualization. This often leads to researchers having to compare large tables of angles and associated p-values among trajectories (e.g., Collard and O'Higgins, 2001; Cobb and O'Higgins, 2004; Singleton et al., 2010). Furthermore, due to the paucity of the paleontological record, analyses of trajectories are often limited to extant taxa. Finally, perhaps because of the recognition that phylogenetic patterns are largely the result of changes in ontogeny, some researchers have argued that ontogenetic trajectories of shape change, or sequences of ontogenetic events, can be used to reconstruct phylogenetic relationships (Nelson, 1978; Kluge, 1985; Yoder, 1992; Fink and Zelditch, 1995; Zelditch et al., 1995; Meier, 1997). However, the reliability of using ontogenetic data for phylogenetic reconstruction has also been questioned (Adams and Rosenberg, 1998; Rohlf, 1998; Mabee, 2000).

Chapter III addresses these issues by developing a method for visualizing the similarities and differences of cranial ontogenetic trajectories among extant cercopithecines (via a developmental shape-change trajectory PCA, herein referred to as a  $\delta$ PCA), and a method for reconstructing ancestral ontogenetic trajectories (herein referred to as an ontophylomorphospace) so that these differences can be investigated in a phylogenetic context. The ontogenetic trajectories themselves were also tested for the presence of a phylogenetic signal to determine if they might be reliably used to reconstruct phylogenies.

Results from this investigation demonstrate that the  $\delta$ PCA can reliably illustrate patterns of variation in developmental trajectories in a visually intuitive manner that allows for easier comparisons among taxa. The ontophylomorphospaces revealed that African papionins exhibit extensive homoplasy in the evolution of cranial ontogenetic trajectories, and that Asian species of *Macaca* show highly derived ontogenetic trajectories relative to other cercopithecines. Finally, the null hypothesis of no phylogenetic signal in the ontogenetic trajectories was unable to be rejected, indicating

that using ontogenetic shape trajectories as a character in phylogenetic analyses should be approached with caution, if attempted at all.

### 1.2.3 *Testing for the presence of ontogenetic scaling*

Given that the current research regarding ontogenetic scaling and size as a line of least resistance in primate cranial evolution is equivocal, and that many of the proposed examples of ontogenetic scaling were based on univariate measures of shape, it is important to test for the presence of ontogenetic scaling using multivariate methods of shape analysis. Therefore, Chapter IV employs a large, comparative ontogenetic sample of catarrhine crania, geometric morphometric methods, and an array of multivariate statistical tests to examine ontogenetic allometry and evaluate if differences in cranial shape between closely related large and small catarrhines are mainly driven by size divergence (i.e., that they are merely the product of ontogenetic scaling), thereby also testing the hypothesis of size as a line of least evolutionary resistance in catarrhine cranial evolution. Specifically, species' allometric trajectories were compared to determine if differences were due to trajectory magnitude, direction, or some combination of the two. Trajectories were then also compared using Phenotypic Trajectory Analysis (which uses dental developmental stage to construct the trajectories) to more fully understand differences among ontogenetic trajectories. While trajectories produced using size and developmental stage can track similar aspects of shape change associated with ontogeny (organisms often get larger as they develop), using dental eruption stage as a covariate to construct ontogenetic trajectories can in some cases provide more information about shape transformations than size alone, especially in samples with large amounts of size variation (Gunz and Bulygina, 2012), as is the case in this investigation.

This investigation found that allometric patterns vary among taxa, indicating that ontogenetic scaling *sensu stricto* does not often account for most morphological differences, i.e., many of the previously proposed hypotheses of scaled variants were falsified. These results also call into question the prevalence of size as a line of least evolutionary resistance, as selection appears to be changing the patterns of ontogenetic shape change, not just the size of the organisms.

## CHAPTER II

### CONSTRUCTING CRANIAL ONTOGENETIC TRAJECTORIES

From E. A. Simons and S.R. Frost. 2016. Constructing cranial ontogenetic trajectories: a comparison of growth, development, and chronological age proxies using a known-age sample of *Macaca mulatta*. *American Journal of Physical Anthropology*, 161, 296-308.

#### 2.1 Introduction

The study of ontogeny and its relationship to the production of adult morphologies has a long history in biology and biological anthropology (e.g., Thompson, 1917; Zuckerman, 1926; DeBeer, 1951; Freedman, 1962; Gould, 1977; Ravosa, 1991; Schilling and Thorogood, 2000; O'Higgins et al., 2001; Leigh, 2006). Ontogeny has often been partitioned into two related components: growth and development, with growth characterized as changes in size and development as changes in shape (Gould, 1977). The relationships between these factors, and their roles in ontogenetic shape change, are complex and can make estimates of ontogenetic shape change difficult to interpret, possibly yielding conflicting results depending on whether growth or development are being considered in particular analyses. Here, we explore the relationships between these factors and their impact on interpretations of cranial shape change during ontogeny in a known-age, ontogenetic sample of the papionin *Macaca mulatta*.

There have been many investigations into papionin cranial ontogeny (Cochard, 1985; Cheverud and Richtsmeier 1986; Leigh and Cheverud, 1991; Collard and O'Higgins, 2001; O'Higgins and Collard, 2002; Leigh et al., 2003; Leigh, 2006, 2007; Singleton et al., 2010; Singleton, 2012). In *Papio*, many studies have demonstrated that adults with large body size are also characterized as having relatively long faces (e.g., Freedman, 1962; Singleton, 2002; Frost et al., 2003). Leigh (2006) investigated the ontogenetic basis for this observation, and concluded that members of the genus *Papio* largely have a shared ontogenetic trajectory, but the terminus of this trajectory differs among the subspecies, and accounts for a majority of observed shape variation. That is, having a relatively large face is mostly a function of having a large body, and were smaller varieties of *Papio* to continue along their respective ontogenetic trajectories, they would more closely resemble larger forms (though he does caution that these ontogenetic

allometries are complex). In their investigation of multiple papionin taxa, Collard and O'Higgins (2001) and O'Higgins and Collard (2002) found that, while ontogenetic allometry accounts for a large proportion of shape variation within genera, larger taxa (*Papio* and *Mandrillus*) are not simply scaled-up variants of smaller ones (*Lophocebus* and *Cercocebus*). These authors thus concluded that among papionin genera, ontogenetic trajectories are not shared. A somewhat different result was found by Leigh (2007), who argued that, while the ontogenetic trajectories of *Cercocebus*, *Lophocebus*, and *Mandrillus* are similar to that of macaques (the outgroup in his analysis), the ontogenetic trajectory of *Papio* was strongly divergent from the others. These studies largely investigated shape changes correlated with cranial *growth* (i.e., ontogenetic allometry), rather than *development*. In contrast, Singleton et al. (2010), who were investigating shape changes relating to cranial development, specifically eruption of the molar teeth, concluded that papionins largely have a shared ontogenetic trajectory, or at least that differences between trajectories are not statistically significant given available sample sizes. Thus, there is no consensus if papionins share an ontogenetic trajectory, or the specific role these trajectories play in attaining adult cranial shapes.

There is also a lack of consensus regarding the similarity of cranial ontogenetic trajectories in extant African apes, with some authors arguing that shape change among species follows roughly parallel trajectories, with the majority of morphological differences between species arising early in ontogeny (Ackermann and Krovitz, 2002; Berge and Penin, 2004; Lieberman et al., 2007; Singleton, 2012), while others argue that ontogenetic trajectories of cranial shape change, at least between some African ape species, are divergent (Cobb and O'Higgins, 2004, 2007; McNulty et al., 2006). These different conclusions have been attributed to various factors including: differences in morphometric methodology (e.g., the use of Euclidean Distance Matrix Analysis vs. Procrustes methods), different landmarks or regions of the cranium, using a limited number of PC axes rather than the entirety of shape space, or lack of adequate statistical testing (Cobb and O'Higgins, 2004; McNulty et al., 2006; Baab et al., 2012).

Geometric morphometrics has proven to be a useful asset in studies of primate cranial ontogeny and evolution (Bookstein, 1991; O'Higgins, 2000; Ackermann and Krovitz, 2002; Frost et al., 2003; Cobb and O'Higgins, 2004, 2007; Mitteroecker et al.,

2004, 2005; McNulty et al., 2006; Slice, 2007; Singleton et al., 2010; Singleton, 2012; Baab et al., 2012; Adams et al., 2013). Importantly, these methods allow for quantification and detailed assessment of the influences that initial shape configurations as well as the patterns and amounts of ontogenetic shape change have on the attainment of adult morphology.

Therefore, this study seeks to evaluate these and other issues using landmark based three-dimensional data and geometric morphometric methods on a sample of *Macaca mulatta* crania from individuals with associated ages at death. Ontogenetic trajectories of cranial shape change were computed using three variables as surrogates for ontogeny: overall cranial size, dental developmental stage, and chronological age, in order to compare the effects of original shape, growth, and development on adult morphology. These computed trajectories are linear approximations of what are most likely curvilinear trajectories, and are vectors describing a pattern (direction) and magnitude (length) of ontogenetic shape change (see McNulty et al., 2006; Fig. 2).

Differences among the ontogenetic trajectories, and adult morphologies calculated using different ontogenetic proxies, can be used to inform the choice of investigators when addressing the specific questions of future studies. These differences among ontogenetic proxies, trajectories, and simulated adults also have implications for analyses of heterochrony, and, while the proxies investigated here are tracking similar but distinct aspects of ontogeny, we suggest that dental developmental stage be used to produce the ontogenetic trajectories that can be used in heterochronic analyses, as this is aligned with Gould's (1977) original formalisms for studying heterochrony, and because using size or chronological age proxies may be problematic as they less directly compare homologous developmental phases.

## **2.2 Materials and Methods**

### **2.2.1 Sample**

The study sample is composed of 160 adult and juvenile crania of *Macaca mulatta* from the Cayo Santiago skeletal collection, housed in the Laboratory of Primate Morphology and Genetics in Puerto Rico (Table 2.1). This population was chosen because of the large number of available specimens with documented sex and ages at



death. Specimens were chosen on the criteria of completeness of the cranium and lack of pathologies.

**Table 2.1.** Study sample. Developmental stage defined as molar eruption stage, as described in the text. Age at death is given in years.

Sex	Developmental Stage	N	Age at Death Mean (Min./Max.)	Natural log of centroid size Mean (Min./Max.)
Male	M0	16	1.17 (0.95/1.56)	2.94 (2.9/2.99)
	M1	18	2.56 (1.07/3.75)	3.07 (2.98/3.16)
	M2	25	4.19 (3.11/4.99)	3.22 (3.12/3.31)
	M3	20	9.75 (6.07/17.13)	3.37 (3.13/3.42)
Female	M0	14	1.02 (0.85/1.2)	2.89 (2.86/2.94)
	M1	29	2.21 (1.41/3.43)	3.02 (2.95/3.14)
	M2	19	3.82 (3.01/6.53)	3.13 (3.04/3.22)
	M3	19	11.07 (5.67/17.67)	3.25 (3.19/3.31)

Each of the specimens was also assigned to a developmental stage (ADE) based on their observed dental eruption state: M0: complete deciduous dentition with M1 not yet in occlusion; M1: first molar is erupted to full occlusion and the second is not; M2 second molar is erupted to full occlusion and the third is not; M3 third molar erupted to full occlusion. Individuals younger than M0 could not be measured due to the lack of sutural fusion and/or missing cranial elements. Where possible, a balanced representation of the sexes was obtained for each developmental stage.

Three dimensional landmark data were collected using a Microscribe 3DX digitizer (Immersion Corp., San Jose, CA), following the 45 landmark protocol of Frost et al. (2003). However, two landmarks (the left and right alveolar margin at distal M3, landmarks 36 and 42 of the protocol) were dropped after the measurements were taken

due to a lack of correspondence between specimens of different developmental stages (see Figure 2.1).

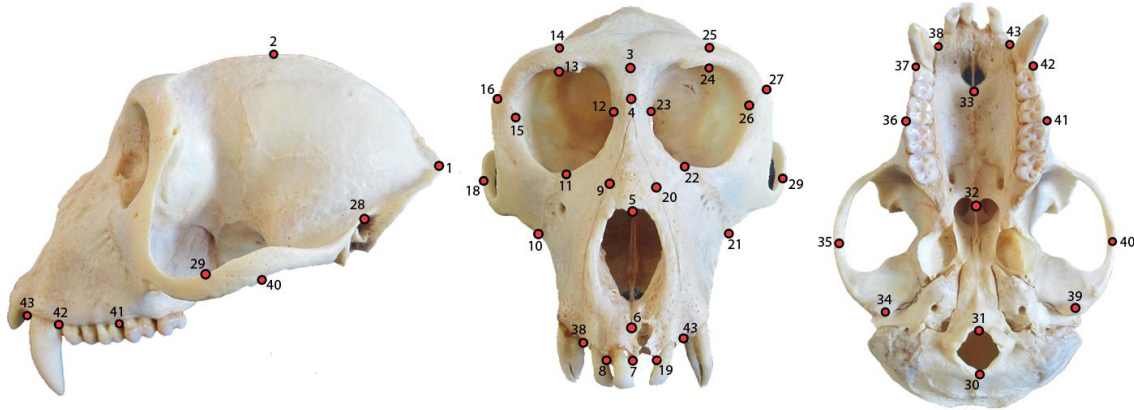


Figure 2.1. *Macaca mulatta* adult male skull with landmarks collected. Definitions of landmarks provided in Frost et al. (2003).

## 2.2.2 Analytical methods

2.2.2.1 *Generalized Procrustes analysis*. Landmark coordinates were subjected to a generalized Procrustes analysis (GPA) in *Morpheus et al.* (Slice, 1998). Size was measured as the natural logarithm of centroid size, the square root of the sum of squared distances of each landmark to the configuration centroid (Bookstein, 1991).

2.2.2.2 *Procrustes Distance*. Shape differences were quantified using Procrustes distance, the square root of the sum of squared distances between corresponding landmarks in optimally superimposed configurations (Bookstein, 1991). Procrustes distance is considered a standard measure of difference, with larger distances implying greater differences in shape (Rohlf, 1996; Dryden and Mardia, 1998). Procrustes distance was used to quantify the differences between mean shapes for each developmental stage, both within and among sexes, between simulated adults produced with each of the ontogenetic trajectories and the actual adults, and thus the verisimilitude of the vectors. Procrustes distances were also used to measure the magnitudes of the calculated trajectories.

*2.2.2.3 Computing ontogenetic trajectories.* Ontogenetic trajectories were computed using multivariate regression of GPA aligned coordinates onto the covariates of the natural logarithm of cranial centroid size (LnCS), dental developmental stage (ADE), and age at death (AAD). LnCS was used due to the size ranges involved in an ontogenetic investigation, as shape changes may be concentrated in the smaller specimens (Bookstein, 1991). These regressions produce vectors of coefficients that describe the shape change correlated with each independent variable, and are linear approximations of ontogenetic shape change of the cranium (Frost et al., 2003; McNulty et al., 2006). These vectors are composed of a direction (pattern of shape change) and magnitude (amount of shape change). In order to fully assess the differences between the three ontogenetic proxies, and their implications for analyses of ontogeny, both direction and magnitude of the trajectories were examined. It should be kept in mind that the actual ontogenetic trajectories are likely not linear (see Neubauer et al., 2009; 2010), but are sufficiently accurate approximations (in some cases more than others, see Results) of the actual trajectories for many purposes (e.g., Richtsmeier et al., 1993; Ponce de León and Zollikofer, 2001; Ackerman and Krovitz, 2002; McNulty et al., 2006; Lieberman et al., 2007; Singleton et al., 2010; Gunz and Bulygina, 2012; Tallman, 2016), though not necessarily always (e.g., Turley and Frost, 2014).

*2.2.2.4 Simulating adult morphologies.* The three ontogenetic shape trajectories for each sex were used to produce simulated adults based on each of the M0-stage juvenile specimens using the methodology of McNulty et al. (2006). Each of the three ontogenetic vectors (specific to the sex of the juvenile specimen) was added to the coordinates of each of the M0-stage specimens to produce simulated adult morphology as predicted from each of the vectors. The ADE vector was first multiplied by a factor of three, the number of developmental stage changes (McNulty et al., 2006; Singleton et al., 2010). The size vector was scaled by the difference in mean LnCS between M0 and M3 individuals for each sex. The age vector was scaled by the difference in mean age between M0 and M3 individuals for each sex. These length adjusted vectors were then added to the coordinates of the juveniles in order to simulate adult morphology.

*2.2.2.5 Assessment of simulated adult morphologies.* The morphologies of simulated adult crania produced by the different developmental vectors were evaluated in two ways. First, the Procrustes distances from the means of each group of simulated adults produced by each augmented vector to the adult means of both sexes were calculated. Permutation tests (1,000 replicates) were used to assess the significance of differences in mean shape between different groups, using SAS routines in the IML module (McNulty, 2005), with  $\alpha=0.05$ . Second, we determined if the Procrustes distances from individual simulated adults to the actual adult means fell within 95% of the range of Procrustes distances between actual adults of each sex and that sex's mean (McNulty et al., 2006).

*2.2.2.6 Comparison of trajectories.* Angles between each of the sex-specific trajectories for ADE, LnCS, and AAD were computed as the arccosine of their inner dot product, quantifying the magnitude of differences in pattern of shape change among trajectories (Collard and O'Higgins, 2001). A small angle between vectors indicates they are tracking similar changes in shape, while a larger angle indicates more divergent patterns of shape change (Cobb and O'Higgins, 2004).

In order to assess the relative contributions of 1) the initial juvenile shape, 2) the pattern and 3) the magnitude of shape change to adult morphology, these components of the six ontogenetic trajectories were interchanged into all possible combinations: i.e., all M0 males and females were each 'grown up' using 1) male pattern/male magnitude, 2) male pattern/female magnitude, 3) female pattern/ male magnitude, and 4) female pattern/female magnitude for each of the three covariates (ADE, LnCS, and AAD). This procedure thus produced a total of twelve sets of simulated adult configurations for each sex. These twelve simulations were then compared to each other and with actual adult males and females using the Procrustes distance metric and permutation test described above. This procedure allowed us to determine if the initial shape, pattern, magnitude, or some combination thereof is most influential in producing adult phenotypes in this species. If the initial shape of juveniles is driving adult morphology, and adult males and females are sexually dimorphic, then we expect male and female juveniles to be significantly different in shape. Additionally, we would expect that, e.g., when a male pattern/magnitude is applied to a juvenile female, the result would resemble actual adult

females more than actual adult males (indicating that initial shape is a highly influential factor). Alternatively, if the pattern of shape change is the most influential aspect of the trajectory, we expect that a male pattern applied to a juvenile female would produce a simulated adult that resembles actual adult males more so than actual adult females. Finally, if the magnitude is the most influential aspect of the trajectory, we expect that, e.g., when a female pattern but a male magnitude is applied to a juvenile female, the resulting simulation would resemble actual adult males more so than actual adult females. This result would indicate that males and females are scaled variants of each other.

*2.2.2.7 Principal components analysis.* Principal components analyses were performed on the actual specimens, and simulated adults, in order to visualize the multidimensional shape-space of cranial ontogeny in a reduced dimensional shape-space. Plots of the first two PCs were used to understand where in shape-space the simulated adults are situated in relation to actual adult specimens. It is important to note that the PCA was strictly for visualization purposes. Actual analyses were performed using the trajectories computed from multivariate regression, not on specific principal components.

*2.2.2.8 Visualization.* Visualizations of simulated adults were produced in Landmark Editor (Wiley, 2006), where mean configurations of simulated adults were computed and then used to warp an exemplar (i.e., a juvenile cranium) surface.

## **2.3 Results**

Adult males and females of *Macaca mulatta* are different in both size and shape. Student's t-tests of LnCS demonstrate that males and females are significantly different in size at all developmental stages (Stage M0:  $p < 0.001$ ; Stage M1:  $p = 0.013$ ; Stage M2:  $p < 0.001$ ; Stage M3:  $p < 0.001$ ). Permutation tests indicate that differences in shape between the sexes are not found until the M2 stage (Stage M0:  $\alpha = 0.052$ ; Stage M1:  $\alpha = 0.089$ ; Stage M2:  $\alpha = 0$ ; Stage M3:  $\alpha = 0$ ). Similar results have also been found in previous investigations of other papionins (O'Higgins and Jones, 1998; O'Higgins and Collard, 2002).

2.3.1 *Comparison of trajectories.* The angles computed from pair-wise comparisons of the trajectories for each of the three independent variables by sex are presented in Table 2.2. All of these angles are acute, indicating that all of the proxies are tracking similar aspects of ontogenetic cranial shape change. For both sexes, however, the vectors computed from AAD are more divergent from those computed from ADE and LnCS.

**Table 2.2.** Angular differences (in degrees) of trajectories produced from the three ontogenetic proxies. Males below diagonal, females above diagonal.

	LnCS	ADE	AAD
LnCS	-	3.95	7.99
ADE	2.74	-	8.59
AAD	5.85	6.84	-

2.3.2 *Comparison of simulated adults.* Procrustes distances between each of the simulated and actual adult mean configurations, and the alpha values from the permutation tests for differences in mean shape, are presented in Table 2.3. For both males and females, the smallest Procrustes distance between simulated and actual adults was produced using the ADE vector, followed by LnCS, and AAD was the most distant. A significant difference in shape between simulated and actual adults was only found for the AAD vector. This result is reflected in the scores for PC1-2 as well (Fig. 2 (A)). Both male and female simulated adults produced using the ADE and the LnCS vectors are closer to actual adult configurations than are those produced using the AAD vector. Additionally, for both sexes, the AAD vector produced simulated adults that were more juvenile in shape, most closely resembling M2 individuals. While neither the ADE nor LnCS vector showed a significant difference in shape between simulated and actual adults, the smaller Procrustes distance of the ADE vector for both males and females suggests that this vector may produce more accurate estimations of adult morphology.

**Table 2.3.** Procrustes distances between mean configurations of simulated and actual adults using the ontogenetic proxies by sex. Alpha values from permutation tests in parentheses.

	Males	Females
ADE	0.00508 (1)	0.01234 (1)
LnCS	0.01194 (.998)	0.01481 (.99)
AAD	0.05035 (0)	0.04888 (0)

When simulated adults computed from different ontogenetic trajectories were compared, those produced with the ADE and LnCS vectors were most similar, and were not significantly different in shape. All comparisons based on simulated adults from the AAD vector had larger Procrustes distances, and also differed significantly in shape (Table 2.4).

**Table 2.4.** Procrustes distances from comparison of ontogenetic proxies for simulated adults. Alpha values from permutation tests in parentheses. Males below diagonal, females above diagonal.

	ADE	LnCS	AAD
ADE	-	0.01059 (0.985)	0.04492 (0)
LnCS	0.00977 (0.991)	-	0.04106 (0)
AAD	0.05006 (0)	0.04388 (0)	-

This result was corroborated when the simulated adults were compared with the 95% range of Procrustes distances between actual adults of each sex and their respective means (Table 2.5). All male and female simulated adults fell within the 95% range of actual adults to each sex's mean for both ADE and LnCS. Few of the simulated adults for AAD fell within this 95% range.

**Table 2.5.** Number of simulated adults that fell within 95% range of actual adult scatter around mean configurations by sex. M = Male; F = Female; Number of juveniles used in parentheses.

Sex	LnCS	ADE	AAD
Juvenile M (16)	16	16	1
Juvenile F (14)	14	14	6

*2.3.3 Comparison of interchanged trajectories.* To disentangle the effects of sex specific patterns and magnitudes of shape change during cranial ontogeny, simulated adults were also produced by applying each of the vectors to juveniles of the opposite sex from which the vectors were produced, and by applying trajectories where the pattern and magnitude of shape change were interchanged between the sexes. The results of this analysis are presented in Table 2.6. For males and females, no accurate estimations of adult morphology were produced from any combination of male and female vectors/magnitudes for the AAD vector. The only accurate approximation of adult morphology using the LnCS vector was found using the correct sex's pattern and magnitude (as reported in Table 2.3, above). On the other hand, when the ADE vector from one sex was applied to the other, accurate approximations of sex-specific actual adult morphologies were produced. For example, when a female ADE vector was applied to a male juvenile (M0 Stage) specimen, the resulting simulated adult resembled an adult female more so than an adult male, and vice versa. Although the other proxies did not produce accurate estimations of actual adult morphologies as quantified by Procrustes distance, for both males and females, the simulated adults from all three proxies resembled actual adults from the sex of the vector, more so than the sex of the juvenile specimen (Fig. 2(B)).

**Table 2.6.** Procrustes distances between mean configurations of simulated and actual adults for juvenile males (**A**) and juvenile females (**B**), using both sex's vectors (<sub>v</sub>) and magnitudes (<sub>m</sub>) for each of the ontogenetic proxies. Top row: Procrustes distance (alpha values) from actual male adults; bottom row: Procrustes distance (alpha values) from actual female adults. Note that developmental stage magnitude is the same for both males and females.

(A)				
Males	M <sub>v</sub> M <sub>m</sub>	M <sub>v</sub> F <sub>m</sub>	F <sub>v</sub> M <sub>m</sub>	F <sub>v</sub> F <sub>m</sub>
ADE <sup>a</sup>	0.00508 (1)	-	-	0.04795 (0)
	0.05302 (0)	-	-	0.01931 (0.339)
LnCS	0.01194 (.998)	0.03854 (0)	0.04029 (0)	0.04829 (0)
	0.05235 (0)	0.03719 (0)	0.04662 (0)	0.02299 (0.049)
AAD	0.05035 (0)	0.02861 (0.002)	0.09432 (0)	0.07863 (0)
	0.04249 (0)	0.04749 (0)	0.05514 (0)	0.03998 (0)



**Table 2.6. (continued).**

**(B)**

Females	M <sub>v</sub> M <sub>m</sub>	M <sub>v</sub> F <sub>m</sub>	F <sub>v</sub> M <sub>m</sub>	F <sub>v</sub> F <sub>m</sub>
ADE	0.0229 (0.102) 0.04967 (0)	- -	- -	0.05389 (0) 0.01234 (1)
LnCS	0.02537 (0.026) 0.04898 (0)	0.0525 (0) 0.04264 (0)	0.03482 (0) 0.03049 (0.003)	0.05338 (0) 0.01481 (.99)
AAD	0.0636 (0) 0.04985 (0)	0.04156 (0) 0.04823 (0)	0.10482 (0) 0.06574 (0)	0.08825 (0) 0.04888 (0)

## 2.4 Discussion

### 2.4.1 Properties of cranial shape trajectories

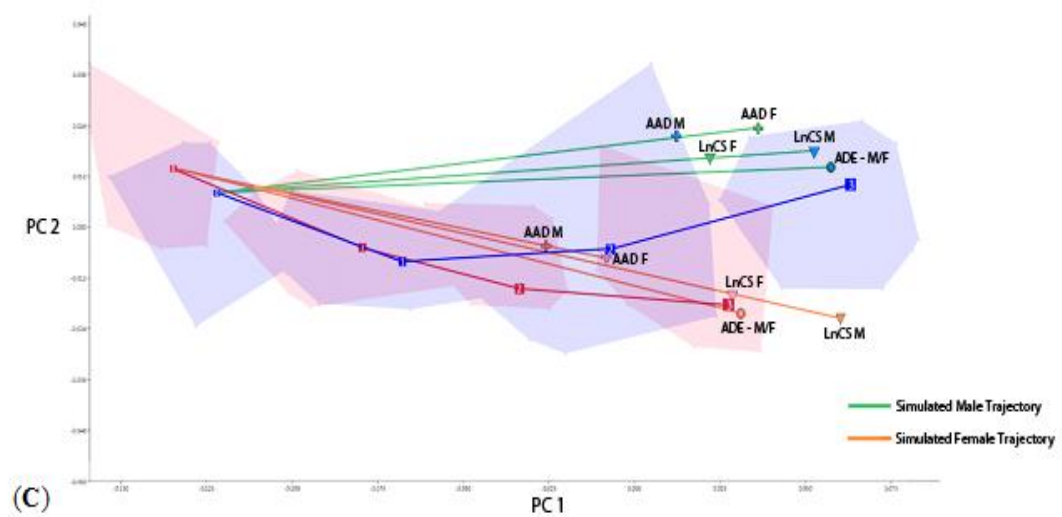
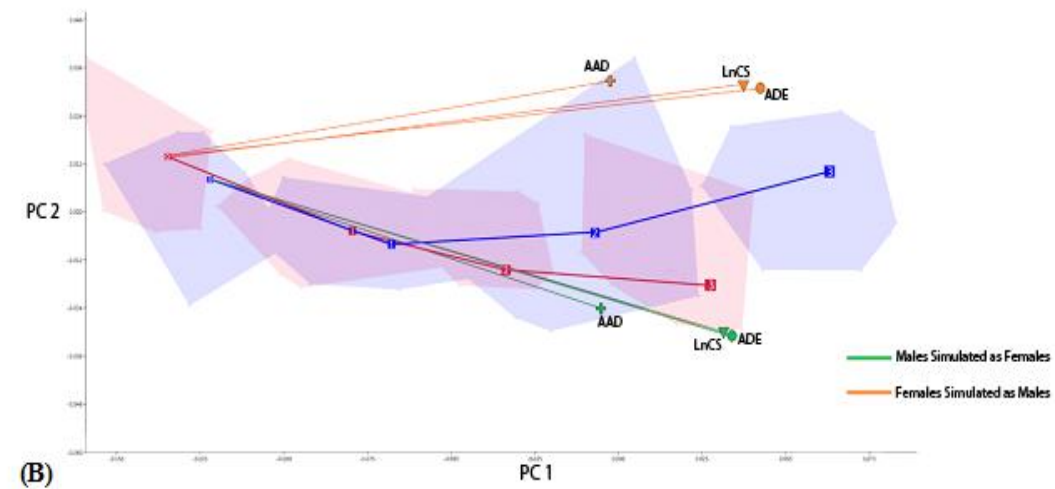
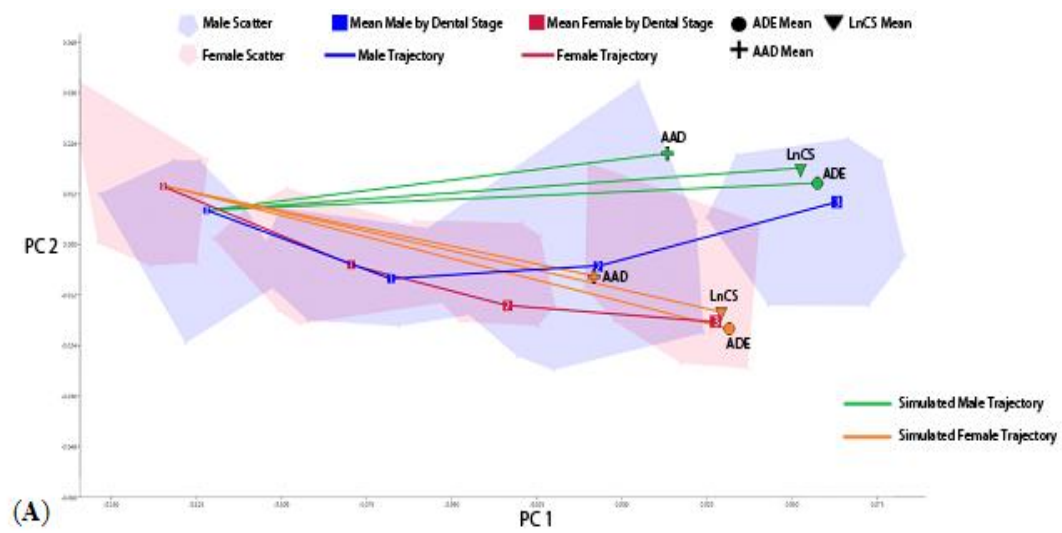
2.4.1.1 *Ontogenetic proxies.* The three different ontogenetic proxies examined in this study estimated relatively similar patterns of shape change associated with ontogeny after the time of eruption of the complete deciduous dentition, although the amount of shape change estimated by chronological age was significantly less than that for the others (Table 2.2). Furthermore, for both males and females, the chronological age vector produced simulated adults that were significantly different in shape from actual adults, and from those of the dental stage and cranial size vectors. This is because of the shorter vector produced by the chronological age proxy, and thus simulated adults that resemble more juvenile crania, being closest in shape to M2 stage individuals. This resemblance to more juvenile crania is illustrated in Figure 3, which is especially apparent in the shorter rostrum and more globular neurocranium of the simulated adults of both sexes for the chronological age vector. The shorter vector is likely due to the large variation in age for the M3 stage (females range from ~5.7 to ~17.7 years, males from ~6.1 to ~17.1 years, see Table 1). In fact, as was noted by McNulty et al. (2006), there is significant variation among individuals in terms of the absolute rate of growth and timing of developmental stages (Table 2.1). In other words, an M3 stage monkey that is older in absolute age may not necessarily be larger than a younger M3 stage individual. Similarly, it is possible for different individuals of the same age at death to be of different developmental stages and cranial shapes. Thus, our results suggest against using chronological age (or other variables that serve as proxies for ages, such as dental wear) in the construction of cranial ontogenetic trajectories in most cases. One exception to this might be in investigations of

shape changes post eruption of M3, where few developmental markers are available, and size change is relatively minor if present at all.

Vectors made using dental stage and cranial size, on the other hand, produced simulated adults that were neither significantly different in shape from each other (Table 2.4; Fig. 3), nor from actual adults (Table 2.3). In this sample at least, amount of growth and timing of developmental stages are tightly correlated and track similar aspects of ontogenetic shape change. That is, as individuals move through developmental stages they also get larger. The cranial size proxy is specifically tracking the size related shape changes of the individuals as they get larger. Therefore, in some cases, overall size is an adequate proxy when producing ontogenetic trajectories, especially when organisms without large size disparities are being considered. Additionally, for investigations involving edentulous organisms, or of postcrania, size may be the only proxy available. Size will also be the most appropriate covariate when allometry is the explicit subject of interest (Klingenberg, 1998; Frost et al., 2003; Mitteroecker and Gunz, 2009).

---

**Figure 2.2.** (next page). Principal components plot. (A), (B), and (C): Squares: mean configurations by sex and dental eruption stage for actual specimens; numbers show ADE (dental eruption stage); Red: Female; Blue: Male; Red polygons: female scatter; Blue polygons: male scatter; Pluses: mean configuration for simulated adults using AAD (age at death); Circles: mean configuration for simulated adults using ADE; Inverted triangles: mean configurations using the natural log of centroid size. (A) Simulated adults for both males and females using each of the three proxies. Orange: female simulations; Green: male simulations. The mean simulated adults using the ADE and LnCS vectors are closer to actual adult means for both sexes than simulations produced with the AAD vector. (B) Pattern is shuffled between sexes, so that female trajectories are used for developmental simulations of juvenile males, and vice versa. Orange: simulated adults generated from juvenile females with a male pattern; Green: simulated adults generated from juvenile males with a female pattern. Note that, for all proxies, when a male trajectory is applied to juvenile females, the simulated adults resemble males more than females, and vice versa. (C) Magnitude is shuffled between sexes, so that male and female developmental simulations have a sex specific pattern, but both male and female magnitudes. Pink shapes: simulated adults generated with a trajectory based on female pattern and female magnitude; Orange shapes: female pattern and male magnitude; Blue shapes: male pattern and male magnitude; Green shapes: male pattern and female magnitude; Orange lines: female trajectory; Green lines: male trajectory. A male magnitude extends the trajectory for the ADE and LnCS proxies, while the opposite is true for the AAD proxy.



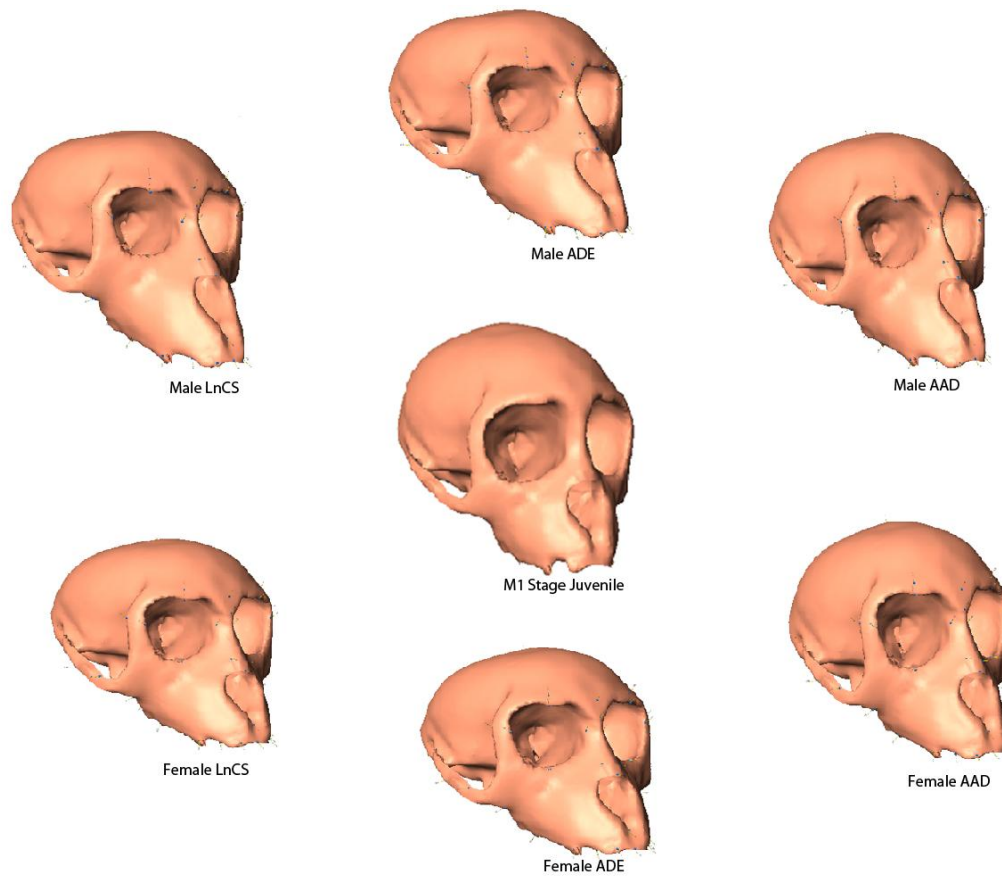


**Figure 2.3.** Visualization of simulated adults. Center: Juvenile female cranium. Top: Male developmental simulations based on size (LnCS), developmental stage (ADE), and chronological age (AAD). Bottom: Female developmental simulations. All visualizations scaled to approximately the same size to facilitate shape comparisons.

These findings have implications for the lack of consensus of previous researchers regarding the similarity of cranial ontogenetic trajectories of primates. The observation that ontogenetic trajectories constructed using either size or molar eruption as proxies are similar indicates that differences in methods of constructing ontogenetic trajectories are not likely to cause the differing results of, e.g., Collard and O'Higgins (2001) and Singleton et al. (2010). However, it should be kept in mind that this is a single species sample, and results regarding trajectories composed from centroid size could differ when multiple taxa are considered. That is, in multi-taxon analyses where taxa vary greatly in size, or in a pooled-sex analysis including taxa with high degrees of sexual dimorphism,

it is likely that dental stage and cranial size would not be as tightly correlated as they are here, and it is possible that using cranial size would lead to over- or underestimates of adult morphologies. In previous investigations, centroid size has also been found to explain substantially less shape variance than linear regressions with dental stage as the covariate (Gunz and Bulygina, 2012). Thus, it may be preferable to use a developmental marker to construct ontogenetic trajectories in analyses that are not explicitly concerned with tracking the correlation of size and shape, as these markers estimate the amount of shape change associated with knowable and discrete stages of development that are approximately equivalent across taxa and sexes, rather than those associated with a continuum of sizes that may differ radically among analytical groups. Other methods, such as the common allometric component (and other group mean centered approaches) may mitigate this effect as well (Mitteroecker et al., 2004).

Since ontogenetic proxy choice does not appear to result in significantly different trajectories of ontogenetic shape change, it may be that using a single principal component (Collard and O'Higgins, 2001; Cobb and O'Higgins, 2004), rather than the entirety of shape space (Singleton et al., 2010) to construct ontogenetic trajectories may have led to the contrasting conclusions of these studies regarding the similarity of papionin cranial ontogenetic trajectories.

*2.4.1.2 Trajectories.* For each of the three proxies, we evaluated the relative contribution of: 1) the shape of the juvenile specimen, 2) the pattern of development and 3) the magnitude of development in the attainment of adult morphologies. The results were similar for both sexes and for each method: the pattern of development, more so than the shape of the juvenile specimen or trajectory magnitude, strongly influenced the attainment of sex-specific adult morphologies. However, the magnitude of development is also important, in that males have larger magnitudes (longer trajectories), which contribute to observed adult morphologies. For example, as can be seen in Figure 2 (C), when a vector representing the female pattern of shape change but extended to male magnitude was applied to juvenile female specimens, the resulting simulated adults "overshot" actual adult females, but still remain closer to the mean configuration of actual adult females than to the mean of actual adult males, and vice versa for males grown with

a female magnitude. Similarly, when the male chronological age pattern but female magnitude was applied to juvenile males it extends the trajectory and actually results in simulated adults closer to the real adult males. In the opposite case, a female chronological age pattern with male magnitude applied to juvenile females, "undershot" female adult morphology to an even greater degree.

This has implications for how sexual dimorphism is achieved in this species. Although males do have a longer trajectory, males and females are not simply scaled variants of each other, which has been argued in previous investigations (Cochard, 1985; Cheverud and Richtsmeier, 1986). If this were the case, we would expect that when a female pattern of development with a male magnitude was applied to juveniles, the simulated adults would resemble actual adult males. The fact that this was not observed indicates that a sex specific pattern of development, along with differences in amount of shape change, is driving sexual dimorphism in this species, rather than only a difference of magnitude along a shared trajectory.

*2.4.1.3 Initial shape of specimens.* Most cranial shape has already been established by the time of the eruption of the complete deciduous dentition (the earliest point examined in this sample), and even more so by the emergence of M1 (as used in other studies, e.g. McNulty et al., 2006). Additionally, we observed that male and female crania are not significantly different in shape at the earliest developmental stage in this sample. Thus, the initial shape of an individual in this investigation played less of an important role in the attainment of sex-specific adult morphology than the pattern and magnitude of shape change. For example, when a male vector of shape change was applied to juvenile females, the resulting simulation (for all three proxies) was closer to actual adult males than to adult females, and vice versa (Fig. 2 (B)). Despite playing less of a role, the simulated adults in the sex-swapped analysis were nonetheless different from simulated adults where the correct sex vector was used (cf. Fig. 2 (A) and (B)), indicating that the initial shape of the specimen does have an effect, even when studying sexes within a single species. Obviously, the impact of the initial configuration would be greater in studies where multiple species or higher taxa are compared (e.g., Collard and O'Higgins 2001; O'Higgins and Collard 2002; Cobb and O'Higgins, 2004; 2007; Mitteroecker et al.,

2004; 2005; Singleton et al., 2010; Singleton, 2012), or, where the earliest dental eruption stage used is more mature (e.g., McNulty et al., 2006) than in this investigation.

#### 2.4.2 The use of ontogenetic trajectories

Ontogenetic trajectories, and the developmental simulations computed from them, have been used to assess the taxonomic affinities of juvenile specimens (McNulty et al., 2006; Singleton et al., 2010; Gunz and Bulygina, 2012). These particular investigations used dental developmental stage, rather than overall cranial size as the covariate to construct their trajectories, as expected adult cranial size was unknown. Additionally, as noted by McNulty et al. (2006), the sex of their specimen (Taung) was also unknown, and using a size variable for species that exhibit sexual dimorphism could conflate older females with younger males. The results of our investigation confirms the choices of these studies, which were based on *a priori* requirements, that developmental stage is likely the preferred covariate to use when predicting the phenotype of a juvenile specimen.

For studies of ontogenetic allometry, on the other hand, size (rather than developmental stage) is the preferred covariate when constructing trajectories using multivariate regression (Bookstein, 1996; Klingenberg, 1998; Frost et al., 2003; Mitteroecker and Gunz, 2009). A major benefit of this method is that all of shape space is being used to investigate allometry, rather than relying on a limited number of principal components to represent allometric shape changes. Because these trajectories are explicitly tracking size related shape changes, they can possibly determine if intra- or interspecific morphological differences are mostly due to allometric scaling, and are therefore produced through extending or truncating ontogenetic trajectories. For example, using allometric trajectories, and growth simulations computed from these trajectories, one could determine if the cranial morphology of the relatively large papionin *Mandrillus* is a scaled-up version of the relatively smaller *Cercocebus*, as it has been suggested that mandrill growth trajectories are similar to mangabey growth trajectories extended into a new size range (Leigh, 2007). While, as stated above, there is debate as to whether the crania of these taxa are scaled variants of each other, the use of these methods could aid

in determining if increasing the magnitude of the allometric trajectory of *Cercocebus* would result in a cranium that is phenotypically similar to that of *Mandrillus*.

Ontogenetic trajectories can also be used to address other long standing issues in physical anthropology, though in some cases it may be preferable to use both a developmental stage proxy and a size proxy to calculate the trajectories. For example, as hypothesized by Giles (1956), and later argued by Shea (1983, 1985, 1988), the cranial morphology of gorillas can be considered as similar to that of chimpanzee, were it to continue along its ontogenetic trajectory. While other studies have demonstrated that these primates do not strictly share an ontogenetic trajectory (e.g., Cobb and O'Higgins, 2004; Mitteroecker et al., 2004; 2007), and are thus not simply scaled variants of each other, an actual test of this hypothesis using the methods of developmental simulation has yet to be attempted. One way to approach this is to quantify the cranial ontogenetic trajectory of chimps using multivariate regression, and, using developmental simulation, extend the trajectory of the mean configuration adult chimps. These results could then be compared with the mean configuration of adult gorillas using the metric of Procrustes distance, and permutation procedures can be used to statistically assess similarities and differences (see Singleton (2012) for a similar analysis performed on a *Mandrillus* cranium). In this case, two trajectories, calculated using size and dental stage respectively, may be preferable as this would facilitate a comparison of the morphological consequences of allometry with those of differences in ontogenetic shape change (see also Mitteroecker et al., 2004). Thus, a chimp trajectory computed from centroid size could be extended to the mean gorilla centroid size, and a chimp trajectory computed from developmental stage would be extended beyond its actual terminus by augmenting the coefficient vector by additional developmental stages (Singleton, 2012). Stated another way, one could compare the results of a chimp cranium continuing along a developmental trajectory (dental stage as a covariate) with those of a trajectory computed from extended ontogenetic scaling (size as a covariate), with both approaches incorporating the entirety of shape space to construct the trajectories. If the simulated 'super-chimp' cranium resembles an adult gorilla's, then this would lend support to Giles' (1956) and Shea's (1983, 1985, 1988) hypotheses.



### 2.4.3 Implications of proxies for heterochrony

There has been seemingly endless debate regarding the proper way to study heterochrony (e.g., Gould, 1977; 1988; 2000; Alberch et al., 1979; Shea, 1983; 1989; Hall, 1984; McNamara, 1986; McKinney, 1988; Raff and Wray, 1989; McKinney and McNamara, 1991; Godfrey and Sutherland, 1995; 1996; Reilly et al., 1997; Rice, 1997; Klingenberg, 1998; Smith, 2001; Minugh-Purvis and McNamara, 2002). More recently, this debate has focused on the proper ways to apply geometric morphometrics to heterochronic investigations (Penin et al., 2002; Berge and Penin, 2004; Mitteroecker et al., 2004; 2005; Lieberman et al., 2007; Baab et al., 2012; McNulty 2012). The consensus view is that geometric morphometrics is especially suited for conducting heterochronic investigations, as a possible outcome of heterochrony is the separation of size and shape (Berge and Penin, 2004; Mitteroecker et al., 2005; Mitteroecker and Gunz, 2009). However, some investigators (e.g., Mitteroecker et al., 2004; 2005) have suggested that the original formulation of heterochrony cannot be directly translated to multivariate methodology. Mitteroecker et al. (2005) argue that biological interpretations should not be predicated on an analysis of a limited number of PC axes (as has been done in several investigations, e.g., Penin et al., 2002; Berge and Penin, 2004; Lieberman et al., 2007), as this does not incorporate the entirety of shape space. Mitteroecker et al. (2004; 2005) have concluded that unless the taxa being compared overlap entirely in shape space (i.e., when all PCs are considered), traditional definitions and interpretations of heterochrony are inapplicable.

As noted by Baab et al. (2012), an alternative to the problems encountered when conducting heterochronic analyses using ordination methods such as PCA is to avoid them altogether, and instead make direct comparisons of ontogenetic trajectories (e.g., by measuring the angle between them) that have been constructed from the entirety of shape space, using multivariate regression of shape coordinates onto centroid size or dental developmental stage, as was done here. From our results, dental stage, rather than size or chronological age should be the preferred covariate to use when constructing cranial ontogenetic trajectories for heterochronic analyses, as they better approximate homologous stages of ontogeny, whereas size and chronological age do not.

Although the ontogenetic trajectories created in our investigation using size and dental development stage were similar, we advocate for the use of dental developmental stage rather than centroid size to produce trajectories for several reasons. First, our sample is from a single species, and the use of centroid size to construct trajectories from a multi-taxon sample with greater size disparity may lead to different results. Additionally, despite size and shape being intimately related, shape can be assessed independently of size (as it is in geometric morphometrics), and ontogenetic trajectories should be computed with this in mind. Second, as has been argued by Gould (1977) and Godfrey and Sutherland (1995), growth allometries are problematic for identifying heterochrony, as 1) the techniques of measuring allometry reinforce a prejudice against the possibility of dissociation between size and shape, and 2) similar growth allometries can be produced by different heterochronic processes. Lastly, Gould (1977) suggested that the best way to identify heterochrony was through the comparison of homologous developmental stages (which he did via a clock model). One drawback to this was that the model was static. Alberch et al. (1979) expanded the clock model to incorporate comparisons of ontogenetic trajectories, but did not retain the standardized developmental stages initially advocated by Gould (1977; see also Klingenberg, 1998; Alba, 2002). As Alba (2002) suggested, these two models should be combined so that there is a standardization of developmental stages at both the onset and offset of development. Actual onset of development, however, is extremely difficult to quantify, and, in many landmark based investigations, will begin around the eruption of M1 (see however Mitteroecker et al., 2004; Gunz and Bulygina, 2012). Additionally, dental developmental stages have been shown to be strongly correlated with life history variables (Harvey and Clutton-Brock, 1985; Smith, 1989), allowing for comparisons among salient life history events.

While chronological age is often considered a *sine qua non* of assessments of heterochronic processes (Gould, 1977; Shea, 1989; Zelditch et al., 2004; Leigh, 2006; Lieberman et al., 2007; though see Strauss, 1987), we recommend against using chronological age to construct ontogenetic trajectories for use in heterochronic investigations that incorporate geometric morphometrics. Although we are aware of the conceptual and etymological implications of not using chronological age in analyses of

heterochrony, the results of this investigation demonstrated that an ontogenetic trajectory computed from chronological age is more unreliable in developmental simulations than those from dental stage or size. Therefore, if one is constructing ontogenetic trajectories for heterochronic analyses using multivariate regression, chronological age should not be used as a covariate. In addition to this, there are several reasons why chronological age (as opposed to developmental or maturational age) may not be as valuable to heterochrony as once thought. First, chronological age is rarely available, and is especially problematic for investigations involving fossil taxa. Second, as captive vs. wild primates have been shown to differ in the chronological timing of tooth eruptions (e.g., Zihlman et al., 2004), chronological age has only an approximate relationship to biological age (Strauss, 1987). Finally, even when chronological ages are known, heterochronic processes (and even heterochronic results) may still be obscured. For example, the knowledge that humans reach dental eruption stages chronologically later than chimpanzees has done little to settle the debate about whether humans are neotenuous relative to chimps (see and cf. Gould, 1977; Shea, 1989; McKinney and McNamara 1991; Godfrey and Sutherland, 1996; McNamara, 2002). Thus, while chronological age can be used to understand the relative rate at which developmental stages are reached, and therefore can be enlightening in certain respects, it is not particularly useful for multivariate analyses of heterochrony that incorporate geometric morphometrics.

## 2.5 Conclusion

This investigation used geometric morphometrics to compare some of the ontogenetic surrogates that can be used to investigate cranial growth and development in a sample of *Macaca mulatta* crania with associated ages at death. Direct comparisons of trajectories produced using dental eruption stage, cranial size, and age at death found that these variables track similar aspects of ontogenetic shape change, with size and dental stage being most similar. The size and dental stage trajectories were also found to produce highly similar simulated adult configurations when applied to juvenile specimens, with dental stage producing the most accurate estimates of adult morphology. Chronological age, on the other hand, was distinct compared to the other proxies, and produced the least accurate estimates of adult morphology. Additionally, while the

pattern, magnitude, and initial shape of the specimen all play a role in the attainment of adult morphologies, the pattern of ontogenetic shape change appears to play the largest role.

Results from this investigation have important implications for the following chapters. First, while size and age proxies were similar, developmental simulations demonstrated that the most reliable is dental developmental stage, which is the covariate that will be used in subsequent chapters. Secondly, of the parameters of initial specimen shape, the pattern of ontogenetic shape changes, and the magnitude of ontogenetic shape changes, the pattern of shape changes was found to have the strongest influence on the production of adult cranial morphology. This indicates that directly comparing patterns of development is a functional means of elucidating how adult shape differences are produced. The next chapter introduces two novel methodologies for these comparisons.

## CHAPTER III

### ONTOGENY AND PHYLOGENY OF THE CERCOPITHECINE CRANIUM

From E.A. Simons, S.R. Frost, and M. Singleton. 2018. Ontogeny and phylogeny of the cercopithecine cranium: a geometric morphometric approach to comparing shape change trajectories. *Journal of Human Evolution*, 124, 40-51.

#### 3.1 Introduction

Investigations of the morphological aspects of growth and development have increased in number and in sophistication in recent decades. In part, this increase is due to the appreciation that evolutionary changes in adult form are the consequence of changes to the ontogenetic routes that lead to that form (Gould, 1977; Hall, 2003; Zelditch et al., 2004; McNulty, 2012). The availability of advanced methodologies for data collection (e.g., 3D digitizers and scanners) and analysis (typified by the ‘geometric morphometric revolution’; Rohlf and Marcus, 1993; Adams et al., 2004) have also provided researchers with improved means to quantify and evaluate relationships between ontogeny and biological form. Investigations of ontogeny incorporating these methods have proven to be useful in a broad array of analyses, including: prediction of adult morphologies from juvenile specimens (Ackermann and Krovitz, 2002; McNulty et al., 2006; Singleton et al., 2010; Singleton et al., 2016), estimation of the morphology of adult specimens were they to continue further along their ontogenetic trajectory (Singleton, 2012), and investigations of the evolutionary changes along extinct lineages (Simons and Frost, 2014). Additionally, ontogenetic investigations further aid in identifying the influence of allometry on shape, and can reduce the inclination to produce adaptive scenarios to explain particular cranial shapes that are in fact the byproduct of selection for body size (Ravosa and Profant, 2000; Marroig and Cheverud, 2005; Gilbert, 2011; Singleton, 2013). Thus, an ontogenetic perspective contributes to investigations of morphology, especially when coupled with advanced methods of shape analysis, as in geometric morphometrics.

Landmark-based geometric morphometrics is a type of statistical analysis that investigates the shape variation of landmark coordinates after factors of non-shape variation have been held constant, while also preserving the geometry of these coordinates (Bookstein, 1991; Rohlf and Marcus, 1993; Dryden and Mardia, 1998;

O'Higgins, 2000; Frost et al., 2003; Slice, 2007; Mitteroecker and Gunz, 2009; Baab et al., 2012). A major benefit of geometric morphometric analysis is the ability to visually represent statistical results as actual shapes, allowing for visual comparison of analytical results with actual specimens (Rohlf and Marcus, 1993; Baab et al., 2012; Adams et al., 2013). Additionally, it allows for a determination of the magnitude and pattern of shape differences between data sets. For these reasons, the geometric morphometrics toolkit is especially suited to address hypotheses regarding shape changes that occur during ontogeny (Collard and O'Higgins, 2001; Ponce de León and Zollikofer 2001; Penin et al., 2002; McNulty et al., 2006; Mitteroecker et al., 2004; O'Higgins and Pan, 2004; Cobb and O'Higgins, 2007; Singleton 2012).

Comparisons of ontogenetic shape trajectories (i.e., the pattern and magnitude of shape changes associated with ontogeny) are a standard approach in geometric morphometrics (Cheverud and Richtsmeier 1986; Leigh and Cheverud, 1991; O'Higgins and Jones, 1998; O'Higgins, 2000; Collard and O'Higgins, 2001; O'Higgins and Collard, 2002; Ackermann and Krovitz, 2002; Leigh et al., 2003; Cobb and O'Higgins, 2004; Leigh, 2006, 2007; McNulty et al., 2006; Singleton et al., 2010; McNulty, 2012; Simons and Frost, 2016). Previous investigations of primate cranial ontogenetic trajectories involving multiple taxa have compared either the first principal component axis of cranial shape change associated with development, as in Collard and O'Higgins (2001), O'Higgins and Collard (2002), and Mitteroecker et al. (2004), or the beta coefficients from a multivariate regression of Procrustes aligned shape coordinates against the covariate of developmental stage, as in McNulty et al. (2006) and Singleton et al. (2010). However, comparing the trajectories of many taxa simultaneously can be cumbersome and time-consuming, as the number of pairwise comparisons increases as a factorial function ( $n-1!$ ) relative to the number of trajectories being evaluated.

This investigation presents two new approaches to compare the cranial developmental shape trajectories of cercopithecines, and visually assess the similarities and differences among them. Specifically, we wished to compare the relative magnitudes of development in various aspects of the cranium, and compare these magnitudes across taxa. We also investigated the importance of ontogenetic allometry in the production of adult phenotypes, and evaluated if any taxa exhibit aspects of their trajectories that are

not correlated with size. Finally, we investigated how developmental trajectories have changed over evolutionary time, in order to determine if there are identifiable evolutionary trends, such as parallel evolution or lineage diversification among clades.

### 3.2 Materials and Methods

#### 3.2.1 Materials

3.2.1.1 *Sample*. The dataset is composed of 17 cercopithecine species partitioned by dental eruption stage (Table 3.1), and is further described in Singleton et al. (2010) and Singleton (2012). The majority of specimens were wild-shot, however, a small number of zoo specimens (16 of 522 specimens) were used for genera that were poorly represented in collections (i.e., *Allenopithecus* [2], *Macaca sylvanus* [9], *Mandrillus* [2] and *Theropithecus* [3]).

**Table 3.1.** Study sample by dental stage, as defined by full eruption of nominal tooth. Both sexes are included in the calculation of trajectories. C = Male with M<sup>1</sup>–M<sup>3</sup>, but canine not erupted.

	Abbreviation	pre-dP <sup>4</sup>	dP <sup>4</sup>	M <sup>1</sup>	M <sup>2</sup>	C	M <sup>3</sup>	Total
<i>Allenopithecus nigroviridis</i>	Ani	0	1	4	8	1	13	27
<i>Chlorocebus aethiops</i>	Cae	0	1	7	5	2	16	31
<i>Cercocebus agilis</i>	Cag	0	0	6	9	0	17	32
<i>Cercocebus atys</i>	Cat	0	1	6	6	0	20	33
<i>Cercocebus torquatus</i>	Cto	1	1	4	4	4	21	35
<i>Lophocebus albigena</i>	Lal	0	4	4	6	1	30	45
<i>Lophocebus aterrimus</i>	Lat	0	4	5	7	0	21	37
<i>Macaca assamensis</i>	Mas	0	2	2	0	4	11	19
<i>Macaca fascicularis</i>	Mfa	2	7	19	7	9	42	86
<i>Macaca leonina</i>	Mnl	0	1	3	3	1	5	13
<i>Macaca mulatta</i>	Mmu	0	4	5	5	0	8	22
<i>Macaca nemestrina</i>	Mne	0	1	2	1	0	8	12
<i>Macaca sylvanus</i>	Msy	0	3	2	3	0	25	33
<i>Mandrillus leucophaeus</i>	Mle	0	1	1	1	1	9	13
<i>Mandrillus sphinx</i>	Msp	2	0	2	5	0	12	21
<i>Papio hamadryas anubis</i>	Pha	0	5	9	6	1	28	49
<i>Theropithecus gelada</i>	Tge	0	0	0	4	2	8	14

3.2.1.2 *Data collection*. Three-dimensional landmark data were collected using a Microscribe 3DX digitizer (Immersion Corp., San Jose, CA), using the 45 landmark protocol of Frost et al. (2003). However, because two landmarks (the left and right

alveolar margin at distal M<sup>3</sup>, landmarks 36 and 42 of the protocol) were not able to be collected for the youngest specimens in our sample, these landmarks were subsequently dropped from all specimens, leaving a total of 43 landmarks (see Figure 2.1).

### 3.2.2 Analytical methods

3.2.2.1 *Generalized Procrustes analysis*. Landmark coordinates were subjected to a generalized Procrustes analysis (GPA; (Bookstein, 1991; Marcus and Corti, 1996; Rohlf, 1999). The GPA was performed in Morpheus (Slice, 1998), as this program allows for superimposition even when some specimens are missing landmarks (which was the case in our sample). All specimens underwent reflected averaging allowing reflections to provide aligned mirror images, which were averaged. Then, a small number of missing landmarks were reconstructed using thin-plate spline (TPS) estimation (Gunz et al., 2009), whereby a reference stage specific mean was calculated for each species (e.g. M<sup>1</sup> stage *Macaca mulatta*), and each incomplete specimen was mapped to its group reference using all landmarks present in that specimen. Swapping and averaging were performed in SAS Version 9.2 (SAS Institute Inc., Cary, NC, USA), using code written by one of the authors (M.S.). For more information, see Singleton et al. (2011).

It is important to note that, when analyzing shapes, the orientation of those shapes is a ‘nuisance variable’ that must be accounted for. However, when analyzing developmental trajectories, the orientation of the trajectories provides valuable information that will be lost if a second Procrustes superimposition is performed on the trajectories. Therefore, only one GPA was performed: the GPA on the original shape variables prior to any analyses.

3.2.2.2 *Ontogenetic trajectories*. Ontogenetic trajectories were computed using multivariate regression of GPA aligned tangent space coordinates onto the covariate of dental eruption stage to produce vectors of coefficients that describe the shape changes correlated with development. These are linear approximations of ontogenetic shape change in the cranium (Frost et al., 2003; McNulty et al., 2006; Singleton et al., 2010). Due to the relative paucity of subadult specimens in museum collections, the uncertain sex of a few subadults, and the need to obtain reasonable sample sizes, mixed-sex



samples were used to construct each species' ontogenetic trajectory. The use of mixed-sex samples to construct ontogenetic trajectories is justified by previous investigations, which found that male and female ontogenetic trajectories do not typically diverge until late in ontogeny, and that mean juvenile cranial shapes between sexes in cercopithecines are indistinguishable (O'Higgins and Jones, 1998; Collard and O'Higgins, 2001; O'Higgins and Collard, 2002; Leigh, 2006). Landmarks 36 and 41 (Fig. 3.1) were treated as missing data in the calculation of trajectories for dP<sup>4</sup> and younger individuals, who were missing these datapoints.

*3.2.2.3 Developmental shape-change trajectory PCA ( $\delta$ PCA).* Rather than the more common approach in geometric morphometrics of a relative warps analysis (i.e., a PCA on the tangent space of the superimposed coordinates of each of the specimens), the ontogenetic cranial trajectories themselves (i.e., the vectors of coefficients from the multivariate regression) were entered into a principal components analysis to produce the  $\delta$ PCA. Principal components analysis reduces the number of variables in the original dataset to produce a summary of the shape variance in the original data. Principal component (PC) axes are the projections of shapes onto the space spanned by the eigenvectors and are mutually orthogonal. In the context of geometric morphometrics, the mean centered landmark coordinates (after Procrustes superimposition) are used to produce an eigendecomposition of the sample covariance matrix. Because PCA is a rigid rotation of the data, the Procrustes distances among the specimens are preserved (Mitteroecker and Gunz, 2009). PCs can be visualized as shape deformations (e.g., thin-plate spline deformation grids, sensu Bookstein, 1989), but, it is important to keep in mind that PCs are statistical artifacts that are largely dependent on the composition of the sample and should not be interpreted as one-to-one representations of biological factors (Mitteroecker et al., 2004, 2005). The  $\delta$ PCA provides an ordination of taxa in ontogenetic shape space for visual comparisons that are easier to evaluate than a large matrix of pairwise angles (e.g., Singleton et al., 2010; Table 3.2). It should be noted that, as PCA is an ordination method that is used more in data exploration than hypothesis testing, the  $\delta$ PCA obviously does not obviate the need to statistically assess any relevant hypotheses.

A conceptually similar analysis to the  $\delta$ PCA was performed by Tallman (2016) on the distal femur of hominids, in which she produced an ontogenetic PCA. In her investigation, Tallman (2016) computed ten equidistant shape means from a multivariate regression of shape on centroid size, and performed a PCA on those, whereas in our PCA we focus on the analysis of trajectories themselves, computed from multivariate regression of shape on dental eruption stage. While in principle any covariate (such as centroid size) may be used, we chose dental eruption stage as this has been demonstrated to be very effective in describing cranial shape changes over ontogeny, and as it incorporates homologous and size-independent developmental events to construct the trajectories (Simons and Frost, 2016). Additionally, when used in developmental simulations, ontogenetic trajectories constructed using dental eruption stage as the covariate produce highly accurate estimations of adult morphology, further supporting their reliability as estimators of shape changes associated with ontogeny (Simons and Frost, 2016). We therefore termed our analysis a  $\delta$ PCA to reflect these different approaches.

*3.2.2.4 Comparison of cranial trajectories.* Pairwise angles between each of the taxa were computed as the arccosine of their inner dot product, quantifying the magnitude of differences in pattern of shape change among trajectories (Collard and O'Higgins, 2001). Permutation tests were used to test for significant differences among trajectories, using the method of McNulty et al. (2006). This method performs pairwise tests from randomized groups of equal size and number of specimens in each dental stage, using individuals from both species in the comparison. A sequential Holm-Bonferroni correction, which is less conservative than a standard Bonferroni correction, was used to account for multiple comparisons (Quinn and Keough, 2002). To determine if the  $\delta$ PCA was adequately representing these differences in trajectory patterns, we performed a matrix correlation test (Dray and Dufour, 2007) on the matrices of the angles for all pairwise species comparisons and pairwise species comparisons of the Euclidean distance among all non-zero  $\delta$ PCs.

3.2.2.5 *Ontophylomorphospace*. In order to examine ontogenetic trajectories in a phylogenetic context, we used the rotation matrix from the  $\delta$ PCA to project a previously determined phylogeny onto the major axes of this developmental morphospace to produce an ‘ontophylomorphospace.’ The ontophylomorphospace is an augmentation of the phylomorphospace approach, which maps principal components of shape onto a phylogenetic tree, draws branches between taxa and estimates internal nodes, produces ancestral state reconstructions, and estimates changes in shape along any branch of the phylogeny (Rohlf, 2002; Sidlauskas, 2008; Klingenberg and Gidaszewski, 2010; Monteiro, 2013; Adams, 2014). Whereas the phylomorphospace approach has traditionally been used to analyze changes among adult forms over evolutionary time, we use it here to analyze changes in ontogenetic trajectories over evolutionary time. The ontophylomorphospace process treats a shape-change trajectory as a single character, though a complex, multidimensional one (Klingenberg and Gidaszewski, 2010). Multivariate trajectory shape change variables are then fit to a phylogeny such that relative warp values at the internal nodes of a phylogeny are estimated from morphometric tip data using squared-change parsimony, in which the sum of squared changes over all branches and all coordinates is minimized (Rohlf, 2002; Sidlauskas, 2008; Klingenberg and Gidaszewski, 2010). Ancestral node character reconstruction via squared-change parsimony has maximum posterior probability under a Brownian motion model of evolution, and has several statistical advantages, such as being invariant under rotation of the coordinate system (Maddison, 1991; Klingenberg and Gidaszewski, 2010). The trajectory changes estimated along each branch of a phylogeny equal the Euclidean distance between the nodes to the terminal taxa bracketing that branch, calculated along all morphospace axes using the Pythagorean theorem, and illustrates the direction and magnitude of morphological change estimated along each branch (Sidlauskas, 2008).

The patterns of morphology in this phylogenetic context can give insights into several aspects of morphological evolution, such as possible constraints on diversification (if there is a high lineage density in one or more groups), if there has been convergent/parallel evolution (if taxa come from widely separated parts of the morphospace and converge on another area), or if morphological evolution has occurred in a diversifying fashion (radiating from a central morphological point as exemplified by

ancestral reconstructions; Sidlauskas, 2008; Almécija et al., 2013; 2015; Sherratt et al., 2014; Adams, 2014). One can also visually assess phylogenetic signal in the data, as more closely related taxa would be expected to occupy similar areas of morphospace, though hypotheses of phylogenetic signal still need to be tested statistically (Klingenberg and Gidaszewski, 2010).

To produce the plot of the ontophylomorphospace, a consensus molecular phylogenetic tree was projected onto the major axes of trajectory shape variation, with branches connecting tree tips and interior nodes, which were estimated using squared-change parsimony (Rohlf, 2002; Sidlauskas, 2008; Strelin et al., 2018). The phylogenetic tree (Fig. 3.1) was downloaded from the open access website 10kTrees (Arnold et al., 2010), which uses molecular data from the NIH genetic sequence database GenBank to produce the tree. Molecular-based trees were used due to the near universal acceptance of their accuracy in regards to cercopithecines (Cronin and Sarich, 1976; Disotell et al., 1992; Perelman et al., 2011), and to avoid the *petitio principii* of drawing conclusions about morphological relationships in a phylogenetic context from morphologically based phylogenies.

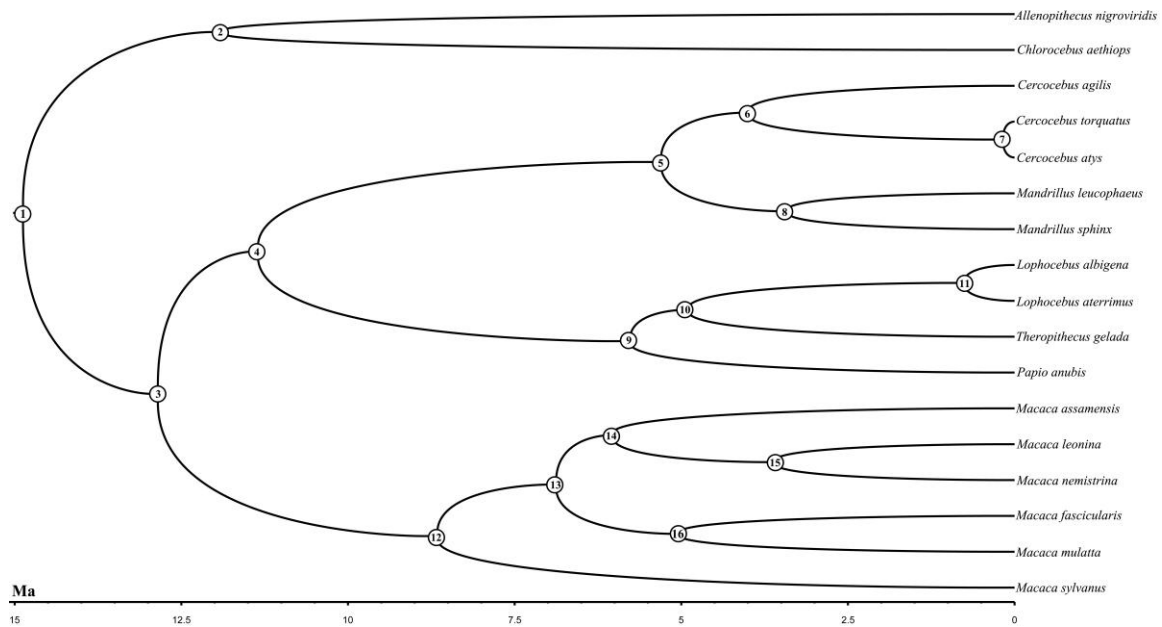


**Figure 3.1.** Molecular phylogenetic tree of the species in this investigation. Numbers show branching order. Scale bar shows branching dates in millions of years (Ma).

3.2.2.6 *Phylogenetic signal*. Phylogenetic signal refers to a situation in which there is a statistical non-independence between species' traits and phylogenetic relatedness (Klingenberg and Gidaszewski, 2010). When shape data are plotted onto a phylogeny, a strong phylogenetic signal is indicated when closely related species are closer to each other in morphometric space than more distantly related species (Adams, 2014). Thus, when a phylogenetic signal is present, the average amount of shape change (the sum of squared changes) along tree branches is relatively small for closely related species. To quantitatively test for phylogenetic signal in the high-dimensional, multivariate trait space of the ontogenetic trajectories used here, a multivariate extension of the Kappa statistic,  $K_{mult}$ , was calculated (Adams, 2014).  $K_{mult}$  is desirable in situations where trait dimensions exceed the number of species in the data set, as is the case in our investigation.  $K_{mult}$  provides an estimate of phylogenetic signal relative to what is expected under a Brownian motion model of evolution, and is numerically identical to standard K statistic estimates (Adams, 2014). Values of  $K_{mult} < 1.0$  suggest the data have less phylogenetic signal than expected under Brownian motion, while values of  $K_{mult} > 1.0$  suggest greater phylogenetic signal than expected. Significance values are obtained via permutation, whereby data at the tips of the phylogeny are randomized and the values of each randomization are then compared with observed tree values (Blomberg et al., 2003; Adams, 2014); 10,000 permutations were used, with  $\alpha = 0.05$ . Our null hypothesis was that there is no phylogenetic signal in the cranial ontogenetic trajectories of our sample.

Analyses for the ontophylomorphospace and for phylogenetic signal were performed in R (R Development Core Team, 2014), using routines in the library 'geomorph' (Adams et al., 2017).

**Table 3.2.** Angular differences and Euclidean distances. Below diagonal: angular differences (in degrees) between species developmental trajectories; no angles were significant after sequential Holm-Bonferroni adjustment for multiple comparisons. Above diagonal: Euclidean distance among the principal component scores from the dPCA.

	Ani	Cae	Cag	Cat	Cto	Lal	Lat	Mas	Mfa	Mnl	Mmu	Mne	Msy	Mle	Msp	Pha	Tge
Ani	—	0.014	0.010	0.014	0.020	0.011	0.013	0.014	0.023	0.023	0.025	0.019	0.016	0.025	0.017	0.020	0.019
Cae	23.01	—	0.015	0.015	0.027	0.016	0.014	0.024	0.029	0.031	0.033	0.027	0.021	0.033	0.017	0.029	0.024
Cag	17.74	24.82	—	0.014	0.02	0.011	0.012	0.017	0.024	0.025	0.027	0.019	0.016	0.026	0.017	0.022	0.02
Cat	19.25	21.01	17.61	—	0.018	0.016	0.011	0.019	0.024	0.023	0.026	0.022	0.015	0.025	0.018	0.023	0.024
Cto	21.33	33.21	<b>19.81</b>	<b>20.99</b>	—	0.022	0.019	0.018	0.024	0.017	0.022	0.018	0.015	0.018	0.025	0.015	0.024
Lal	18.22	25.83	17.59	14.69	<b>17.75</b>	—	0.014	0.017	0.028	0.026	0.029	0.019	0.019	0.028	0.018	0.023	0.023
Lat	20.67	21.76	18.31	13.73	21.49	16.81	—	0.018	0.024	0.024	0.027	0.019	0.015	0.025	0.016	0.022	0.021
Mas	19.73	35.22	23.51	26.22	21.19	21.06	25.77	—	0.017	0.015	0.018	0.017	0.017	0.021	0.021	0.016	0.022
Mfa	24.81	<b>34.48</b>	<b>25.85</b>	<b>29.06</b>	28.41	<b>28.14</b>	27.69	18.25	—	0.018	0.017	0.026	0.024	0.026	0.026	0.025	0.028
Mnl	29.11	41.08	28.22	30.11	20.13	27.12	28.22	24.27	30.75	—	0.015	0.020	0.021	0.019	0.027	0.017	0.028
Mmu	23.46	37.61	26.11	28.76	24.46	23.38	28.85	<b>15.33</b>	18.21	27.14	—	0.025	0.023	0.024	0.029	0.020	0.030
Mne	18.12	25.71	16.51	18.74	17.51	14.59	18.22	21.24	28.58	27.68	24.88	—	0.021	0.017	0.021	0.016	0.022
Msy	27.37	27.11	26.48	24.47	30.12	27.39	24.59	31.29	30.84	31.85	<b>32.51</b>	29.29	—	0.025	0.023	0.018	0.023
Mle	23.15	37.65	25.49	27.14	20.39	22.52	26.88	13.42	20.32	21.67	15.97	23.73	31.79	—	0.028	0.019	0.024
Msp	28.47	41.05	28.44	30.08	20.73	28.61	28.28	24.32	29.79	16.39	27.02	28.98	32.85	22.22	—	0.026	0.022
Pha	26.29	35.42	24.29	28.18	22.69	24.52	25.92	24.49	<b>32.22</b>	24.36	28.71	22.28	32.87	26.69	29.85	—	0.023
Tge	28.82	36.54	29.87	33.51	29.18	35.49	30.44	31.54	33.26	<b>32.07</b>	34.76	29.85	32.69	32.59	28.39	31.33	—

### 3.3 Results

**3.3.1  $\delta$ PCA.** In a matrix correlation test, the angular differences among species trajectories are significantly positively correlated with the pairwise species comparisons of the Euclidean distances among principal component scores from the  $\delta$ PCA (Mantel:  $r = 0.48$ ,  $p = 0.001$ ), indicating that the  $\delta$ PCA is a reliable way to visualize ontogenetic trajectories among many taxa simultaneously, while being less difficult than a comparison of many angles (Figure 3.2 and Table 3.2). None of the pairwise angular differences in ontogenetic vectors were statistically significant when the sequential Holm-Bonferroni correction for multiple comparisons was employed (Table 3.2). The first three principal components (63% total variance) of ontogenetic shape trajectories from the  $\delta$ PCA plot are presented in Figure 3.2. Presented in Figure 3.3 are visualizations illustrating relative magnitudes and directions of developmental shape changes in the cranium along each of the  $\delta$ PCA axes. For example, a visualization with a smaller neurocranium and larger rostrum indicates a greater magnitude of developmental shape change in the rostrum relative to the neurocranium. Note that the visualizations presented in Figure 3.3 do not represent actual or theoretical shapes, merely relative magnitudes of shape change when compared with other regions of the cranium.

Keeping in mind that interpretations of shape (or, in this case, trajectory) transformations along PCs should be approached with caution, examinations of the respective PC axis loadings indicate that more positive values on  $\delta$ PC1 reflect increased

magnitudes of relative rostral development, and widening of the cranial base compared to the rest of the cranium.  $\delta PC1$  separates *Chlorocebus* from other taxa, whose relative magnitudes of development in these cranial dimensions are lower. The positive end of  $\delta PC2$  reflects increased magnitudes of anterior rostral development relative to the rest of the cranium, and slight dorsal elevation of the anterior rostrum, for which *Mandrillus* is separated. The negative end of  $\delta PC2$  reflects an increased magnitude of neurocranial development relative to the rostrum. Of note on this axis are the relatively low scores of all species of *Macaca*.  $\delta PC3$  reflects relatively lengthening of neurocranium, with positive values on this axis showing an increased magnitude of lengthening. More positive values on  $\delta PC3$  are also related to increased dorsal elevation of the anterior rostrum. This  $\delta PC$  clearly distinguishes *Theropithecus*.  $\delta PC1$  and  $\delta PC2$  reveal a clear African cercopithecine trend, from which Asian *Macaca* deviates. *Macaca sylvanus* and *Allenopithecus*, both of which are considered morphologically primitive (Szalay and Delson, 1979; Strasser and Delson, 1987), group with the mangabeys (save *Cercocebus torquatus*), indicating these taxa may share an ancestral cranial ontogenetic pattern (but see Discussion).

Bivariate regression of each of the first three  $\delta PC$  eigenvectors on the logarithm of centroid size (the average adult  $\ln CS$  for each species was used as the independent variable) showed that both  $\delta PC1$  and  $\delta PC2$ , though not  $\delta PC3$ , were significantly correlated with size ( $\delta PC1$ :  $F_{1,15} = 7.33$ ,  $r^2 = 0.33$ ,  $p = 0.0162$ ;  $\delta PC2$ :  $F_{1,15} = 11.63$ ,  $r^2 = 0.44$ ,  $p = 0.004$ ;  $\delta PC3$ :  $F_{1,15} = 1.03$ ,  $r^2 = 0.06$ ,  $p = 0.33$ ). This indicates that the  $\delta PC1$  and  $\delta PC2$  axes of trajectory shape variation have an allometric scaling component (Bookstein, 1991; Monteiro, 1999; Mitteroecker et al., 2004; Klingenberg, 2016).

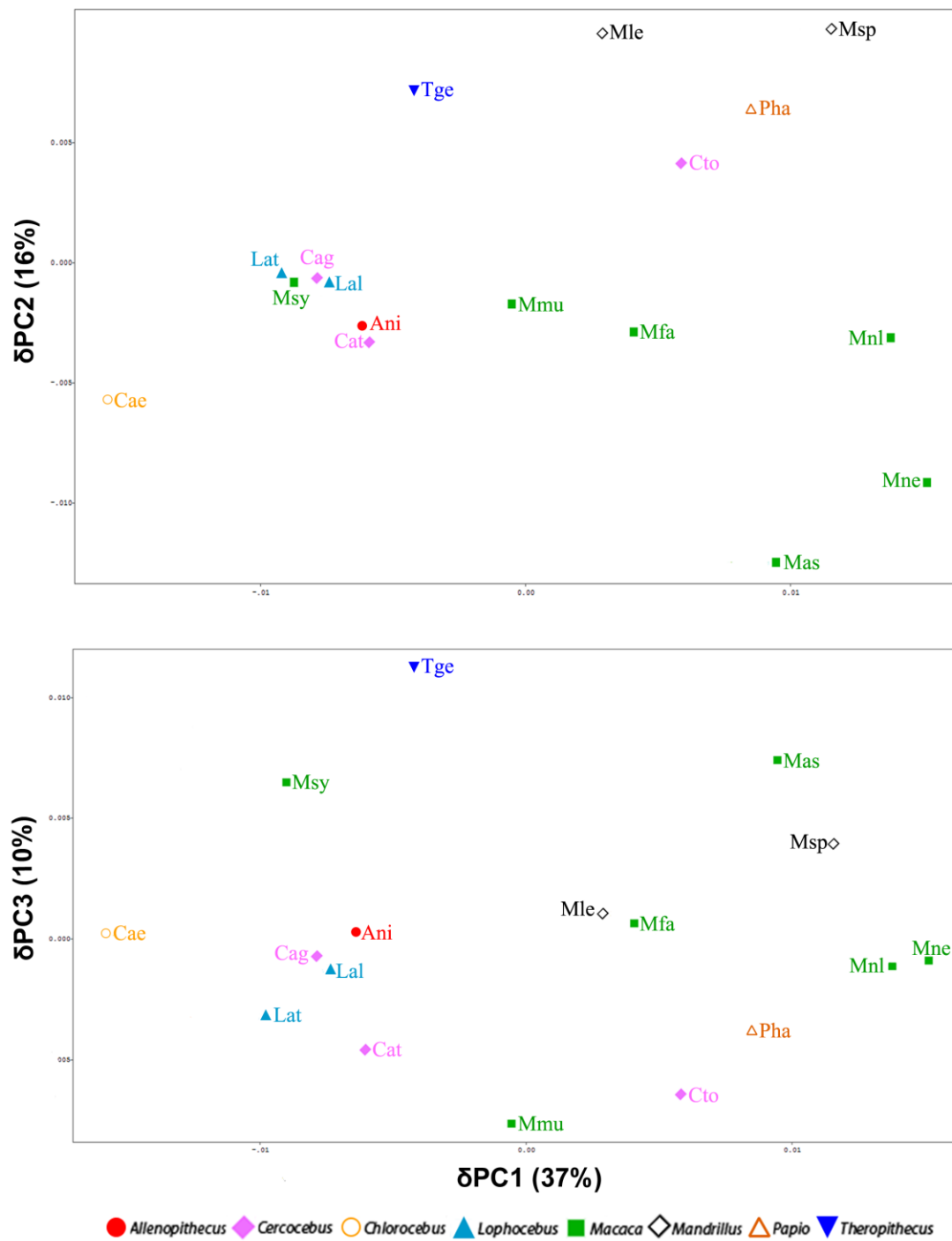


**Figure 3.2.** δPCA plot showing δPC1 (37% total variance) and δPC2 (16% total variance), and δPC1 and δPC3 (10% total variance). Abbreviations correspond to those in Table 3.1.



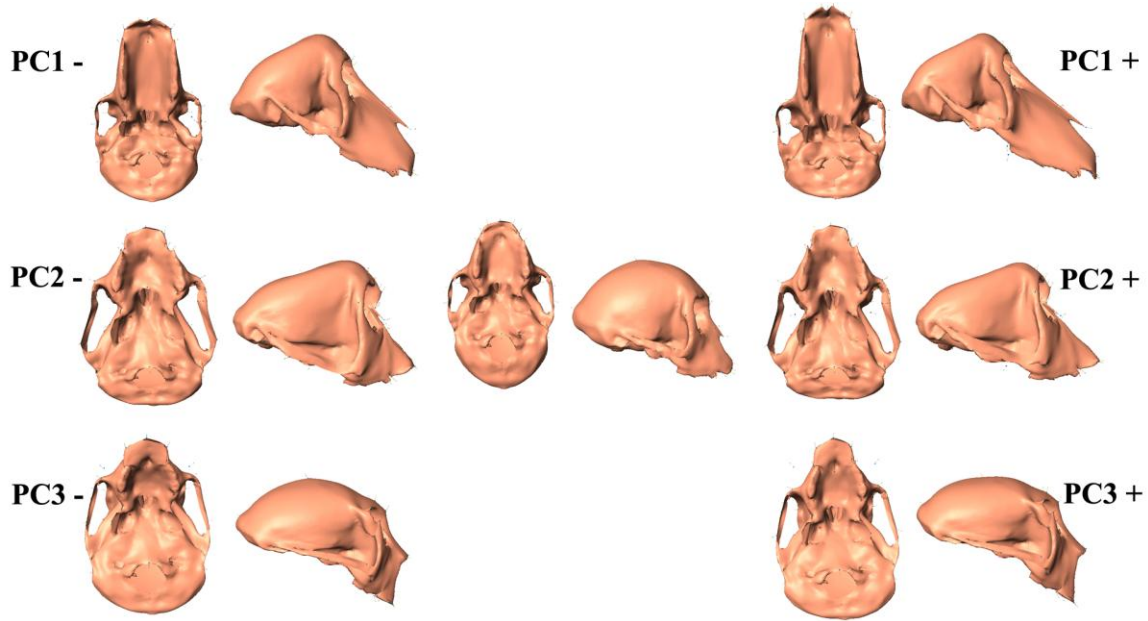


**Figure 3.3.** Visualizations of shape change magnitudes associated with  $\delta$ PC axes 1-3 (lateral and ventral views). Center cranial visualizations based on M1 stage *M. mulatta* specimen, warped to average M1 individual for whole sample. Left and right column cranial visualizations are same surface warped to simulated adult configuration produced by adding scaled trajectory from positive and negative ends of  $\delta$ PCA axes, and depict relative magnitudes of development in aspects of the cranium relative to others. For example, a larger rostrum and smaller neurocranium indicates an increased magnitude of rostral development relative to neurocranial development, and vice versa. Right column: positive end of  $\delta$ PC axis. Left column: negative end of  $\delta$ PC axis. Note that these visualizations do not represent actual or theoretical shapes, merely relative magnitudes of shape change of aspects of the skull when compared with other aspects of the skull. Additionally, warping is limited to the locations of our landmarks.

**3.3.2 Ontophylomorphospace.** A plot of the ontophylomorphospace (OPMS), representing the first two principal components axes of ontogenetic shape trajectory space, is presented in Figure 3.4. Branches connect the tips, which represent the positions of the observed trajectories of extant taxa, and internal nodes (numbered), which represent the positions of the reconstructions of ancestral trajectories using squared change parsimony.

The estimated ancestral cercopithecine cranial ontogenetic pattern (Fig. 3.4, Node 1), as reconstructed here, had similar magnitudes of relative rostral and neurocranial development (the morphologically distinguishing factors reflected by these axes, see above). The estimated ancestral papionin ontogenetic pattern (Node 3) lies near the center of the OPMS plot, indicating that ancestral papionin crania also had similar relative magnitudes of both rostral and cranial base development. It is similar to the ancestral

cercopithecine pattern, and among extant species is most similar to *Macaca mulatta*. Relative to the rest of the cranium, the reconstructed ancestral macaque pattern (Node 12) shows an increased magnitude of rostral and cranial base development than both the ancestral cercopithecine and papionin pattern (more positive value on OPMS1). The estimated ancestral trajectory for both *Mandrillus/Cercocebus* (Node 5) and *Papio/Lophocebus/Theropithecus* (Node 9) clades are similar to each other, and differ from ancestral cercopithecines, papionins, and macaques, by having relatively increased magnitudes of rostral development coupled with decreased magnitudes of neurocranial development.

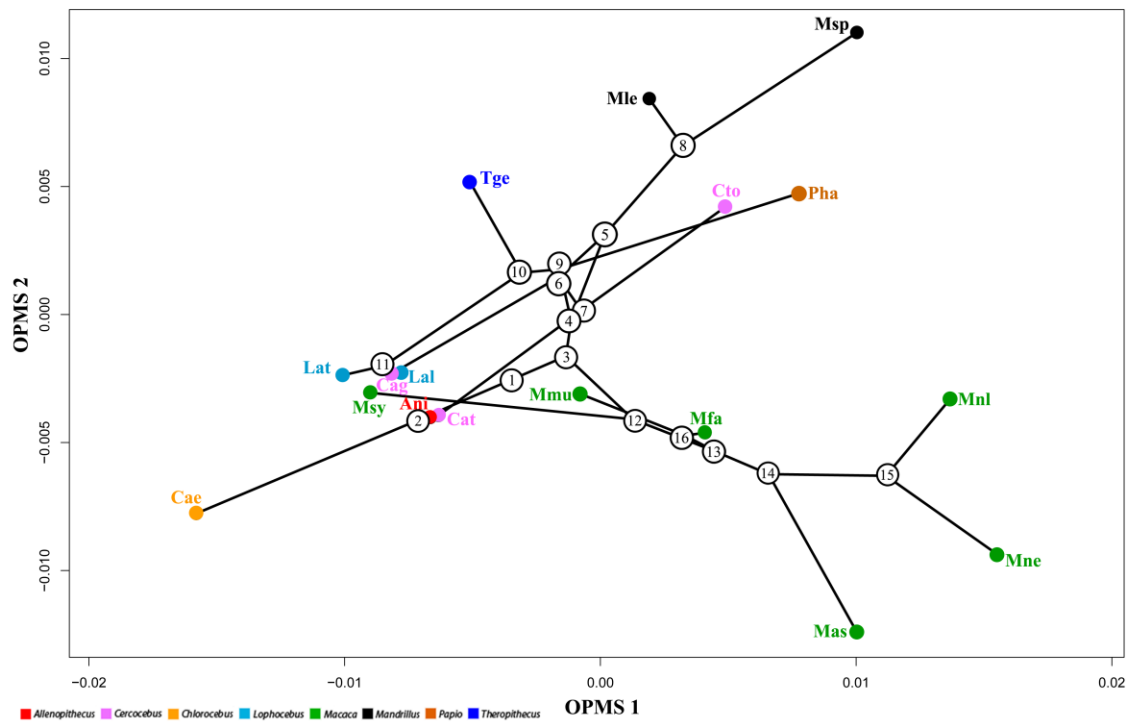


**Figure 3.4.** Ontophylomorphospace of cranial ontogenetic trajectories. The molecular phylogeny (Fig. 3.1) is projected onto the first two principal axes of trajectory morphospace of extant taxa and internal nodes, which were estimated using squared-change parsimony. Abbreviations correspond to those in Table 3.1. Numbers correspond to nodes in Figure 3.1. Colors correspond to those in Figure 3.2. Note the crossing of the branches of the African papionins (indicating parallel evolution of trajectories), and the diversification of trajectories of Asian Macaca (indicating derived trajectories relative to other cercopithecines).

Of the non-papionin cercopithecines in this analysis, *Allenopithecus*, shows the least amount of change from the estimated last common ancestor (LCA) of these species

(Node 2). *Chlorocebus* is comparatively derived, and occupies a distinct trajectory space compared to the other taxa.

Branches for *Macaca* largely emanate outward from their common ancestor with little overlap, indicating a diversification of cranial ontogenetic trajectories, which are derived relative to other cercopithecines. However, when compared with other species of *Macaca*, the branch of *M. sylvanus*, considered plesiomorphic among extant macaques (Szalay and Delson, 1979), occupies an area of trajectory morphospace most similar to *Lophocebus* and *Cercocebus agilis*, indicating a convergence of trajectories, rather than each of these species retaining an ancestral ontogenetic trajectory. In fact, *M. sylvanus*, while possessing a primitive cranial morphology, and a cranial ontogenetic trajectory that is similar to *Lophocebus* and *Cercocebus agilis*, is rather derived in its ontogenetic trajectory, as indicated by the branch length emanating from Node 12. Within *Macaca*, *M. mulatta* has a cranial ontogenetic trajectory most similar to the reconstructed ancestral trajectory of all papionins (Node 3). *Macaca fascicularis* possesses a cranial ontogenetic trajectory similar to the reconstructed trajectory of Asian macaques (Node 13). This, coupled with a relatively short branch length, indicates that *M. fascicularis* retains a similar cranial ontogenetic trajectory as the common ancestor of Asian macaques.

The frequent crossing of the branches among African papionins indicates that there has been extensive parallel evolution of cranial ontogenetic trajectories in this clade, as species that are not closely related share relatively similar ontogenetic trajectories. The most derived cranial ontogenetic trajectories of the African papionins (i.e., those with the longest branch lengths and positioned further from the main grouping in the ontophylomorphospace) are: *Mandrillus leucophaeus*, *Mandrillus sphinx*, *Papio anubis*, and *Cercocebus torquatus*. The trajectories of these species radiate in the same direction, indicating that their trajectories are similar even though they are not ancestrally shared. *Mandrillus leucophaeus* has a less derived ontogenetic trajectory than *Mandrillus sphinx* compared to the *Mandrillus* LCA (Node 8). One notable deviation from these African papionins is the ontogenetically distinct *Theropithecus gelada*. It lies apart from all other cercopithecines in trajectory space and does not converge on any other cercopithecine trajectory, despite being only moderately derived relative to its estimated LCA (i.e., the branch is of moderate length, Node 10).

Both species of *Lophocebus* have short branch lengths from their reconstructed common ancestor (Node 11), indicating a limited amount of evolutionary change in their ontogenetic trajectories. *Lophocebus* and *Cercocebus* (save *Cercocebus torquatus*) occupy similar areas of ontogenetic trajectory space, and *Cercocebus* has long overlapping branches, indicating parallel evolution of *Cercocebus* ontogenetic trajectories. In the phylogeny used in this investigation (Fig. 3.1), *Cercocebus torquatus* and *Cercocebus atys* are more closely related than either is to *Cercocebus agilis*, but *Cercocebus atys* and *Cercocebus agilis* trajectories have converged, and are most similar to the trajectory of *Lophocebus*. *Cercocebus atys* has a cranial ontogenetic trajectory that is highly similar to *Allenopithecus*. With *Allenopithecus* and *M. mulatta*, it lies near the reconstructed ancestral trajectory of all cercopithecines (Node 1). As noted above, *Cercocebus torquatus* has an ontogenetic trajectory most similar to that of *Papio* and *Mandrillus*.

3.3.3 *Phylogenetic signal*. Tests failed to reject the null hypothesis of no phylogenetic signal ( $p$ -value = 0.1339) and yielded a  $K_{mult}$  of  $<1.0$  ( $K_{mult} = 0.21863$ ) indicating that cranial ontogenetic trajectories lack strong phylogenetic signal in cercopithecines.

### 3.4 Discussion

3.4.1 *Extant ontogenetic trajectories*. The principal components axes from the  $\delta$ PCA are able to illustrate cranial shape changes associated with ontogeny in a visually intuitive manner. Additionally, aspects of developmental trajectories that would otherwise be difficult to interpret become apparent in a  $\delta$ PCA plot. For example, the distinctiveness of the Asian macaque trajectories, when contrasted with other cercopithecines, is clear for the first two  $\delta$ PCA axes (Fig. 3.2). Moreover, the  $\delta$ PCA allows for a visualization of ontogenetic shape trends in the cranium by warping an  $M^1$ -stage individual to the adult shapes implied along major axes of trajectory shape variation (Fig. 3.3). The conjunction of these two forms of visualization allows for an evaluation of the similarities and differences of ontogenetic trajectories, and the influence of these trajectories on adult morphologies.

Previous investigations of papionins have noted that generic, and even specific cranial morphologies are present in M<sup>1</sup>-stage juveniles (Collard and O'Higgins, 2001; Singleton, 2009; Gilbert et al., 2011; Singleton, 2012). Our results indicate that species-typical post-M<sup>1</sup> developmental patterns augment this initial distinctiveness through differential developmental magnitudes, and lead to the identifiable cranial features associated with adult taxa. For example, the  $\delta$ PCA illustrates relatively increased magnitudes of rostral development in *Mandrillus*, the adults of which are characterized, in part, by pronounced rostral development, in conjunction with the pronounced development of paranasal ridges (McGraw and Fleagle, 2006). This indicates that, for this aspect of its cranial morphology, *Mandrillus* at least partially achieves this phenotypic trait through an increased developmental magnitude in this feature relative to other aspects of the cranium. The more positive values on  $\delta$ PC3, which are related to increased dorsal elevation of the anterior rostrum, clearly distinguish *T. gelada*, whose adult anterior rostral morphology has been noted as relatively elevated when compared with other papionins (Delson and Dean, 1993). Thus, in addition to providing a visually intuitive representation of ontogenetic trajectories (in comparison to a matrix of pairwise angles), the  $\delta$ PCA also provides a means for determining the contributions of post-natal ontogeny in attaining adult morphologies.

As noted above, both  $\delta$ PC1 and  $\delta$ PC2 are significantly correlated with cranial size. In Figure 3.2, there is a clear African papionin size trend in the first two  $\delta$ PCs, with smaller species having relatively lower values for both  $\delta$ PC1 and  $\delta$ PC2. Interestingly, Asian macaques deviate from this trend, indicating that their trajectories are not as highly correlated with size as other cercopithecines. Compared to African papionins, their trajectories show an increased developmental magnitude of cranial base width relative to the rest of the cranium coupled with increased development of the neurocranium relative to the rostrum, leading to generally broader neurocrania, and less elongated faces. This corroborates previously identified divergences in cranial growth allometries between macaques and African papionins (Ravosa and Profant, 2000).

The lack of significant differences in pairwise vector angle comparisons is most likely related to the fact that there were 136 comparisons, so that with the sequential Holm-Bonferroni adjustment the threshold for significance is 0.0004. Nonetheless, the *p*-

values are strongly related to sample size. For example, *Macaca fascicularis* has the most robust sample size, and the most  $p$ -values less than 0.05 (see Table 1). This suggests that larger samples across developmental stages in more taxa would likely lead to more significantly different pairwise angles. This relationship between significance and sample size was also encountered by Singleton et al. (2010). On the other hand, our total sample size of 522 specimens from 17 species is relatively robust, even if individual developmental stages within particular taxa are smaller than ideal. Therefore, while individual pairwise trajectory differences may not be significant, overall patterns of variation among trajectories can still be evaluated.

The significant positive correlation between pairwise vector angles and pairwise Euclidean distances among  $\delta$ PCs demonstrated that species with more obtuse vector angles are often further from each other in  $\delta$ PCA space, and thus the  $\delta$ PCA provides an accurate representation of vector similarities and differences (though some information is being lost in the ordination, see subsection 3.4.4 about limitations below). For example, the two most distinct taxa in terms of angular difference were *Chlorocebus aethiops*, who showed the largest angular differences with other taxa, and *Theropithecus gelada*, who showed the next largest (Table 3.2). While none of the angles among taxa were significantly different, these two species are in unique trajectory spaces relative to other taxa in the  $\delta$ PCA (Fig. 3.2). Therefore, this method is a useful way to explore overall patterns of trajectory variation in the dataset, even in cases where pairs of vector comparisons are statistically indistinguishable. Once these patterns of ontogenetic trajectory variation have been evaluated, targeted hypotheses can be developed to test specific aspects of the observed patterns.

**3.4.2. Estimated ancestral trajectories.** The ontophylomorphospace is a useful method for comparing ontogenetic trajectories in a phylogenetic context. Some conclusions that could be drawn from the  $\delta$ PCA may in fact be misleading when phylogeny is not considered. For example, the close positions of *M. sylvanus*, *Chlorocebus*, and *Allenopithecus* in trajectory space shown by  $\delta$ PC1 and  $\delta$ PC2 (Fig. 3.2), suggests that they share an ancestral trajectory. The ontophylomorphospace (Fig. 3.4), however, indicates

that this is too simplistic, and that these species have likely converged on their similar ontogenetic trajectories.

Similarly, the branches of the African papionins cross each other to occupy similar areas of the ontophylomorphospace, indicating homoplasy in cranial ontogenetic trajectories. This result is not unexpected, as extensive homoplasy has also been noted in the adult cranial morphology of this clade (Disotell et al., 1992; Fleagle and McGraw, 1999; Singleton, 2005; McGraw and Fleagle, 2006; Gilbert, 2007; Perelman et al., 2011; Gilbert, 2013). Thus, *Papio* and *Mandrillus*, as well as *Lophocebus* and *Cercocebus*, were observed to be more similar in their ontogenetic trajectories than expected given their actual phylogenetic relationships. One notable exception to this is *Cercocebus torquatus*, which has an ontogenetic trajectory more like those of *Papio* and *Mandrillus* than the other mangabeys. This result is concordant with previous ontogenetic and morphological studies of *Cercocebus torquatus*. For example, Singleton et al. (2010) found that developmental simulations using the developmental trajectory of *Cercocebus torquatus* resulted in relatively prognathic simulated adults that also had relatively shallow suborbital fossae and moderately inflated maxillary ridges. These findings indicate that the ontogenetic trajectory of *Cercocebus torquatus* would be expected to be more similar to the other papionins which also share these traits (as *Papio* and, especially *Mandrillus*, do). McGraw and Fleagle (2006) also noted several aspects of adult craniofacial morphology of *Cercocebus torquatus* that are similar to those of *Mandrillus*, and likely to be reflected in their developmental trajectories.

Due to the paucity of the paleontological record, it is extremely difficult to quantify the cranial ontogenetic trajectories of extinct species, as this requires an ontogenetic series of nearly complete crania with well-defined taxonomic attributions. The lack of these ancestral ontogenetic trajectories also preclude investigations of heterochrony in primates, as these investigations rely on the ability to determine if there have been changes in ontogenetic shape trajectories among ancestors and descendants. Because these data are inherently rare, most investigations of heterochrony in primates have focused on comparing the ontogenetic trajectories of extant taxa (Shea, 1981, 1983, 1985; Leigh et al., 2003; Mitteroecker et al., 2004, 2005; Leigh, 2007; Lieberman et al., 2007), rather than among ancestors and descendants, even if these could be reasonably

identified in the fossil record. Therefore, until more complete datasets are acquired, a method for estimating ancestral trajectories is required for investigations of heterochrony to be carried out. While a thorough discussion of heterochrony in the cercopithecine cranium is beyond the scope of this investigation, the ontophylomorphospace procedure allows for the estimation of ancestral ontogenetic trajectories, and is thus a step toward comparisons of ancestor/descendant ontogenetic relationships. Additionally, the reconstructed nodes of ancestral shape change trajectories could be used in developmental simulations of juvenile fossils to better predict adult shapes (as opposed to using trajectories computed from extant taxa; e.g., see McNulty et al., 2006).

*3.4.3 Phylogenetic signal.* While the historically recognized putative parallelisms between ontogeny and phylogeny have rightly fallen into disrepute (in the strict sense of ontogeny recapitulating phylogeny, Gould (1977)), it has long been thought that ontogenetic information could be used to infer phylogenetic relationships, at least in terms of providing information about character polarity which could then be used to bolster phylogenies constructed using other methods (Nelson, 1978; Kluge, 1985; Yoder, 1992; Meier, 1997; for counterarguments, see Mabee, 2000). The majority of these investigations focused on analyzing ontogenetic sequences, rather than phenotypic trajectories in shape space. However, some have argued that ontogenetic trajectories of shape change (i.e., not just the sequence of character ontogeny) may provide insights into phylogeny (Fink and Zelditch, 1995; Zelditch et al., 1995; but see Adams and Rosenberg, 1998; Rohlf, 1998).

Our results indicate that cranial ontogenetic trajectories themselves do not have a strong phylogenetic signal. This is not to say that adult cranial shape does not have a phylogenetic signal, which was not tested here (see Lockwood et al., 2004; Cardini and Elton, 2008; Gilbert, 2011). Thus, using ontogenetic shape trajectories as a character in phylogenetic analyses is ill-advised. Additionally, the large amount of homoplasy observed in the cranial ontogenetic trajectories of the cercopithecines in our investigation, especially in the African papionins, severely complicates using ontogenetic trajectories to infer phylogenetic relationships among these primates. Still, it may be the case that ontogenetic trajectories contain phylogenetic information, but cercopithecines (especially



African papionins), due to their pervasive homoplasy, are not the best taxon with which to investigate this hypothesis.

The lack of a phylogenetic signal could be due to several factors. One possibility is that the lack of signal is due to only analyzing post-M1 ontogeny. Given that distinctive morphologies are present by M1 eruption (Collard and O'Higgins, 2001; Singleton, 2009, 2012; Gilbert et al., 2011), more phylogenetic signal may be found in pre-M1 individuals. As it has been argued that partitioning the cranium into modules provides more reliable phylogenetic information (Lockwood et al., 2004; Cardini and Elton, 2008; Gilbert, 2011), it is possible that analyzing the ontogenetic trajectories of the entire cranium will not capture a phylogenetic signal, but the trajectory of, e.g., the basicranium alone would. It may also be the case that ontogeny is not an independent 'trait' that can be used in phylogenetic analysis. Alternatively, ontogenetic trajectories may be too dynamic to provide a reliable estimate of phylogeny, as factors of phenotypic plasticity, such as biomechanical forces, can work to shape the cranium in ways not directly connected to a genetic lineage. Additionally, in this investigation, phylogenetic signal was tested against the expectations of Brownian motion, but there are multiple processes which may produce a pattern of phylogenetic signal (Revell et al., 2008; Adams, 2014), that were not tested here. Finally, as noted by Rohlf (1999, 2002), there is no reason to expect tangent space coordinates to correspond to taxonomically or biologically meaningful variables, as the coordinates are defined a priori. Thus, the difficulties encountered when attempting to infer the correct phylogenetic tree from morphometric data are also likely to be found in the trajectories of shape change derived from them.

*3.4.4 Limitations.* While the  $\delta$ PCA method allows for a comparison of ontogenetic trajectories in a visually appealing manner, there are some limitations to this approach that are similar to those encountered when performing a standard PCA. For example, the reduction of an ontogenetic trajectory to a single point overlooks nuances that are likely present in the data, e.g., if the amount of shape variation associated with ontogenetic development differs among taxa. In such a case, a method which allows for a direct comparison of how well shape variation correlates with development would be useful

(Tallman, 2016). Additionally, the results of our matrix correlation test between pairwise trajectory angles and the Euclidean distances among principal component scores from the  $\delta$ PCA returned a moderate  $r$ -value. While statistically significant, this result indicates that there is variation present in the trajectories that is not explained by the Euclidean space of the  $\delta$ PCA, further illustrating that caution should be used when reducing a complex, multivariate trait (i.e. ontogenetic shape change trajectories) to a single point. Despite these limitations, we feel that the  $\delta$ PCA is still a useful way to compare ontogenetic trajectories of diverse taxa in a visually intuitive manner.

### 3.5 Conclusion

Biological form is a complex, multivariate trait, whose complexity is only compounded when analyzed over ontogenetic and evolutionary time. The relatively recent advent of advanced geometric morphometric methodologies has allowed for innovative investigations into the relationship between ontogeny and morphology, and how these should be interpreted in an evolutionary framework. In this investigation, we used these geometric morphometric methods to estimate cranial ontogenetic trajectories and from these produced a developmental shape change trajectory PCA ( $\delta$ PCA), which provides an ordination and visual representation that reliably facilitates comparison of ontogenetic trajectories among taxa. We next used the rotation matrix from the  $\delta$ PCA to project a phylogeny onto the major axes of this developmental morphospace to produce an ‘ontophylomorphospace’ in order to examine cranial ontogeny in a phylogenetic context. We found that, similar to results of previous investigations of adult craniofacial morphology, there has been extensive homoplasy in the evolution of cranial ontogenetic trajectories, especially in the African papionins. Additionally, our results indicate a diversification of cranial ontogenetic trajectories for Asian species of *Macaca* that are derived relative to other cercopithecines. Finally, we found that there is no phylogenetic signal in the cranial ontogenetic trajectories of cercopithecines. While there are several possible explanations, the extensive amount of homoplasy in these primates may be responsible for this result.

This chapter focused on developing methods for the comparison of the ontogenetic trajectories of extant taxa, and for estimating ancestral patterns of

ontogenetic development. One of the findings of this investigation was a clear allometric component in the the ontogenetic trajectories of African papionins. As size is an integral aspect of cranial shape production, the following chapter will more thoroughly explore the role of size and allometry in the evolution of primate cranial morphology.

Specifically, the investigations will test several long-standing hypotheses regarding the presence of ontogenetic scaling among catarrhine taxa, and will evaluate the likelihood of size as a line of evolutionary least resistance in the evolution of primate cranial shape.

## CHAPTER IV

### ONTOGENETIC ALLOMETRY AND SCALING IN CATARRHINE CRANIA

#### 4.1 Introduction

Size is highly influential in the physiological, physical, behavioral, and ecological aspects of organisms, and allometry, the relationship between size and shape, has been invoked to explain patterns of morphological evolution in a broad array of taxa (Thompson, 1917; Huxley, 1932; Gould, 1966, 1971; Schmidt-Nielsen, 1984; Jungers, 1985; Shea, 1985, 1995; Klingenberg, 1998, 2010, 2016; Gerber et al., 2008; Cardini and Polly, 2013). Allometry has also been considered an evolutionary constraint, whereby evolutionary changes in shape are driven by the necessity to maintain functional roles despite variations in size (Frankino et al., 2005; Klingenberg, 2010). Researchers have differentiated between three levels of allometric inquiry: static allometry, which compares size-shape covariation among individuals within a population at a particular ontogenetic stage; evolutionary allometry, which compares size-shape covariation among ancestors and descendants; and ontogenetic allometry, where size-shape covariation is examined over the course of growth and development (Cock, 1966; Cheverud, 1982; Klingenberg, 1998).

Several previous investigations of ontogenetic allometry have posited that many aspects of shape evolution can be attributed to ontogenetic scaling (*sensu* Gould, 1966; Shea, 1985; 1995), which occurs when comparisons of allometric trajectories reveal that closely related taxa differ by either extension or truncation of a common ontogenetic allometry, i.e., there is a difference merely in the length, but not in the direction of their trajectories (see also Klingenberg, 1998). When this is the case, differences between juvenile and adult individuals within a species will resemble each other in a similar manner as smaller and larger adults (Shea, 1985). Many investigations have invoked ontogenetic scaling to explain some or all of observed shape differences between closely related species who vary in size (Freedman, 1962; Pilbeam and Gould, 1974; Jungers and Fleagle, 1980; Shea, 1981, 1983a,b, 1985, 1995; McKinney, 1986; Atchley and Hall, 1991; Ravosa et al., 1993). However, many of these investigations were performed on

broad morphological patterns (e.g., cranial length vs. cranial width), and relied on bivariate comparisons of ontogenetic trajectories.

As vertebrate cranial shape, and its ontogenetic trajectories of shape change are multidimensional, it is important to evaluate if ontogenetic scaling is a common pattern in the evolution of catarrhine cranial shape using the advanced methods of multidimensional shape analysis such as geometric morphometrics, or, GM (Rohlf and Marcus, 1993; Adams et al., 2004). Several investigations have used GM to compare multidimensional ontogenetic trajectories, but these have led to discrepant conclusions regarding the presence of ontogenetic scaling in catarrhine crania. For example, some investigations have found that intertaxon adult cranial morphological variation results from sharing a common allometric trajectory, but that morphological differences arise from extensions or truncations of that trajectory (Marroig and Cheverud, 2001, 2005; Leigh et al., 2003; Leigh, 2006, 2007; Gonzalez et al., 2011). Other studies, often investigating the same taxa, have found that divergent ontogenetic trajectories are largely responsible for observed morphological differences among adults, and that bigger species aren't merely 'scaled up' versions of smaller ones (Collard and O'Higgins, 2001; Cobb and O'Higgins, 2004; Mitteroecker et al., 2004, 2005; Schaefer et al., 2004; Perez et al., 2011). These differences are in addition to cranial shape differences already observed in the youngest measured specimens. One possible cause of these discrepancies could be that some studies used limited dimensions of the shape space (e.g. the subspace defined by PC1 and PC2) to summarize trajectories rather than the whole of shape space (Cobb and O'Higgins, 2004; Mitteroecker et al., 2004a, 2005; Schaefer et al., 2004). PCs may be misleading in such comparisons because they do not indicate whether trajectories are similar in all of shape space, and may include shape differences unrelated to ontogeny (Mitteroecker et al., 2004; Baab et al., 2012). These discrepancies highlight the need to thoroughly evaluate the role of ontogenetic scaling in studies of catarrhine cranial evolution using GM methods that don't rely on data reduction techniques.

Evidence that adult morphological variation is produced via ontogenetic scaling would support the hypothesis that changes in shape are linked to selection for body size differences rather than differences in shape per se (Gould, 1966, 1975; Shea, 1985; Ravosa, 1991, 1992; Ravosa et al., 1993; Ravosa and Profant, 2000). Alternatively, if

taxa show divergent allometric patterns, i.e., if there are significant differences in the direction of allometric trajectories, then it is possible that there has been selection on shape itself rather than on size *qua* size (Ravosa and Profant, 2000). The comparison of ontogenetic trajectories in this way has been termed a 'criterion of subtraction,' and has been argued to be a fruitful way of elucidating possible selective forces operating over evolutionary time. That is, one can evaluate whether observed shapes are likely the product of selection for those shapes, or if they are the product of differential end points on a shared ontogenetic trajectory (Gould, 1966, 1975; Shea, 1985, 1995; Ravosa and Vinyard, 2002). It is important to note that the criterion of subtraction is one line of evidence for the presence of selection, but alternative evolutionary forces such as genetic drift, epigenesis, and phenotypic plasticity may also be possible explanations for evolutionary shape changes that are not merely the product of size changes. Extending this to an evolutionary timescale, some have suggested that size is possibly a 'line of least evolutionary resistance' (Marroig and Cheverud, 2005, 2010; Ungar and Hlusko, 2016), and that size changes may be a first step in adaptation and diversification, with size responding more quickly than shape to environmental change (Elton et al., 2010). Thus, finding that the morphologies of closely related taxa are the product of differential end points on a shared ontogenetic trajectory (i.e. ontogenetic scaling) among closely related taxa would indicate that size was a strongly influential evolutionary pressure on cranial shape, and would provide support for, or at least be consistent with, the hypothesis of size as a path of least evolutionary resistance.

To address these issues, this investigation uses a large, taxonomically diverse, ontogenetic sample and geometric morphometric methods to examine ontogenetic allometry among catarrhines. It therefore focuses on differences in cranial shape between closely related species of differing sizes to determine if they are consistent with the predictions of ontogenetic scaling, thereby also testing the hypothesis of size as a line of least evolutionary resistance in catarrhine cranial evolution. Analyses were performed on two aspects of cranial postnatal ontogeny: 1) trajectories of shape change associated with size (allometric trajectories), and 2) trajectories of shape change associated with dental eruption stage. While these trajectories frequently track similar aspects of shape change associated with ontogeny (organisms often get larger as they develop), using molar

eruption stage as a covariate to construct ontogenetic trajectories can in some cases provide more information about shape transformations than size alone, especially in samples with large amounts of size variation (Gunz and Bulygina, 2012). We therefore used both of these covariates in a multivariate, comparative approach to gain a more thorough understanding of how common ontogenetic scaling is in catarrhines, and if there are factors other than size that are driving cranial morphological evolution in this evolutionary radiation.

## 4.2 Materials and Methods

4.2.1.1 *Sample*. The dataset is composed of an ontogenetic series of 1,503 crania from 31 catarrhine species partitioned by dental eruption stage: M0: deciduous dentition with first molar not in occlusion; M1: first molar erupted to full occlusion, second is not; M2: second molar erupted to full occlusion, third is not; M3: fully erupted adult dentition (Table 4.1). Due to the scarcity of subadult specimens available in museum collections for some species, and the need to obtain reasonable sample sizes, mixed-sex samples were used to construct each species' ontogenetic trajectory. The use of mixed-sex samples to construct ontogenetic trajectories is justified by previous investigations which found that male and female ontogenetic trajectories do not typically diverge until late in ontogeny, and that mean juvenile cranial shapes between sexes are indistinguishable (O'Higgins and Jones, 1998; Collard and O'Higgins, 2001; O'Higgins and Collard, 2002; Leigh, 2006; Singleton et al., 2010; Simons and Frost, 2016).

Each of the species in our sample was partitioned into four subclades: Colobinae (6 species), Cercopithecini (5 species), Papionini (13 species), and Hominoidea (7 species) (see Table 18), and statistical analyses were performed separately for each subclade. This sample was selected so that multiple genera would be represented in each subclade, and to reflect the major phyletic transitions in catarrhine evolutionary history. This partitioning allowed us to compare closely related taxa and not, e.g., *Miopithecus talapoin* and *Gorilla gorilla*, which have never been posited to be scaled variants of each other.

4.2.1.2 *Data collection.* Forty-three three dimensional landmarks were collected using a Microscribe 3DX digitizer (Immersion Corp., San Jose, CA). These landmarks are based on the 45 landmark protocol of Frost et al. (2003), however, landmarks 36 and 42 of the original protocol were not collected in this sample, leaving a total of 43 landmarks (see Figure 2.1).

**Table 4.1.** Study sample by dental stage, as defined by full eruption of nominal tooth. Both sexes are included in the calculation of trajectories.

	dP <sup>4</sup>	M <sup>1</sup>	M <sup>2</sup>	M <sup>3</sup>	Total
<i>Allenopithecus nigroviridis</i>	2	8	11	19	40
<i>Chlorocebus aethiops</i>	12	11	14	13	50
<i>Cercocebus agilis</i>	7	11	12	13	43
<i>Cercocebus atys</i>	3	13	15	16	47
<i>Cercocebus torquatus</i>	2	7	8	21	38
<i>Cercopithecus lhoesti</i>	5	10	12	14	41
<i>Cercopithecus mitis</i>	10	10	14	12	46
<i>Colobus guereza</i>	13	15	12	20	60
<i>Gorilla gorilla</i>	14	14	15	16	59
<i>Homo sapiens</i>	15	21	28	42	106
<i>Hylobates lar</i>	13	15	16	22	66
<i>Lophocebus albigena</i>	5	13	16	20	54
<i>Lophocebus aterrimus</i>	6	10	14	21	51
<i>Macaca fascicularis</i>	13	12	12	14	51
<i>Macaca mulatta</i>	11	11	12	15	49
<i>Macaca sylvanus</i>	1	1	4	14	20
<i>Mandrillus sphinx</i>	5	8	9	18	40
<i>Miopithecus talapoin</i>	10	10	11	19	50
<i>Nasalis larvatus</i>	8	10	13	20	51
<i>Pan paniscus</i>	15	16	12	20	63
<i>Pan troglodytes</i>	17	17	16	26	76
<i>Papio hamadryas anubis</i>	14	14	16	16	60
<i>Papio hamadryas cynocephalus</i>	3	18	19	14	54
<i>Papio hamadryas ursinus</i>	3	5	7	15	30
<i>Piliocolobus badius</i>	4	12	15	14	45
<i>Pongo pygmaeus</i>	10	13	9	22	54
<i>Procolobus verus</i>	1	7	13	16	37
<i>Pygathrix nemaeus</i>	2	2	2	12	18
<i>Semnopithecus entellus</i>	1	5	4	16	26
<i>Symphalangus syndactylus</i>	7	6	10	22	45
<i>Theropithecus gelada</i>	4	3	10	16	33
					1,503

#### 4.2.2 Analytical Methods



All statistical analyses were performed in the R (R Core Team, 2017) package *geomorph* (Adams et al., 2017).

A generalized Procrustes analysis was performed separately on each of the four subclades to remove the effects of scale, orientation, and location of the landmark coordinates (Bookstein, 1991; Marcus and Corti, 1996; Rohlf, 1999). All subsequent analyses were performed on these Procrustes aligned shape coordinates.

**4.2.2.1 Allometric trajectories.** A Homogeneity of Slopes (HOS) test was performed to determine if allometric trajectories varied among species within each of the four clades in the sample. An HOS test determines if species share a common allometry by comparing shape covariation with size (the natural logarithm of centroid size was used in all analyses) and calculates if there is a significant interaction term between LnCS and species (Adams et al., 2017). If the interaction term is significant, the null hypothesis is rejected and at least one of the species differs in its allometric trajectory relative to the others. If this is the case, it is then necessary to parse which species differed, and if this is due to allometric trajectory magnitude, direction, or both. As each of the four clades in our sample was found to have a significant interaction effect between LnCS and species ( $p < 0.0001$ ; see Appendix), we then used a Procrustes ANOVA/RRPP (Reduced Residual Permutation Procedure) to parse which species differed, and if this was due to allometric trajectory magnitude, direction, or some combination of the two. In an RRPP approach, estimates of phenotypic values are made using a linear model that does not contain the species x LnCS interaction effect. The residuals from this model are then randomly assigned to linear estimates (calculated from regression coefficients that describe species and size effects) to reconstruct "random" phenotypic values (Adams and Collyer, 2007; Collyer and Adams, 2007). These random values are then used to calculate species x size means, where the linear model contains the same effect plus the species x size interaction effect. A distribution of random values is then computed from many permutations (here, 10,000), from which the significance of observed values can be inferred (Adams and Collyer, 2007; Collyer and Adams, 2007). In these allometric trajectories, trajectory magnitude refers to the amount of shape change per unit LnCS

change, and trajectory direction refers to the pattern of allometric shape change. A sequential Holm-Bonferroni correction, which is less conservative than a standard Bonferroni correction, was used to account for multiple comparisons within clades (Quinn and Keough, 2002). As ontogenetic scaling requires a similar pattern of allometry to different endpoints, if species are found to differ in the pattern of allometric shape change, then by definition ontogenetic scaling alone cannot explain shape differences among specimens. Alternatively, the finding of no significant difference in allometric trajectory pattern provides support for hypotheses of ontogenetic scaling, though in itself would not conclusively demonstrate it, as the path distance of the ontogenetic trajectory would also need to vary among species.

*4.2.2.2 Phenotypic trajectory analysis.* Comparisons among species' ontogenetic shape change trajectories (as opposed to allometric trajectories) were performed using a phenotypic trajectory analysis (PTA, Adams and Collyer, 2009; Collyer and Adams, 2013). To evaluate shape change relative to unit developmental change, Procrustes aligned shape coordinates were used as the response variables and dental eruption stage (M0-M3) was used as the independent variable. When constructing ontogenetic trajectories, the use of dental eruption stage as the independent variable has been shown to produce trajectories that are a highly reliable approximation of ontogenetic shape changes in the cranium which are (conceptually) independent of size differences among species (McNulty et al., 2006; Singleton et al., 2010; Simons and Frost, 2016).

A PTA produces pair-wise comparisons of the magnitude, direction, and shape of phenotypic trajectories, which allows for an evaluation of how specific aspects of the trajectories vary. Trajectory magnitude is defined as the path-length distance along the trajectory, and is found from the set of Euclidean distances between sequential levels; trajectory direction is found from the first principal component of the covariance matrix estimated from the trajectory points, standardized by the starting (here, the M0 juvenile stage) point; trajectory shape is found as the Procrustes distances between pairs of phenotypic trajectories (Adams and Collyer 2009; Collyer and Adams, 2013). An important distinction between the PTA and the allometric analyses above is that in PTA, trajectory magnitude refers to the length of the entire trajectory from juvenile to adult

(rather than change in shape per unit size change). Statistical significance of differences in these trajectory parameters were also assessed using permutation procedures (10,000 iterations).

We used the PTA to test the null hypothesis that differences in catarrhine cranial morphology are due solely to differences in trajectory path-length, i.e., to an extension or truncation of a common developmental shape change trajectory. If the null hypothesis is not falsified, then shape differences among taxa are consistent with an extension or truncation of a similar ontogenetic trajectory, and cranial size differences likely account for the morphological diversity observed among taxa. This finding would be consistent with an adaptive radiation along an evolutionary path of least resistance (size). If the null hypothesis is falsified, this can be due to y-intercept transpositions and/or different slope coefficients, or a combination of these as well as magnitude differences (see Figure 9 in Klingenberg, 1998). The finding of y-intercept transpositions may indicate the evolution of a shared covariance pattern while maintaining a similar shape at different sizes, or that differences may have occurred ontogenetically prior to the developmental stage where specimens are reasonably able to be measured (Klingenberg, 1998; Collard and O'Higgins, 2001; Singleton, 2012). In the case of this study, that would mean differences in shape had already appeared prior to the eruption of dp4. A difference in slope may indicate positive or negative allometry and selection for shape differences independent of size (Klingenberg, 1998; Ravosa and Vinyard, 2002).

A major benefit of both the Procrustes ANOVA and PTA methods is that the trajectories of shape change are compared directly using all dimensions of multivariate space, and therefore do not rely on data reduction techniques, such as PCA (Adams and Collyer, 2009; Collyer and Adams, 2013). This is important because the conclusions drawn from comparisons of ontogenetic trajectories using proxies derived from data reduction techniques can be misleading (Mitteroecker et al., 2005; Baab et al., 2012), and have possibly led to the discrepant conclusions of prior investigations (Cobb and O'Higgins, 2004).

The comparison of trajectories using these procedures allows for a determination of if there has merely been an extension/truncation of similar ontogenetic trajectories, or

if other aspects of the trajectories have changed, indicating a decoupling of size and shape.

### 4.3 Results

**4.3.1 Allometric trajectories.** Results from the Procrustes ANOVA (Tables 4.2 - 4.9) show that shape difference per unit LnCS is mostly conserved among catarrhines and variation among allometric trajectories is largely due to differences in trajectory direction, that is, they generally differed in pattern, not magnitude. For colobines, almost all comparisons of allometric trajectory pattern are significantly different (Table 4.2). The exceptions are *Pygathrix nemaeus* x *Colobus guereza* and *Pygathrix nemaeus* x *Ptilocolobus badius*. However, the non-significant results for *Pygathrix nemaeus* are possibly due to the species' small sample size ( $n = 18$ ), which can affect the detection of significant differences in ontogenetic trajectories (Singleton et al., 2010; Simons et al., 2018). Few of the magnitude comparisons among colobines were different (Table 4.3). Cercopithecini shows no significant differences in the magnitude of allometric trajectories (Table 4.5), but does have significant differences in allometric pattern, particularly for *Miopithecus talapoin*, which differs from all other taxa (Table 4.4).

**Table 4.2.** Angles among Colobinae allometric trajectories. Below diagonal: angular difference (in degrees) between allometric trajectories. Above diagonal: p-values from permutation tests of angular differences (10,000 iterations). Shading indicates a significant difference after Holm-Bonferroni correction.

	C. gue	N. lar	P. bad	P.nem	P. ver	S. ent
C. gue	—	0.0001	0.0013	0.2559	0.0001	0.0001
N. lar	24.1662	—	0.0001	0.0005	0.0001	0.0001
P. bad	18.3362	29.5298	—	0.0517	0.0004	0.0005
P.nem	14.7317	25.4386	19.3302	—	0.0002	0.0016
P. ver	36.9665	38.8752	30.1635	37.5293	—	0.0063
S. ent	24.5715	24.4999	22.5749	24.8427	25.6404	—

**Table 4.3.** Allometric magnitude comparison of Colobinae allometric trajectories. Allometric magnitude (amount of shape change per unit LnCS increase) p-values from permutation tests (10,000 iterations). Shading indicates a significant difference after Holm-Bonferroni correction.

	C. gue	N. lar	P. bad	P.nem	P. ver	S. ent
C. gue	—					
N. lar	0.3682	—				
P. bad	0.3214	0.0819	—			
P.nem	0.6935	0.3269	0.7041	—		
P. ver	0.1003	0.0309	0.3729	0.2558	—	
S. ent	0.0002	0.0001	0.0178	0.015	0.3662	—

**Table 4.4.** Angles among Cercopithecini allometric trajectories. Below diagonal: angular difference (in degrees) between allometric trajectories. Above diagonal: p-values from permutation tests of angular differences (10,000 iterations). Shading indicates a significant difference after Holm-Bonferroni correction.

	A. nig	C. aet	C. lho	C. mit	M. tal
A. nig	—	0.0017	0.0132	0.0002	0.0001
C. aet	17.8898	—	0.0257	0.0856	0.0001
C. lho	16.4257	14.6443	—	0.027	0.0001
C. mit	19.5203	12.9512	14.659	—	0.0001
M. tal	30.554	24.3182	28.2028	26.5987	—

**Table 4.5.** Allometric magnitude comparison of Cercopithecini allometric trajectories. Allometric magnitude (amount of shape change per unit LnCS increase) p-values from permutation tests (10,000 iterations). Shading indicates a significant difference after Holm-Bonferroni correction.

	A. nig	C. aet	C. lho	C. mit	M. tal
A. nig	—				
C. aet	0.7058	—			
C. lho	0.2314	0.3707	—		
C. mit	0.0209	0.0357	0.2622	—	
M. tal	0.3134	0.4762	0.9253	0.2604	—

For tribe Papionini, the majority of significant differences lie in the pattern of allometry, rather than in the magnitude (cf. Tables 4.6 and 4.7). Of note is that the larger bodied African papionins (i.e., *Mandrillus*, *Papio*, and *Theropithecus*) significantly differ from

each other as well as the smaller bodied African papionins (i.e., *Cercocebus* and *Lophocebus*). The smaller bodied African papionins however do not significantly differ from each other in either allometric magnitude or pattern (Tables 4.6 and 4.7). The majority of differences in allometric trajectory magnitude are found in *Macaca mulatta* (Table 4.7). All of the hominoids significantly differ in the pattern of their allometric trajectories (Table 4.8). There are also several differences in allometric magnitude, particularly for *Pongo pygmaeus* (Table 4.9).

**Table 4.6.** Angles among Papionini allometric trajectories. Below diagonal: angular difference (in degrees) between allometric trajectories. Above diagonal: p-values from permutation tests of angular differences (10,000 iterations). Shading indicates a significant difference after Holm-Bonferroni correction.

	C. agi	C. aty	C. tor	L. alb	L. ate	M. fas	M. mul	M. sph	M. syl	P. anu	P. cyn	P. urs	T. gel
C. agi	—	0.0945	0.0414	0.063	0.2623	0.0046	0.09	0.0002	0.0141	0.0001	0.0001	0.0001	0.0129
C. aty	18.29394	—	0.2729	0.234	0.0415	0.005	0.0831	0.0018	0.054	0.0003	0.0001	0.0002	0.0183
C. tor	16.21879	14.43787	—	0.1314	0.0209	0.0019	0.0027	0.0001	0.098	0.0001	0.0001	0.0001	0.013
L. alb	16.24501	15.31156	13.08168	—	0.4364	0.0028	0.0025	0.0001	0.0465	0.0001	0.0001	0.0001	0.0004
L. ate	14.29184	19.32527	16.65897	12.03925	—	0.0009	0.0051	0.0001	0.0203	0.0001	0.0001	0.0001	0.0007
M. fas	18.67923	20.71435	16.79365	17.70978	19.75329	—	0.0026	0.0001	0.0056	0.0003	0.0001	0.0001	0.007
M. mul	14.71944	16.50114	16.62479	17.6531	17.97051	16.21379	—	0.0001	0.0121	0.0001	0.0001	0.0001	0.0021
M. sph	20.33571	21.12712	18.08375	20.88065	24.07997	18.81756	21.11405	—	0.0001	0.0001	0.0001	0.0012	0.0001
M. syl	22.48978	21.13399	16.85087	18.87761	21.30121	21.33796	20.38484	28.1523	—	0.0001	0.0001	0.0001	0.0174
P. anu	21.27583	24.05581	19.2218	22.27396	23.65006	16.23622	22.58029	13.17453	28.56169	—	0.0149	0.0078	0.0001
P. cyn	28.05218	28.11048	23.59328	27.41734	30.42082	22.30089	29.42768	17.48627	33.95011	12.23938	—	0.1549	0.0001
P. urs	28.18627	28.14987	24.37509	29.00141	32.27726	21.36872	28.73369	15.62377	33.67278	13.50644	11.57349	—	0.0001
T. gel	17.97783	19.47835	15.3522	20.16363	20.44335	15.46518	16.82789	20.0986	19.89386	19.05238	25.34367	23.89219	—

To visually compare allometric trajectories, Figure 4.1 (A-D) shows the first PC of predicted values of cranial shape versus LnCS (Adams and Nistri, 2010). These figures illustrate that within each clade, allometric trajectories are broadly oriented in a similar direction, but that some differences among species are apparent. Note that the PCs of predicted shape values are used for visualization purposes only and statistical tests were performed on the entirety of the data space.

**Table 4.7.** Allometric magnitude comparison of Papionini allometric trajectories. Allometric magnitude (amount of shape change per unit LnCS increase) p-values from permutation tests (10,000 iterations). Shading indicates a significant difference after Holm-Bonferroni correction.

	C. agi	C. aty	C. tor	L. alb	L. ate	M. fas	M. mul	M. sph	M. syl	P. anu	P. cyn	P. urs	T. gel
C. agi	—												
C. aty	0.6062	—											
C. tor	0.4519	0.2183	—										
L. alb	0.3555	0.7718	0.0595	—									
L. ate	0.923	0.5418	0.5101	0.2916	—								
M. fas	0.4028	0.868	0.0591	0.8623	0.3221	—							
M. mul	0.0193	0.0077	0.0679	0.00009	0.0229	0.00009	—						
M. sph	0.8606	0.6504	0.2135	0.3042	0.7587	0.3388	0.0007	—					
M. syl	0.1596	0.0694	0.3866	0.0202	0.1738	0.0208	0.6533	0.0684	—				
P. anu	0.5198	0.2423	0.8057	0.0469	0.5811	0.036	0.0141	0.1825	0.2684	—			
P. cyn	0.0218	0.1587	0.0003	0.1606	0.0143	0.0805	0.00009	0.0026	0.0007	0.00009	—		
P. urs	0.4911	0.963	0.0922	0.7571	0.4077	0.882	0.0003	0.4665	0.0317	0.0763	0.0647	—	
T. gel	0.9011	0.6575	0.299	0.3531	0.7995	0.4025	0.0035	0.9658	0.0971	0.321	0.0107	0.508	—

**Table 4.8.** Angles among Hominoidea allometric trajectories. Below diagonal: angular difference (in degrees) between allometric trajectories. Above diagonal: p-values from permutation tests of angular differences (10,000 iterations). Shading indicates a significant difference; all angles were significant after sequential Holm-Bonferroni correction.

	G. gor	H. lar	H. sap	P. pan	P. pyg	P. tro	S. syn
G. gor	—	0.0001	0.0001	0.0001	0.0001	0.0001	0.0001
H. lar	34.471	—	0.0001	0.0001	0.0001	0.0001	0.0122
H. sap	50.051	45.3291	—	0.0001	0.0001	0.0001	0.0001
P. pan	25.573	29.6278	37.0951	—	0.0014	0.0081	0.0001
P. pyg	22.7248	33.6796	40.1357	17.9162	—	0.0001	0.0001
P. tro	26.8547	24.1118	38.3067	15.6444	20.1351	—	0.0001
S. syn	41.7531	19.584	45.5668	31.7667	38.2642	27.1183	—

**Table 4.9.** Allometric magnitude comparison of Hominoidea allometric trajectories. Allometric magnitude (amount of shape change per unit LnCS increase) p-values from permutation tests (10,000 iterations). Shading indicates a significant difference after Holm-Bonferroni correction.

	G. gor	H. lar	H. sap	P. pan	P. pyg	P. tro	S. syn
G. gor	—						
H. lar	0.0013	—					
H. sap	0.0643	0.1898	—				
P. pan	0.012	0.2696	0.7412	—			
P. pyg	0.0001	0.2072	0.004	0.0057	—		
P. tro	0.0157	0.1846	0.8611	0.8441	0.0009	—	
S. syn	0.6901	0.001	0.0399	0.01	0.0001	0.0081	—

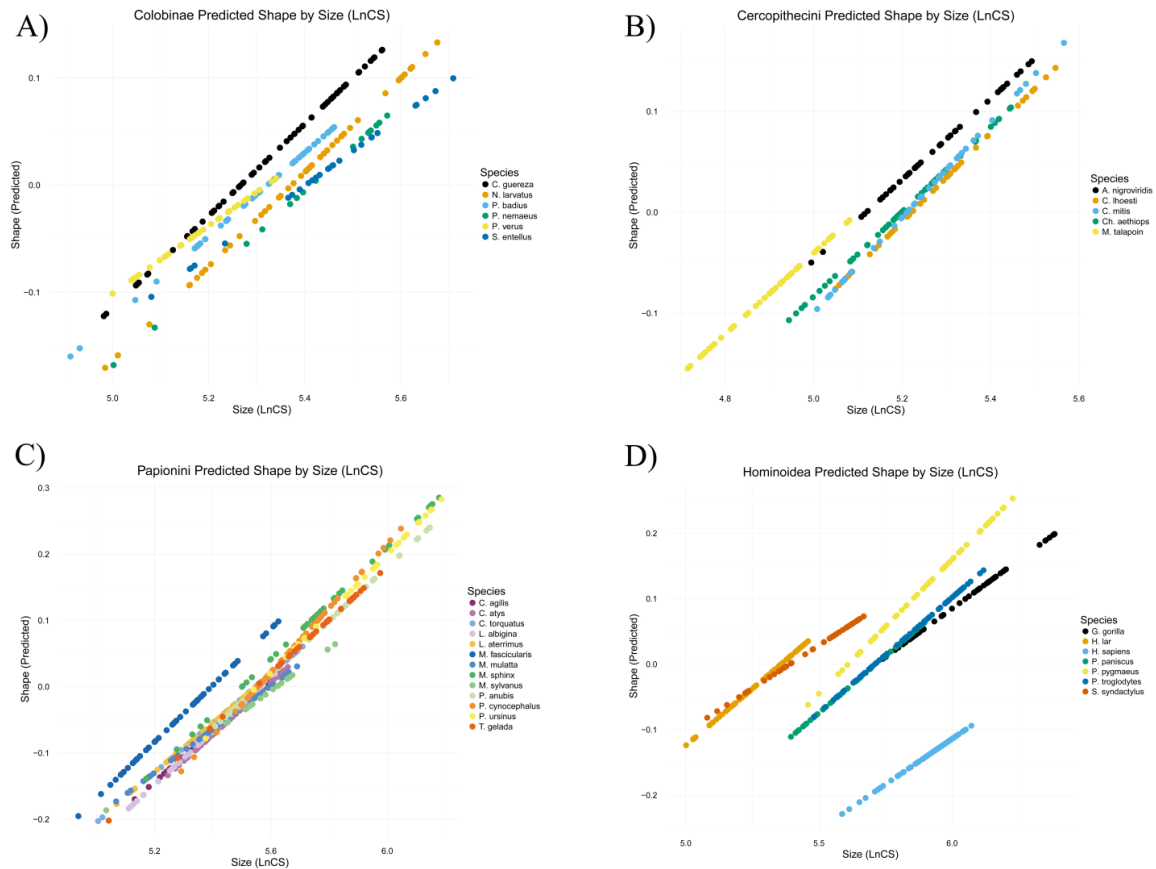


Figure 4.1 (A-D). Visual comparison of allometric trajectories for: A) Colobinae; B) Cercopitheciini; C) Papionini; D) Hominoidea. Figures are linear regressions of the first PC of predicted values of cranial shape versus LnCS (Adams and Nistri, 2010). These illustrate that within each clade, allometric trajectories are broadly oriented in a similar direction, but that some differences among species are apparent.



4.3.2 *Ontogenetic trajectories*. Results of the PTA comparison for magnitude, direction, and shape of cranial ontogenetic shape trajectories (associated with dental developmental stage, rather than size) are presented in Tables 4.10 - 4.17. Similar to the Procrustes ANOVA results above, much of the trajectory variation lies in the pattern of ontogenetic shape change, rather than in magnitude or trajectory shape. For colobines, no significant differences in trajectory magnitude were found, but there were significant differences in the direction of the trajectories, particularly for *Procolobus verus*, which differed from all other colobines (Table 4.10). Additionally, *Procolobus verus* was found to have a significantly different trajectory shape than *Nasalis larvatus* (Table 4.11). Within Cercopithecini, the majority of differences among species involved comparisons including *Miopithecus talapoin*, which significantly differed in ontogenetic trajectory direction from all other species (Table 4.12), and had a significantly shorter trajectory magnitude than *Cercopithecus lhoesti* and *Cercopithecus mitis* (Table 4.13). None of the cercopithecine species differed in ontogenetic trajectory shape. Among Papionini, none of the species differed in the shape of their ontogenetic trajectories, but there were notable differences in their magnitude and direction (Table 4.15). For example, both *Mandrillus sphinx* and *Papio hamadryas anubis* have significantly longer trajectories than the mangabeys and macaques (Table 4.18). Also of note, within the genus *Cercocebus*, *Cercocebus torquatus* has a significantly longer trajectory than *Cercocebus atys* or *Cercocebus agilis*, though it has a similar pattern (Tables 4.15 and 4.18).

**Table 4.10.** Phenotypic trajectory analysis results: Colobinae trajectory angle comparison. Below diagonal: angular difference (in degrees) between ontogenetic trajectories. Above diagonal: p-values from permutation tests of angular differences (10,000 iterations). Shading indicates a significant difference after Holm-Bonferroni correction.

	C. gue	N. lar	P. bad	P.nem	P. ver	S. ent
C. gue	—	0.0001	0.0033	0.368	0.0002	0.2653
N. lar	21.87608	—	0.0001	0.0112	0.0001	0.0545
P. bad	18.16662	27.49541	—	0.1167	0.0011	0.3559
P.nem	15.46659	24.3401	20.09972	—	0.0006	0.5501
P. ver	54.78672	61.06547	51.24614	54.87367	—	0.006
S. ent	20.03278	26.30464	20.49669	21.10598	48.17089	—

**Table 4.11.** Phenotypic trajectory analysis results: Colobinae trajectory shape and magnitude comparison. Below diagonal: p-values from comparison of ontogenetic trajectory. Above diagonal: p-values from comparison of ontogenetic trajectory path distances (magnitude). Significance tested using permutation procedures (10,000 iterations). Shading indicates a significant difference after Holm-Bonferroni correction.

	C. gue	N. lar	P. bad	P.nem	P. ver	S. ent
C. gue	—	0.249	0.9793	0.6937	0.2622	0.4483
N. lar	0.1832	—	0.3548	0.8725	0.089	0.6922
P. bad	0.0091	0.0758	—	0.6273	0.238	0.4034
P.nem	0.615	0.4038	0.4617	—	0.0812	0.8975
P. ver	0.0148	0.0018	0.0118	0.1616	—	0.0347
S. ent	0.1771	0.19	0.2893	0.1125	0.0386	—

In terms of ontogenetic trajectory pattern, there were no significant differences among the larger bodied African papionins (i.e., *Mandrillus*, *Papio*, and *Theropithecus*), or among the smaller bodied African papionins (i.e., *Cercocebus* and *Lophocebus*). However, there were significant differences found in the comparisons between these two groups (Table 4.14). Among hominoids, almost all species significantly differ in the pattern of their ontogenetic trajectories (Table 4.16). *Homo sapiens* have a significantly different trajectory shape than all other hominoids, save *Hylobates lar* (Table 4.17). *Homo sapiens* and *Pongo pygmaeus* significantly differ from all other taxa in path distance (trajectory magnitude), with the former having a significantly shorter trajectory than the other species, and the latter having a significantly longer one (Tables 4.17 and 4.18).

**Table 4.12.** Phenotypic trajectory analysis results: Cercopithecini trajectory angle comparison. Below diagonal: angular difference (in degrees) between ontogenetic trajectories from Phenotypic Trajectory Analysis. Above diagonal: p-values from permutation tests of angular differences (10,000 iterations). Shading indicates a significant difference after Holm-Bonferroni correction.

	A. nig	C. aet	C. lho	C. mit	M. tal
A. nig	—	0.0398	0.0564	0.0193	0.0003
C. aet	20.90201	—	0.1313	0.0039	0.0001
C. lho	21.49333	14.43591	—	0.2343	0.0001
C. mit	22.47408	16.19522	13.96147	—	0.0001
M. tal	32.43516	23.35495	27.28559	27.25868	—

**Table 4.13.** Phenotypic trajectory analysis results: Cercopithecini trajectory shape and magnitude comparison. Below diagonal: p-values from comparison of ontogenetic trajectory shape. Above diagonal: p-values from comparison of ontogenetic trajectory path distances (magnitude). Significance tested using permutation procedures (10, 000 iterations). Shading indicates a significant difference after Holm-Bonferroni correction.

	A. nig	C. aet	C. lho	C. mit	M. tal
A. nig	—	0.5814	0.8711	0.7123	0.01
C. aet	0.5473	—	0.3314	0.1826	0.007
C. lho	0.6112	0.9492	—	0.7759	0.0004
C. mit	0.6263	0.2847	0.3626	—	0.0002
M. tal	0.1637	0.1171	0.0552	0.1174	—

**Table 4.14.** Phenotypic trajectory analysis results: Papionini trajectory angle comparison. Below diagonal: angular difference (in degrees) between ontogenetic trajectories. Above diagonal: p-values from permutation tests of angular differences (10,000 iterations). Shading indicates a significant difference

	C. agi	C. aty	C. tor	L. alb	L. ate	M. fas	M. mul	M. sph	M. syl	P. anu	P. cyn	P. urs	T. gel
C. agi	—	0.0499	0.0758	0.0142	0.0294	0.0002	0.006	0.0004	0.1334	0.0001	0.0013	0.0002	0.0082
C. aty	16.07156	—	0.0178	0.0337	0.0115	0.0017	0.0149	0.0006	0.0674	0.0001	0.0002	0.0002	0.0064
C. tor	17.38219	22.39064	—	0.2752	0.0398	0.0327	0.0386	0.0291	0.7244	0.0059	0.0097	0.0041	0.0482
L. alb	15.73232	17.21826	14.83883	—	0.1859	0.0004	0.001	0.0002	0.2158	0.0001	0.0004	0.0001	0.0011
L. ate	14.29126	18.73683	18.79492	12.04493	—	0.0001	0.0006	0.0001	0.0747	0.0001	0.0001	0.0001	0.0006
M. fas	18.95554	20.96989	18.53579	18.67923	22.19747	—	0.0201	0.0005	0.3507	0.0001	0.008	0.0019	0.0545
M. mul	15.21137	17.4233	18.32523	17.9038	19.10809	12.56511	—	0.0006	0.2039	0.0001	0.0023	0.0003	0.0275
M. sph	21.42614	25.12782	20.11015	23.60657	26.34826	18.32035	19.03587	—	0.0664	0.1132	0.4318	0.3367	0.0108
M. syl	22.764	26.94193	17.22237	21.17309	25.33622	18.44927	20.72746	26.14589	—	0.065	0.0762	0.0452	0.238
P. anu	22.65237	27.84922	22.47539	25.84734	27.9412	17.86946	20.47295	11.89885	25.36573	—	0.5473	0.2346	0.0029
P. cyn	22.28705	27.69412	23.73059	26.45374	28.68514	18.44547	20.72429	12.45632	26.40488	10.56741	—	0.6504	0.0238
P. urs	27.22573	30.08434	26.50051	30.36615	32.90061	21.29989	24.90144	13.32804	28.96468	12.72585	12.50429	—	0.0094
T. gel	18.83699	21.55316	19.89924	22.03545	22.59245	14.72414	15.86073	19.07006	21.44786	18.81131	19.24911	21.44188	—

**Table 4.15.** Phenotypic trajectory analysis results: Papionini trajectory shape and magnitude comparison. Below diagonal: p-values from comparison of ontogenetic trajectory shape. Above diagonal: p-values from comparison of ontogenetic trajectory path distances (magnitude). Significance tested using permutation procedures (10, 000 iterations). Shading indicates a significant difference

	C. agi	C. aty	C. tor	L. alb	L. ate	M. fas	M. mul	M. sph	M. syl	P. anu	P. cyn	P. urs	T. gel
C. agi	—	0.5987	0.001	0.1549	0.7677	0.0157	0.5834	0.00009	0.0116	0.00009	0.0037	0.0007	0.0005
C. aty	0.6231	—	0.0003	0.0686	0.7938	0.0097	0.2966	0.00009	0.0077	0.00009	0.0016	0.0004	0.0004
C. tor	0.097	0.0252	—	0.0094	0.0004	0.0318	0.0017	0.0579	0.3053	0.6957	0.1828	0.6372	0.9813
L. alb	0.569	0.2652	0.3135	—	0.0752	0.3755	0.3301	0.00009	0.0335	0.0011	0.0918	0.0186	0.0082
L. ate	0.1889	0.0672	0.6933	0.4371	—	0.0069	0.3821	0.00009	0.0102	0.00009	0.0013	0.0002	0.0002
M. fas	0.5629	0.291	0.1034	0.7945	0.1215	—	0.054	0.00009	0.0563	0.0082	0.334	0.0806	0.0348
M. mul	0.7911	0.2855	0.2486	0.55	0.4771	0.3237	—	0.00009	0.0169	0.00009	0.0126	0.0025	0.0011
M. sph	0.0606	0.0103	0.6372	0.2762	0.1794	0.1385	0.128	—	0.871	0.0045	0.0005	0.0166	0.0618
M. syl	0.2961	0.1982	0.4827	0.2967	0.6247	0.1553	0.3945	0.1795	—	0.3296	0.1252	0.2033	0.2928
P. anu	0.1567	0.0359	0.0376	0.0844	0.0092	0.1044	0.1431	0.0929	0.0863	—	0.217	0.9495	0.6928
P. cyn	0.4216	0.1086	0.3981	0.6585	0.3394	0.4212	0.6725	0.5526	0.2534	0.4184	—	0.377	0.1839
P. urs	0.3755	0.1323	0.4605	0.7696	0.3353	0.58	0.4605	0.8463	0.1821	0.5171	0.9689	—	0.629
T. gel	0.1067	0.0389	0.9261	0.2981	0.8592	0.0929	0.2335	0.3077	0.6182	0.0185	0.2496	0.2675	—

Presented in Figure 4.2 (A-D) are the first two PCs of trajectory space by clade, illustrating ontogenetic trajectories of shape change. As in the visualizations of the allometric trajectories, the PCs of the ontogenetic trajectories are used for visualization purposes only and statistical tests were performed on the entirety of the data space.

**Table 4.16.** Phenotypic trajectory analysis results: Hominoidea trajectory angle comparison. Below diagonal: angular difference (in degrees) between ontogenetic trajectories. Above diagonal: p-values from permutation tests of angular differences (10,000 iterations). Shading indicates a significant difference after Holm-Bonferroni correction.

	G. gor	H. lar	H. sap	P. pan	P. pyg	P. tro	S. syn
G. gor	—	0.0001	0.0001	0.0001	0.0003	0.0001	0.0001
H. lar	34.9887	—	0.0001	0.0001	0.0001	0.0001	0.0039
H. sap	54.7329	45.2974	—	0.0001	0.0001	0.0001	0.0001
P. pan	26.6267	32.5592	42.3263	—	0.0672	0.0194	0.0001
P. pyg	23.5446	35.082	45.259	15.8822	—	0.0024	0.0001
P. tro	26.2878	24.6453	42.8167	15.7027	19.4845	—	0.0001
S. syn	40.8226	21.5244	45.1336	32.5131	36.8023	27.2483	—

**Table 4.17.** Phenotypic trajectory analysis results: Hominoidea trajectory shape and magnitude comparison. Below diagonal: p-values from comparison of ontogenetic trajectory shape. Above diagonal: p-values from comparison of ontogenetic trajectory path distances (magnitude). Significance tested using permutation procedures (10,000 iterations). Shading indicates a significant difference after Holm-Bonferroni correction.

	G. gor	H. lar	H. sap	P. pan	P. pyg	P. tro	S. syn
G. gor	—	0.0116	0.0001	0.1089	0.0003	0.9524	0.7451
H. lar	0.2514	—	0.0034	0.3393	0.0001	0.0049	0.1441
H. sap	0.0024	0.0597	—	0.0003	0.0001	0.0001	0.0009
P. pan	0.4169	0.017	0.0007	—	0.0001	0.0752	0.4059
P. pyg	0.3951	0.0226	0.0001	0.2261	—	0.0005	0.0007
P. tro	0.6151	0.0464	0.0012	0.8584	0.4603	—	0.7472
S. syn	0.8121	0.6578	0.0592	0.3769	0.2426	0.5288	—

**Table 4.18.** Path distances from phenotypic trajectory analyses, by clade.

Colobinae	Cercopithecini			Papionini	Hominoidea		
C. guereza	0.226717	A. nigroviridis	0.206538	C. agilis	0.208713	G. gorilla	0.221973
N. larvatus	0.23972	C. aethiops	0.196704	C. atys	0.1984	H. lar	0.192836
P. badius	0.227087	C. lhoesti	0.209183	C. torquatus	0.300985	H. sapiens	0.160365
P. nemaus	0.259476	C. mitis	0.212781	L. albigina	0.234671	P. paniscus	0.203538
P. verus	0.199541	M. talapoin	0.166397	L. aterrimus	0.203434	P. pygmaeus	0.266836
S. entellus	0.255574			M. fascicularis	0.249741	P. troglodytes	0.222652
				M. mulatta	0.218233	S. syndactylus	0.216797
				M. sphinx	0.344751		
				M. sylvanus	0.361892		
				P. anubis	0.291654		
				P. cynocephalus	0.268243		
				P. ursinus	0.290218		
				T. gelada	0.301559		

#### 4.4 Discussion

In general, the results of the allometric analyses in this investigation demonstrate that the magnitude of allometric trajectories (i.e. the amount of shape change over ontogeny) is mostly conserved among catarrhines, and variation among allometric trajectories is largely due to differences in trajectory direction (i.e., the pattern of shape change over ontogeny). As allometric patterns vary among taxa, ontogenetic scaling

*sensu stricto* cannot often account for most morphological differences, i.e., many of the previously proposed hypotheses of scaled variants were falsified (see below). However, within each of the clades, allometric trajectories were largely oriented in the same direction (Figure 4.2, A-D), and it was rare for the ontogenetic trajectories themselves to differ in shape. This indicates that catarrhines are achieving differences in adult cranial morphology through similar modes of ontogenetic shape change, but in relatively slight (though still statistically detectable) differences in the direction of those changes. These results are in line with previous investigations of static allometry in adult papionins which found evidence for the presence of allometric trends, even if allometries aren't strictly shared (Singleton, 2002). Using the 'criterion of subtraction,' the presence of a variety of ontogenetic pathways

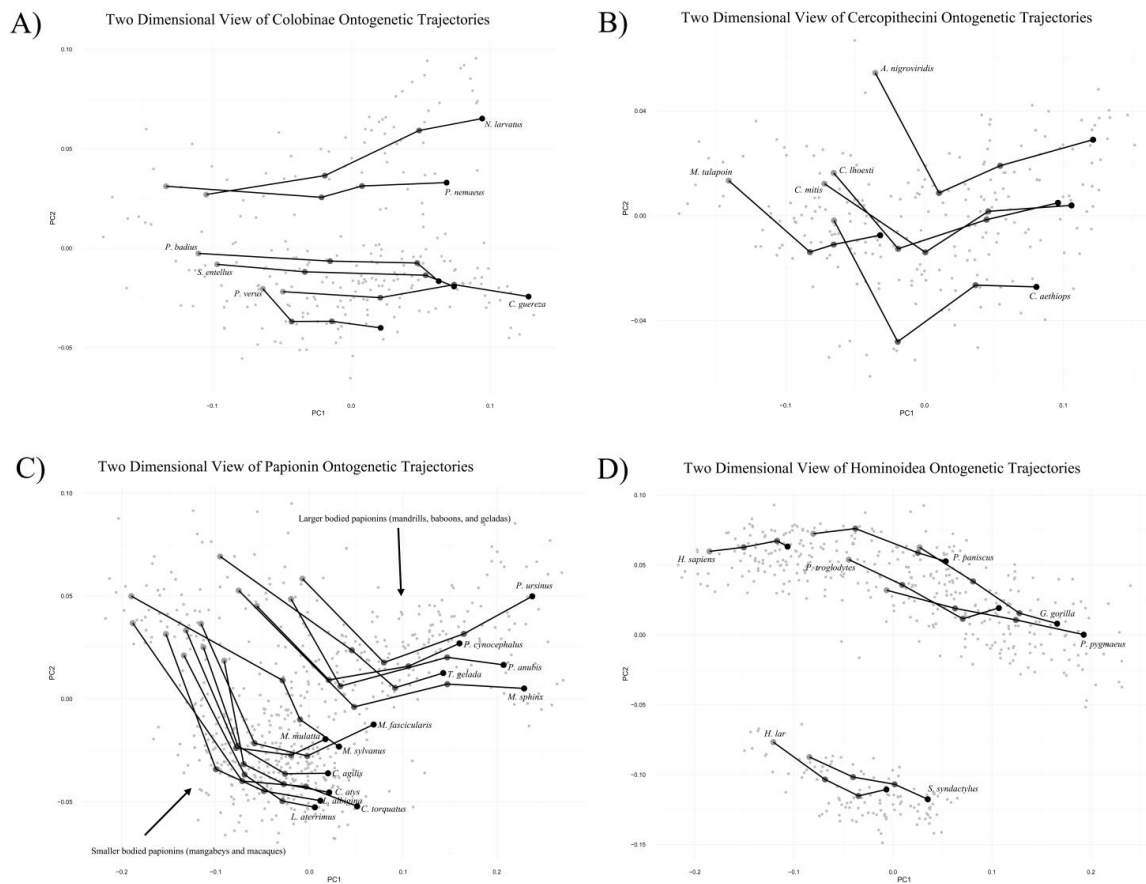


**Figure 4.2 (A-D).** The first two PCs of trajectory space by clade, illustrating ontogenetic trajectories of shape change. A) Colobinae, B) Cercopitheciini, C) Papionini, and D) Hominoidea.

provides indirect evidence for selection on cranial shapes themselves, rather than on body size alone (Ravosa and Profant, 2000), though it is more than reasonable to assume that selection on body size has also occurred. Like the allometric analyses, results from the Phenotypic Trajectory Analyses showed that the direction of ontogenetic trajectories (pattern) rather than amount of shape change (magnitude) is most influential in producing morphological differences in adult crania. This further supports the interpretation that selection is operating on more than size alone, and that shape differences are likely reflecting the maintenance of biomechanical functionality of the cranium at different sizes (Shea, 1985; Ravosa and Vinyard, 2002).

4.4.1.1 *Colobinae*: While there has been some research into adult colobine cranial morphometric variation (e.g. Koyabu and Endo, 2008; Cardini and Elton, 2009; Koyabu and Endo, 2010), there have been few investigations describing cranial shape changes associated with ontogeny in this clade (Ravosa, 1991; O'Higgins and Pan, 2004). In their investigation of colobine cranial ontogeny, O'Higgins and Pan (2004) determined that the larger African colobines (*Colobus guereza* and *Piliocolobus badius*) share a common allometric trajectory, but the smaller *Procolobus verus* exhibits a divergent ontogenetic trajectory. They therefore concluded that cranial shape differences between the larger and smaller colobines are not due solely to a variable extension/truncation of a shared ontogenetic trajectory.

The results of the present investigation largely comport with the findings of O'Higgins and Pan (2004), with some exceptions. Comparisons among allometric trajectories reveal that the magnitude of shape change per unit size change is largely shared across taxa, however, the angle between the trajectory vectors is significantly different for most taxa, with all three African colobine species differing in the direction of their allometric trajectories (see Table 4.2). These results indicate that African colobines share a similar amount of shape change per unit LnCS increase, but that shape is changing in different ways. The results of the PTA echo the results of the allometric analyses, in that significant differences exist in the direction of the ontogenetic trajectories of shape change, but there are no significant differences in the length of the ontogenetic trajectories. This indicates that differences in shape among smaller and larger

colobines, and between Asian and African colobines, are not the result of allometric scaling, but of differences in how adult shapes are accomplished.

4.4.1.2 *Cercopithecini*: Previous investigations have argued that size differences have played a major role in the evolution of guenon cranial morphology (Cardini and Elton, 2008). Comparisons among guenon allometric trajectories in the present investigation show that the magnitude of shape change per unit size change is shared across taxa (Table 4.5), but differences exist in the direction of the allometric trajectories of shape change. Notably, *Miopithecus talapoin* is distinct in its trajectory direction from all other species in our sample. This indicates that the ways in which *Miopithecus* attains its adult cranial shape is distinct from the other guenons. Additionally, results of the PTA demonstrate that in addition to differences in allometric and ontogenetic trajectory direction, *Miopithecus* has a significantly shorter ontogenetic trajectory compared to several other guenon species (Tables 4.13 and 4.18). Previous investigations (Shea, 1992) have argued that *Miopithecus* is a scaled variant of other, larger guenons, but our results suggest that this may be the coincident outcome of having an absolutely shorter trajectory. Because *Miopithecus* significantly differs in the direction of its allometric and ontogenetic trajectories, it cannot be considered a scaled variant of other, larger guenons, and shape differences are attributable to more than a common developmental pattern terminating at different adult body sizes.

4.4.1.3 *Papionini*: Because of phenotypic affinities, particularly facial prognathism, *Papio* and *Mandrillus* were historically considered to form a monophyletic group, while the shorter faced and smaller *Cercocebus* and *Lophocebus* were thought to form another (Szalay and Delson, 1979). However, since molecular relationships in Papionini have been more thoroughly resolved, it is now widely acknowledged that *Papio* and *Lophocebus* comprise one monophyletic group, and *Cercocebus* and *Mandrillus* another (Cronin and Sarich, 1976; Disotell et al., 1992; Fleagle and McGraw, 1999; Gilbert, 2007; Leigh, 2007; Perelman et al., 2011; Gilbert, 2013; Pugh and Gilbert, 2018). The implication of this is that the similar phenotypes of *Papio/Mandrillus* (i.e., relatively long faces, relatively large body size) and *Cercocebus/Lophocebus* (i.e., relatively short faces,



relatively small body size) are the product of parallel evolution (Fleagle and McGraw, 1999; Gilbert, 2007; Leigh, 2007). Ravosa and Profant (2000) have suggested that identifying different allometric patterns between *Papio* and *Mandrillus*, and between *Cercocebus* and *Lophocebus* could help explain this homoplasy, especially if *Papio* and *Lophocebus* share one pattern and *Mandrillus* and *Cercocebus* another.

The results of the present investigation somewhat comport with those of Collard and O'Higgins (2001), in that allometric trajectory pattern differences were found between the larger bodied (*Mandrillus*, *Papio*, and *Theropithecus*) and smaller bodied (*Cercocebus* and *Lophocebus*) African papionins, with the former also significantly differing from each other. Thus, larger papionins (*Papio* and *Mandrillus*) are not merely 'scaled up' versions of their respective sister taxa (*Lophocebus* and *Cercocebus*) (cf. Leigh, 2007). However, unlike Collard and O'Higgins (2001), we found no differences in the pattern of allometric trajectories within the smaller bodied African papionins. Furthermore, as revealed by the PTA, larger papionins do not significantly differ in the direction of their ontogenetic trajectories, only in their allometric pattern (cf. Tables 4.6 and 4.14). This indicates that the ontogenetic shape changes in the larger papionins are occurring in the same vein, which is the likely cause of their homoplasy, but that adult morphological differences between these two species are mostly arising from different patterns of allometry. These results, coupled with the finding that smaller papionins also have similar allometric and ontogenetic trajectories, indicates that large papionins develop in a similar manner, and small papionins develop in a similar manner, but *Cercocebus* and *Mandrillus* do not share one pattern and *Papio* and *Lophocebus* another (see Figure 4.2 C). While *Cercocebus torquatus* does not significantly differ from *Mandrillus* or *Papio* in either length or direction of ontogenetic trajectory, it does differ in allometric pattern, and therefore cannot be considered a scaled variant of these larger taxa. This further supports the conclusion that, in papionins, different patterns of allometry play a large role in the production of adult morphologies.

Tribe Papionini does provide some evidence for ontogenetic scaling, however. For example, *Cercocebus torquatus*, while sharing a similar allometric pattern and pattern of ontogenetic shape change with both *Cercocebus atys* and *Lophocebus aterrimus*, has a significantly longer trajectory than either of these species (Tables 4.13

and 4.18). This indicates that these species have a common developmental program terminating at different adult body sizes, and thus can be considered as scaled variants. Additionally, members of *Papio* don't differ in the pattern of either their allometric or ontogenetic trajectories, indicating that the smaller members of this genus are possibly scaled variants on a common theme, as was also found by Freedman (1962). However, this does not appear to be a widespread trend among the tribe.

4.4.1.4 *Hominoidea*: There have been relatively few multivariate investigations of cranial shape evolution in the gibbons (Hylobatidae) (but see McNulty 2004; Neaux, 2017). However, the size disparities between them and the larger apes have not gone unnoticed, and allometry has been acknowledged as a possible explanation for cranial shape differences among them (Leslie and Shea, 2016). While size is undoubtedly a factor in the evolution of hominoid cranial shape, the results of this investigation suggest unique allometric and ontogenetic trajectories both within and among the greater and lesser apes (Tables 4.9 and 4.16). To our knowledge, no one has proposed that gibbons are scaled variants of the larger apes. McNulty (2004, p. 432), however, did pose the question: "If gibbons were to grow to the size of both chimpanzees and gorillas, might we not expect these to look more similar to each other than to the traditional lesser apes?" The results of this study indicate that the larger (i.e., *Symphalangus*) and smaller (i.e., *Hylobates*) gibbons are not even scaled variants of each other, much less the larger apes.

Some previous investigations of cranial ontogeny in the non-human African apes have argued that ontogenetic scaling among species is responsible for variation in adult morphologies. For example, Shea (1983) argued that *Pan paniscus*, *Pan troglodytes*, and *Gorilla gorilla* share a single ontogenetic trajectory of cranial size/shape change for most features of the cranium, which are extended to various size ranges such that *Pan troglodytes* resembles an enlarged *Pan paniscus* and a diminutive *Gorilla gorilla* (and thus shape differences are the product of ontogenetic scaling). Others have argued that while allometry is a factor in the production of extant ape cranial shape, the African apes are not simply scaled variants of a single type, as trajectories diverge when all of the shape space is investigated (Cobb and O'Higgins, 2004; Mitteroecker et al., 2004b). The results of the present study found that all hominoids significantly differ in the pattern

(direction) of their allometric trajectories (Table 4.9) and that nearly all differ in the pattern of their ontogenetic trajectories (Table 4.16). We therefore concur with Cobb and O'Higgins (2004) and Mitteroecker et al. (2004b) that cranial shape differences among non-human African apes are not simply due to sharing an ontogenetic trajectory to different endpoints, and that *Pan paniscus*, *Pan troglodytes*, and *Gorilla gorilla* are not scaled variants of each other.

Several previous investigations have argued that many adult human cranial features resemble those of juvenile *Pan troglodytes* (either due to neoteny (Gould, 1977) or peramorphosis (Shea, 1989; McKinney and McNamara, 1991)). Our investigation demonstrated that *Homo sapiens* evince a unique cranial ontogenetic trajectory when compared with other hominoids (see also e.g., Mitteroecker et al., 2004b; Schaefer et al., 2004). In addition to these ontogenetic pattern differences, we also found that *Homo sapiens* have a significantly shorter ontogenetic trajectory than other hominids (Tables 4.17 and 4.18). These lines of evidence suggest that the resemblance between adult humans and juvenile chimpanzees is superficial, and is likely the result of the resemblance of the general juvenile cranial form of humans and chimpanzees, with humans changing only slightly (comparatively) from this juvenile condition over the course of ontogeny. That is, the 'juvenilized' cranium of adult humans is not due to having a truncated *Pan troglodytes* trajectory, but to having an absolutely smaller amount of shape transformation from the juvenile condition, although in a different direction (as was also found for *Miopithecus talapoin*).

4.4.2 *Size as a line of least evolutionary resistance.* In general, primates have increased in body size over their evolutionary history (Fleagle, 1978, 2013; Steiper and Seiffert, 2012). As changes in body size are known to have allometric consequences for the shape of the skull (Cheverud, 1982; Shea, 1985; Klingenberg, 1998; Frost et al., 2003; Gerber et al., 2008), it has been argued that size may be a line of least evolutionary resistance (*sensu* Schluter, 1996), and that evolutionary shape changes in cranial morphology are in fact largely the allometric consequence of these size changes (Marroig and Cheverud, 2005, 2010; see also Ungar and Hlusko, 2016). For example, supporting size as a line of least resistance, Marroig and Cheverud (2005, 2010) argued that body size evolution is

the most significant factor in producing observed cranial morphologies in Platyrrhines, and that most taxa are scaled variants of each other. Similarly, Shea (1992) and Cardini and Elton (2007) argued that size evolution has played a large role in the cranial morphological evolution of Tribe Cercopithecini. However, other researchers have questioned the influence of size on the evolution of cranial morphological variation. For example, in their investigation of platyrrhine crania, Perez et al. (2011) found that size does not account for a large proportion of cranial shape variation once phylogenetic structure is considered. In their investigation of *Chlorocebus*, a geographically widespread cercopithecine, Elton et al. (2010) determined that forces other than size are instrumental in producing cranial morphological variation. Additionally, Leigh et al. (2003) concluded that size change cannot in itself explain morphological differences among Papionins.

A general trend of sharing allometric and ontogenetic patterns to different termini (i.e., differing solely in trajectory magnitude and therefore exhibiting ontogenetic scaling) would lend support to the hypothesis of size as a line of least evolutionary resistance in the production of catarrhine cranial shape. In broad terms, the results of this investigation indicate that a variety of allometric patterns underlie the production of adult morphological variation, i.e., within each clade, there is not a commonly inherited developmental trajectory leading to strictly allometric changes in cranial morphology. Using the ‘criterion of subtraction’ (Gould, 1966, 1975; Shea, 1985, 1995; Ravosa and Vinyard, 2002), this demonstrates that selection is often acting directly on shapes themselves, rather than size alone (see also Ravosa and Profant, 2000). This is not to say that evolutionary changes in body size have no effect on shape, there is plenty of evidence to support this (Thompson, 1917; Huxley, 1932; Gould, 1966; Klingenberg, 1998; Cardini and Polly, 2013). However, rarely does it ever seem to be the case that differences in cranial shape between closely related larger and smaller catarrhines are solely the product of a shared ontogenetic trajectory to different endpoints. Alternatively, it is also possible that size induced shape changes and concomitant diversification occurs early in the evolution of a clade, and the sample used in this investigation is capturing a point in time in which this diversification has already occurred, and selection (or some other evolutionary force, such as drift) has since begun to operate on the shapes

themselves rather than on size alone, as it initially may have. This investigation found some support for this interpretation, as there was evidence for scaled variants within some of the more densely (in terms of species) sampled genera (e.g., within *Cercocebus* and within *Papio*). This indicates that more recently separated species are possibly more likely to be scaled variants, and thus that size may be an important initial factor in shape diversification. However, there was no evidence for the presence of scaled variants in the two species of *Pan*, who speciated relatively recently (Prüfer et al., 2012), indicating that this might not be true across all catarrhines. This could be further examined in future investigations by having denser sampling within a speciose genus whose speciation was relatively recent, such as in *Cercopithecus*, to determine if they provide further examples of scaled variants. Additionally, one could test for an association among evolutionary rates of cranial size and shape evolution and lineage diversification. If rates of size evolution are driving shape evolution and diversification, as size as a line of least evolutionary resistance predicts, a positive correlation among these three variables would be expected.

## CHAPTER V

### CONCLUSION

Ontogenetic studies have played an integral role in understanding patterns of cranial shape evolution in primates. While there have been many investigations into primate cranial ontogeny, many of those employing geometric morphometric methods have reached disparate conclusions regarding the similarities and differences of compared trajectories. It is possible that this is due to the different proxies that are used to calculate the trajectories, and therefore important to differentiate which aspects of ontogeny each of the proxies is describing, so that investigators can use targeted means of addressing their specific research questions. Furthermore, while comparing ontogenetic trajectories is common in ontogenetic studies, comparing the trajectories of many taxa simultaneously can be cumbersome and time-consuming, and, because the calculation of trajectories requires a sequence of ontogenetic stages from a single species (which are often not available from the fossil record), analyses of trajectories are often limited to extant taxa. Finally, there are several long standing hypotheses about the role of size in primate cranial evolution that have yet to be tested using advanced methods of shape analysis.

The studies in this dissertation performed landmark-based three-dimensional shape analyses on ontogenetic samples of extant catarrhine crania to address the issues outlined above. Each of the three data chapters (Chapters II-IV) expands in taxonomic scope as a targeted approach to each of the research questions.

In Chapter II, cranial ontogenetic trajectories were constructed using three common ontogenetic proxies (cranial size, molar eruption stage, and chronological age) in an ontogenetic sample of *Macaca mulatta* crania with associated ages at death. These trajectories were also used in developmental simulations to further evaluate the relative reliability of each of the proxies for constructing ontogenetic trajectories. Two research questions were addressed: 1) which ontogenetic proxy, if any, provide the most reliable linear approximations of cranial ontogenetic trajectories when using multivariate regression models?; 2) of the parameters of initial specimen shape, the pattern of shape change, and the magnitude of shape change, which plays the largest role in the production

of adult cranial morphologies? Results from this investigation have important implications for future investigations of ontogenetic trajectories. First, the analyses strongly suggest that chronological age is the least reliable proxy for the calculation of ontogenetic trajectories. While size, dental developmental stage, and age proxies were similar, developmental simulations demonstrated that the most reliable proxy for constructing ontogenetic trajectories is dental developmental stage. Secondly, of the parameters of initial specimen shape, the pattern of ontogenetic shape changes, and the magnitude of ontogenetic shape changes, the pattern of shape changes was found to have the strongest influence on the production of adult cranial morphology. This indicates that directly comparing patterns of development is a functional means of elucidating how adult shape differences are produced.

Chapter III presents two novel methodologies for the comparison of ontogenetic trajectories. First, to compare a broad sample of the ontogenetic trajectories of extant taxa simultaneously, a developmental shape-change trajectory PCA ( $\delta$ PCA) was developed, which is able to illustrate patterns of variation in developmental trajectories in a visually intuitive manner that allows for easier comparisons among taxa. Second, a method for reconstructing ancestral ontogenetic trajectories (an ontophylomorphospace) was developed so that differences in ontogenetic trajectories could be examined in an evolutionary context. The  $\delta$ PCA was shown to reliably illustrate patterns of variation in developmental trajectories in a visually intuitive manner that allows for easier comparisons among taxa. The ontophylomorphospaces revealed that African papionins exhibit extensive homoplasy in the evolution of cranial ontogenetic trajectories, and that Asian species of *Macaca* show highly derived ontogenetic trajectories relative to other cercopithecines. As some researchers have argued that ontogenetic trajectories of shape change can be used to reconstruct phylogenetic relationships, Chapter III also tests for the presence of a phylogenetic signal in the ontogenetic trajectories themselves. The null hypothesis of no phylogenetic signal in the ontogenetic trajectories was unable to be rejected, indicating that using ontogenetic shape trajectories as a character in phylogenetic analyses should be approached with caution, if attempted at all.

In Chapter IV, a large, comparative ontogenetic sample of catarrhine crania was used to evaluate if differences in cranial shape between closely related large and small

catarrhines are mainly driven by size divergence (i.e., that they are merely the product of ontogenetic scaling), thereby also testing the hypothesis of size as a line of least evolutionary resistance in catarrhine cranial evolution. Two distinct but related aspects of ontogeny were investigated: 1) allometric trajectories (shape changes associated with size) and 2) ontogenetic trajectories (shape changes associated with dental eruption stage). The first (allometric) analysis used Homogeneity of Slopes tests and Procrustes ANOVA to evaluate if allometric trajectories varied among species, and if this was due to trajectory magnitude, direction, or some combination of the two. The second set of analyses used Phenotypic Trajectory Analysis to more fully understand differences among ontogenetic trajectories. The allometric analyses demonstrated that shape difference per unit size change (magnitude) is conserved among catarrhines, and variation among allometric trajectories is largely due to differences in trajectory orientation (pattern). Likewise, the Phenotypic Trajectory Analysis showed that the orientation of ontogenetic trajectories (pattern) rather than amount of shape change from juvenile to adult (magnitude) is most influential in producing differences in adult crania. As allometric patterns vary among taxa, ontogenetic scaling *sensu stricto* does not often account for most morphological differences, i.e., many of the previously proposed hypotheses of scaled variants were falsified. These results also call into question the prevalence of size as a line of least evolutionary resistance, as selection appears to be changing the patterns of ontogenetic shape change, not just the size of the organisms.

Overall, the investigations presented in this dissertation have contributed to our understanding of cranial shape evolution in catarrhines, and to our understanding of geometric morphometric methods for studying ontogeny. The methods presented here can be used in future investigations to better understand patterns of primate cranial evolution. For example, there has been disagreement for decades about ancestral catarrhine morphotypes. Determining ancestral morphotypes has important implications for primate evolution, and has informed influential phylogenetic assessments of relationships among fossil catarrhines (e.g., the taxonomic status of many early catarrhines (Harrison, 1986; Begun, 1994, 2002; Rae, 1997, 1999; Pilbeam, 2002; Andrews and Harrison, 2005; McNulty et al., 2015)). However, the ancestral cranial morphotype for each of major catarrhine clades is currently uncertain. The method



presented in this dissertation for reconstructing ancestral ontogenetic trajectories (ontophylomorphospaces) can be used in future investigations to reconstruct the ontogenetic pathways that led to ancestral morphologies, rather than reconstructing ancestral morphologies from adult forms (which is the commoner method). This is a possible route to addressing the multi-decade debate in anthropology of the cranial morphotype of the last common ancestor of hominoids and cercopithecoids (Delson, 1975; 1977; Delson and Andrews, 1975; Benefit and McCrossin, 1991, 1993; Benefit, 2000). Furthermore, the ontophylomorphospace method, because it provides ancestral reconstructions of ontogenetic trajectories, can be used in conjunction with developmental simulation (McNulty et al., 2006; Singleton et al., 2010) for possibly more reliable developmental simulations of juvenile fossils (e.g. for the recently discovered infant cranium of *Nyanzapithecus alesi*, (Nengo et al., 2017)) that don't rely on using trajectories from extant taxa. This could aid in the taxonomic identification of juvenile specimens (which, compared with adult specimens, are more difficult to place taxonomically), though further testing is needed.

The results from the investigation of ontogenetic scaling questioned the role of size as a line of evolutionary least resistance in catarrhine cranial shape change. Because catarrhines evince varied routes to adult morphologies (i.e., they don't often share an allometric trajectory to different endpoints), factors other than size change have likely played a role in the evolution of those morphologies. If size is a line of least evolutionary resistance, and a first step in adaptation and diversification, it would be expected that 1) rates of shape evolution would be correlated with rates of size evolution (as size changes lead to shape changes), and 2) changes in rates of size evolution would be correlated with rates of lineage diversification. Therefore, future investigations could compare the evolutionary rates of each of these variables to determine if they are related, as the hypothesis of size as a line of least resistance would predict.

## APPENDIX

### ANOVA TABLES FROM HOMOGENEITY OF SLOPES TESTS.

<b>Colobinae</b>	Df	SS	MS	Rsq	F	Z	Pr(>F)
log(size)	1	0.869967	0.869967	0.363886	251.269	58.55374	0.0001
species	5	0.664506	0.132901	0.277947	38.38526	19.82596	0.0001
log(size):species	5	0.077277	0.015455	0.032323	4.463889	4.212319	0.0001
Residuals	225	0.779017	0.003462				
Total	236	2.390766					

	Df	SSE	SS	R2	F	Z	Pr(>F)
Common Allometry	235	1.520799					
Group Allometries	225	0.779017	0.741782	0.31027	21.42458	11.3248	0.0001

Appendix Table A1. HOS test for Colobinae.

<b>Cercopithecini</b>	Df	SS	MS	Rsq	F	Z	Pr(>F)
log(size)	1	1.147836	1.147836	0.522714	346.073	67.44602	0.0001
species	4	0.290105	0.072526	0.132111	21.86668	15.20337	0.0001
log(size):species	4	0.03824	0.00956	0.017414	2.882348	2.818646	0.0001
Residuals	217	0.719734	0.003317				
Total	226	2.195915					

	Df	SSE	SS	R2	F	Z	Pr(>F)
Common Allometry	225	1.048079					
Group Allometries	217	0.719734	0.328345	0.149525	12.37452	8.736299	0.0001

Appendix Table A2. HOS test for Cercopithecini.

<b>Papionini</b>	Df	SS	MS	Rsq	F	Z	Pr(>F)
log(size)	1	5.682687	5.682687	0.605791	1522.124	92.95558	0.0001
species	12	1.47307	0.122756	0.157034	32.88052	18.46284	0.0001
log(size):species	12	0.193883	0.016157	0.020668	4.327678	4.09987	0.0001
Residuals	544	2.030966	0.003733				
Total	569	9.380607					

	Df	SSE	SS	R2	F	Z	Pr(>F)
Common Allometry	568	3.697919					
Group Allometries	544	2.030966	1.666953	0.177702	18.6041	10.5976	0.0001

Appendix Table A3. HOS test for Papionini.

<b>Hominoidea</b>	Df	SS	MS	Rsq	F	Z	Pr(>F)
log(size)	1	3.777703	3.777703	0.369053	845.2132	80.72452	0.0001
species	6	4.208992	0.701499	0.411187	156.9515	44.20929	0.0001
log(size):species	6	0.215881	0.03598	0.02109	8.0501	7.41252	0.0001
Residuals	455	2.033634	0.00447				
Total	468	10.23621					

	Df	SSE	SS	R2	F	Z	Pr(>F)
Common Allometry	467	6.458507					
Group Allometries	455	2.033634	4.424873	0.432276	82.50078	25.45731	0.0001

Appendix Table A4. HOS test for Hominoidea.

## REFERENCES CITED

- Ackermann RR, Krovitz GE. 2002. Common patterns of facial ontogeny in the hominid lineage. *Anat Rec* 269:142-147.
- Ackermann RR. 2005. Ontogenetic integration of the hominoid face. *J Hum Evol* 48:175-197.
- Adams, D.C., Rosenberg, M.S., 1998. Partial warps, phylogeny, and ontogeny: a comment on Fink and Zelditch (1995). *Systematic Biology* 47, 168–173.
- Adams, D.C., Rohlf, F.J., Slice, D.E., 2004. Geometric morphometrics: Ten years of progress following the “revolution.” *Italian Journal of Zoology* 71, 5–16.
- Adams DC, Collyer ML. 2007. Analysis of character divergence along environmental gradients and other covariates. *Evolution* 61(3):510-515.
- Adams D, Collyer ML. 2009. A general framework for the analysis of phenotypic trajectories in evolutionary studies. *Evolution*, 63(5):1143-1154.
- Adams DC, Nistri A. 2010. Ontogenetic convergence and evolution of foot morphology in European cave salamanders (Family: Plethodontidae). *BMC Evol Bio* 10(1):216.
- Adams D, Rohlf FJ, Slice DE, Dean CA, James FR, Dennis ES. 2013. A field comes of age: geometric morphometrics in the 21st century Geometric morphometrics and the “Procrustes paradigm.” *Hystrix, Ital J Mammal* 71:5-16.
- Adams DC, Collyer ML, Kaliontzopoulou A, Sherratt E. 2017. Geomorph: Software for geometric morphometric analyses. R package version 3.0.5.  
<https://cran.rproject.org/package=geomorph>.
- Adams, D.C., 2014. A generalized K statistic for estimating phylogenetic signal from shape and other high-dimensional multivariate data. *Systematic Biology* 63, 685–697.
- Alba DM. 2002. Shape and stage in heterochronic models. In: Minugh-Purvis N, McNamara KJ, editors. *Human evolution through developmental change*. Baltimore: The Johns Hopkins University Press. p 28–50.
- Alberch P, Gould SJ, Oster GF, Wake DB. 1979. Size and shape in ontogeny and phylogeny. *Paleobiology* 5:296–317.
- Almécija, S., Tallman, M., Alba, D.M., Pina, M., Moyà-Solà, S., Jungers, W.L., 2013. The femur of *Orrorin tugenensis* exhibits morphometric affinities with both Miocene apes and later hominins. *Nature Communications* 4, 2888.

- Almécija, S., Orr, C.M., Tocheri, M.W., Patel, B.A., Jungers, W.L., 2015. Exploring phylogenetic and functional Signals in complex morphologies: the hamate of extant anthropoids as a test-case study. *Anatomical Record* 298, 212–229.
- Amundson R. 2005. The changing role of the embryo in evolutionary thought: roots of evo-devo. Cambridge: Cambridge University Press.
- Andrews, P. and Harrison, T., 2005. The last common ancestor of apes and humans. In: Lieberman DE, Smith RJ, Kelley J (Eds). *Interpreting the past: essays on human, primate, and mammal evolution in honor of David Pilbeam*. Brill Academic Publishers, Boston. p103-121.
- Antón SC, Leigh SR. 2003. Growth and life history in *Homo erectus*. In: Thompson JL, Krovitz GL, Nelson, AJ, editors. *Patterns of growth and development in genus Homo*. Cambridge: Cambridge University Press. p 219-245.
- Arnold, C., Matthews, L.J., Nunn, C.L., 2010. The 10kTrees Website: A new online resource for primate phylogeny. *Evolutionary Anthropology* 19, 114–118.
- Atchley WR, Hall BK. 1991. A model for development and evolution of complex morphological structures. *Biological Reviews* 66(2):101-157.
- Baab KL, McNulty KP, Rohlf FJ. 2012. The shape of human evolution: a geometric morphometrics perspective. *Evol Anthropol* 21:151–165.
- Begun, D.R., 1994. Relations among the great apes and humans: new interpretations based on the fossil great ape *Dryopithecus*. *Am J Phys Anthropol*. 37(S19): 11-63.
- Begun, D.R., 2002. European Hominoids. In: Hartwig, W. (ed.) *The Primate Fossil Record*. p 339-368.
- Benefit, B.R. and McCrossin, M.L., 1991. Ancestral facial morphology of Old World higher primates. *PNAS*. 88(12): 5267-5271.
- Benefit, B.R. and McCrossin, M.L., 1993. Facial anatomy of *Victoriapithecus* and its relevance to the ancestral cranial morphology of Old World monkeys and apes. *Am J Phys Anthropol*. 92(3): 329-370.
- Benefit BR. 2000. Old World monkey origins and diversification: an evolutionary study of diet and dentition. In: Whitehead PF and Jolly CJ, editors. *Old World monkeys*. Cambridge: Cambridge University Press. p 133-179.
- Berge C, Penin X. 2004. Ontogenetic allometry, heterochrony, and interspecific differences in the skull of African apes, using tridimensional Procrustes analysis. *Am J Phys Anthropol* 124:124–138.

- Blomberg, S.P., Garland, T., Ives, A.R., 2003. Testing for phylogenetic signal in comparative data: behavioral traits are more labile. *Evolution* 57, 717–745.
- Bookstein FL. 1991. *Morphometric tools for landmark data: geometry and biology*. Cambridge: Cambridge University Press.
- Bookstein FL. 1996. Combining the tools of geometric morphometrics. In: Marcus LF, Corti M, Loy A, Naylor GJP, Slice DE, editors. *Advances in morphometrics*. New York: Plenum Press. p 131-151.
- Cheverud J, Richtsmeier J. 1986. Finite-element scaling applied to sexual dimorphism in Rhesus macaque (*Macaca mulatta*) facial growth. *Systematic Biology* 35: 381-399.
- Cardini A, Elton S. 2008. Variation in guenon skulls (I): species divergence, ecological and genetic differences. *J Hum Evol* 54(5):615-637.
- Cardini A, Elton S. 2008. Does the skull carry a phylogenetic signal? Evolution and modularity in the guenons. *The Biological Journal of the Linnean Society* 93, 813–834.
- Cardini A, Elton S. 2009. Geographical and taxonomic influences on cranial variation in red colobus monkeys (Primates, Colobinae): introducing a new approach to ‘morph’ monkeys. *Global Ecology and Biogeography*, 18(2):248-263.
- Cardini A, Polly PD. 2013. Larger mammals have longer faces because of size-related constraints on skull form. *Nature communications* 4:2458.
- Carlson KB, de Ruiter DJ, DeWitt TJ, McNulty KP, Carlson KJ, Tafforeau P, Berger LR. 2016. Developmental simulation of the adult cranial morphology of *Australopithecus sediba*. *S Afr J Sci.* 112(7-8): 1-9.
- Cheverud, J.M., 1982. Relationships among ontogenetic, static, and evolutionary allometry. *Am J Phys Anthropol.* 59(2): 139-149.
- Cochard, LR. 1985. Ontogenetic allometry of the skull and dentition of the rhesus monkey (*Macaca mulatta*). In: Jungers WJ, editor. *Size and scaling in primate biology*. New York: Plenum Press. p 231-255.
- Cobb SN, O’Higgins P. 2004. Hominins do not share a common postnatal facial ontogenetic shape trajectory. *J Exp Zool B Mol Dev Evol* 302:302–321.
- Cobb SN, O’Higgins P. 2007. The ontogeny of sexual dimorphism in the facial skeleton of the African apes. *J Hum Evol* 53:176–190.
- Cock, A. G. 1966. Genetical aspects of metrical growth and form in animals. *Quarterly Review of Biology* 41:131-190.

- Collard M, O'Higgins P. 2001. Ontogeny and homoplasy in the papionin face. *Evol Dev* 3:322–331.
- Collyer ML, Adams DC. 2007. Analysis of two-state multivariate phenotypic change in ecological studies. *Ecology* 88(3):683–692.
- Collyer ML, Adams DC. 2013. Phenotypic trajectory analysis: comparison of shape change patterns in evolution and ecology. *Hystrix* 24(1):75.
- Cronin, J.E., Sarich, V.M., 1976. Molecular evidence for dual origin of mangabeys among Old World monkeys. *Nature* 260, 700–702.
- De Beer G. 1930. *Embryology and evolution*. Oxford: Clarendon Press.
- De Beer G. 1951. *Embryos and ancestors*. Oxford: Clarendon Press.
- Delson E, Andrews P. 1975. Evolution and interrelationships of the catarrhine primates. In Luckett WP, Szalay FS (Eds). *Phylogeny of the Primates: A multidisciplinary approach*. New York: Plenum. p 405–446.
- Delson, E., Dean, D., 1993. Are *Papio baringensis* R. Leakey, 1969, and *P. quadratiostris* Iwamoto, 1982, species of *Papio* or *Theropithecus*? In: Jablonski, N.G., (Ed.), *Theropithecus: The Rise and Fall of a Primate Genus*. Cambridge University Press, New York, pp. 125–156.
- Delson E. 1975. Evolutionary history of the Cercopithecidae. *Contributions to primatology* 5:167–217.
- Delson E. 1977. Catarrhine phylogeny and classification: Principles, methods and comments. *J Hum Evol* 6(5):433–459.
- Disotell, T.R., Honeycutt, R.L., Ruvolo, M. 1992. Mitochondrial DNA phylogeny of the Old-World monkey tribe Papionini. *Molecular Biology and Evolution* 9, 1–13.
- Dray, S., Dufour, A.B. 2007. The ade4 package: implementing the duality diagram for ecologists. *Journal of Statistical Software* 22(4), 1–20.
- Dryden IL, Mardia KV. 1998. *Statistical shape analysis*. New York: John Wiley & Sons.
- Elton S, Dunn J, Cardini A. 2010. Size variation facilitates population divergence but does not explain it all: an example study from a widespread African monkey. *Biol J Linnean Soc.* 101(4):823–843.
- Fink WL, Zelditch ML. 1995. Phylogenetic analysis of ontogenetic shape transformations: a reassessment of the piranha genus *Pygocentrus* (Teleostei). *Systematic Biology* 44:343–360.

- Fleagle JG, McGraw WS. 1999. Skeletal and dental morphology supports diphyletic origin of baboons and mandrills. *Proceedings of the National Academy of Sciences USA* 96, 1157–1161.
- Fleagle JG. 1978. Size distributions of living and fossil primate faunas. *Paleobiology* 4(1):67-76.
- Fleagle JG. 2013. *Primate adaptation and evolution*. Academic Press.
- Frankino WA, Zwaan BJ, Stern DL, Brakefield PM. 2005. Natural selection and developmental constraints in the evolution of allometries. *Science* 307(5710):718-720.
- Freedman L. 1962. Growth of muzzle length relative to calvaria length in *Papio*. *Growth* 26:117–128.
- Frost SR, Marcus LF, Bookstein FL, Reddy DP, Delson E. 2003. Cranial allometry, phylogeography, and systematics of large-bodied papionins (primates: *Cercopithecinae*) inferred from geometric morphometric analysis of landmark data. *Anat Rec A Discov Mol Cell Evol Biol* 275:1048–1072.
- Garstang W. 1922. The theory of recapitulation: a critical restatement of the biogenetic law. *Proc. Linn. Soc. Lond. zool.* 35:81-101.
- Gerber S, Eble GJ, Neige P. 2008. Allometric space and allometric disparity: a developmental perspective in the macroevolutionary analysis of morphological disparity. *Evolution*, 62(6): 1450-1457.
- Giles E. 1956. Cranial allometry in the great apes. *Hum Biol* 28:43-58.
- Gilbert, C.C., Stanley, W.T., Olson, L.E., Davenport, T.R. Sargis, E.J., 2011. Morphological systematics of the kipunji (*Rungwecebus kipunji*) and the ontogenetic development of phylogenetically informative characters in the Papionini. *Journal of Human Evolution* 60, 731–745.
- Gilbert, C.C., 2007. Craniomandibular morphology supporting the diphyletic origin of mangabeys and a new genus of the *Cercocebus/Mandrillus* clade, *Procercocobus*. *Journal of Human Evolution* 53, 69–102.
- Gilbert, C.C., 2011. Phylogenetic analysis of the African papionin basicranium using 3-D geometric morphometrics: the need for improved methods to account for allometric effects. *American Journal of Physical Anthropology* 144, 60–71.
- Gilbert, C.C., 2013. Cladistic analysis of extant and fossil African papionins using craniodental data. *Journal of Human Evolution* 64, 399–433.



- Godfrey LR, Sutherland MR. 1995. Flawed inference: why size-based tests of heterochronic processes do not work. *J Theor Biol* 172(1):43-61.
- Godfrey LR, Sutherland MR. 1996. Paradox of peramorphic paedomorphosis: heterochrony and human evolution. *Am J Phys Anthropol* 99(1):17-42.
- Gonzalez PN, Perez SI, Bernal V. 2011. Ontogenetic allometry and cranial shape diversification among human populations from South America. *Anat Rec* 294(11):1864-1874.
- Gould SJ. 1966. Allometry and size in ontogeny and phylogeny. *Biological Reviews*, 41(4):587-638.
- Gould SJ. 1971. Geometric similarity in allometric growth: a contribution to the problem of scaling in the evolution of size. *The American Naturalist*, 105(942):113-136.
- Gould SJ. 1975. Allometry in primates, with emphasis on scaling and the evolution of the brain. *Contributions to primatology* 5:244-292.
- Gould SJ. 1977. *Ontogeny and Phylogeny*. Cambridge: Harvard University Press.
- Gould SJ. 1988. The uses of heterochrony. In: McKinney ML, editor. *Heterochrony in Evolution*. New York: Springer US. p 1-13.
- Gould SJ. 2000. Of coiled oysters and big brains: how to rescue the terminology of heterochrony, now gone astray. *Evol Dev* 2(5):241-248.
- Gower JC. 1975. Generalized procrustes analysis. *Psychometrika* 40:33-51.
- Gunz P, Bulygina E. 2012. The Mousterian child from Teshik-Tash is a Neanderthal: A geometric morphometric study of the frontal bone. *Am J Phys Anthropol* 149(3):365-379.
- Gunz, P., Mitteroecker, P., Neubauer, S., Weber, G.W., Bookstein, F.L. 2009. Principles for the virtual reconstruction of hominin crania. *Journal of Human Evolution* 57, 48–62.
- Gunz P. 2012. Evolutionary relationships among robust and gracile australopiths: an “evo-devo” perspective. *Evol Biol* 39:472–487.
- Hall BK. 1984. Developmental processes underlying heterochrony as an evolutionary mechanism. *Can J Zool* 62(1):1-7.
- Hall BK. 1998. *Evolutionary developmental biology*. Second Edition. New York, NY: Thompson Science.

- Hall, B.K., 2003. Descent with modification: the unity underlying homology and homoplasy as seen through an analysis of development and evolution. *Biological Reviews* 78, 409–433.
- Harris EE. 2000. Molecular systematics of the Old World monkey tribe Papionini: analysis of the total available genetic sequences. *J Hum Evol* 38(2):235-256.
- Harrison T. 1986. New fossil anthropoids from the Middle Miocene of East Africa and their bearing on the origin of the Oreopithecidae. *Am J Phys Anthropol* 71(3): 265-284.
- Harvey PH, Clutton-Brock TH. 1985. Life history variation in primates. *Evol* 39(3):559-581.
- Huxley J. 1932. Problems of relative growth. Baltimore: Johns Hopkins University Press.
- Jungers WJ. Editor. 1985. Size and scaling in primate biology. Springer Science & Business Media.
- Jungers WL, Fleagle JG. 1980. Postnatal growth allometry of the extremities in *Cebus albifrons* and *Cebus apella*: a longitudinal and comparative study. *Am J Phys Anthropol* 53(4):471-478.
- Jungers WJ. Editor. 1985. Size and scaling in primate biology. Springer Science & Business Media.
- Klingenberg, C.P., Gidaszewski, N.A. 2010. Quantifying phylogenetic signals and homoplasy in morphometric data. *Systematic Biology* 59, 245–261.
- Klingenberg CP, Marugán-Lobón J. 2013. Evolutionary covariation in geometric morphometric data: analyzing integration, modularity, and allometry in a phylogenetic context. *Sys Bio* 62(4): 591-610.
- Klingenberg CP. 1998. Heterochrony and allometry: the analysis of evolutionary change in ontogeny. *Biological Reviews*, 73(1): 79-123.
- Klingenberg CP. 2010. Evolution and development of shape: integrating quantitative approaches. *Nature Reviews Genetics* 11(9):623.
- Klingenberg CP. 2016. Size, shape, and form: concepts of allometry in geometric morphometrics. *Development genes and evolution* 226(3):113-137.
- Kluge, A.G., 1985. Ontogeny and phylogenetic systematics. *Cladistics* 1, 13–27.

- Koyabu DB, Endo H. 2009. Craniofacial variation and dietary adaptations of African colobines. *J Hum Evol* 56(6):525-536.
- Koyabu DB, Endo H. 2010. Craniodental mechanics and diet in Asian colobines: morphological evidence of mature seed predation and sclerocarp. *Am J Phys Anthropol* 142(1):137-148.
- Leigh SR, Cheverud JM. 1991. Sexual dimorphism in the baboon facial skeleton. *Am J Phys Anthropol* 84:193-208.
- Leigh SR, Shah NF, Buchanan LS. 2003. Ontogeny and phylogeny in papionin primates. *J Hum Evol* 45:285-316.
- Leigh SR. 2001. Evolution of human growth. *Evolutionary Anthropology: Issues, News, and Reviews* 10(6): 223-236.
- Leigh SR. 2006. Cranial ontogeny of *Papio* baboons (*Papio hamadryas*). *Am J Phys Anthropol* 130:71-84.
- Leigh SR. 2007. Homoplasy and the evolution of ontogeny in papionin primates. *J Hum Evol* 52:536-558.
- Leslie ER, Shea BT. 2016. Gibbons to gorillas: Allometric issues in hominoid cranial evolution. U.H. Reichard, H. Hirai, C. Barelli (Eds.), *Evolution of Gibbons and Siamang, Developments in Primatology: Progress and Prospects*. Springer, New York, pp. 185-203.
- Lieberman DE, Ross CF, Ravosa MJ. 2000. The primate cranial base: ontogeny, function, and integration. *Am J Phys Anthropol* 113:117-169.
- Lieberman DE, Carlo J, Ponce de León M, Zollikofer CPE. 2007. A geometric morphometric analysis of heterochrony in the cranium of chimpanzees and bonobos. *J Hum Evol* 52:647-662.
- Lockwood, C.A., Kimbel, W.H., Lynch, J.M., 2004. Morphometrics and hominoid phylogeny: Support for a chimpanzee-human clade and differentiation among great ape subspecies. *Proceedings of the National Academy of Sciences USA* 101, 4356-4360.
- Lovtrup S. 1978. On von Baerian and Haeckelian recapitulation. *Sys Zool* 27(3):348-352.
- Mabee, P. M. (2000). The usefulness of ontogeny in interpreting morphological characters. In: Weins, J.J. (Ed.), *Phylogenetic Analysis of Morphological Data*. Smithsonian Institution Press, Washington, DC, pp. 84-114.

- Maddison, W.P., 1991. Squared-change parsimony reconstructions of ancestral states for continuous-valued characters on a phylogenetic tree. *Systematic Biology* 40, 304–314.
- Marcus LF, Corti M. 1996. Overview of the new, or geometric morphometrics. In *Advances in morphometrics* (pp. 1-13). Boston MA: Springer Press.
- Marroig G, Cheverud, JM. 2001. A comparison of phenotypic variation and covariation patterns and the role of phylogeny, ecology, and ontogeny during cranial evolution of New World monkeys. *Evolution*, 55(12): 2576-2600.
- Marroig G, Cheverud JM. 2005. Size as a line of least evolutionary resistance: diet and adaptive morphological radiation in New World monkeys. *Evolution* 59:1128–1142.
- Marroig G, Cheverud JM. 2010. Size as a line of least resistance II: direct selection on size or correlated response due to constraints? *Evolution* 64(5): 1470-1488.
- McGraw, W.S., Fleagle, J.G., 2006. Biogeography and evolution of the *Cercocebus-Mandrillus* clade: evidence from the face. In: Lehman, S.M. and Fleagle, J.G. (Eds.), *Primate Biogeography: Progress and Prospects*. Springer, New York, pp. 201–224.
- McKinney ML, McNamara KJ. 1991. *Heterochrony*. Springer US.
- McKinney ML. 1986. Ecological causation of heterochrony: a test and implications for evolutionary theory. *Paleobiology* 12(3):282-289.
- McKinney ML. 1988. *Heterochrony in evolution*. New York: Springer US.
- McNamara KJ. 1986. A guide to the nomenclature of heterochrony. *J Paleontol* 60:4-13.
- McNamara KJ. 2002. Sequential hypermorphosis: stretching ontogeny to the limit. In: Minugh-Purvis N, McNamara KJ, editors. *Human evolution through developmental change*. Baltimore: The Johns Hopkins University Press. p 102–121.
- McNulty KP, Frost SR, Strait DS. 2006. Examining affinities of the Taung child by developmental simulation. *J Hum Evol* 51:274–296.
- McNulty KP. 2004. A geometric morphometric assessment of hominoid crania: conservative African apes and their liberal implications. *Annals of Anatomy* 186(5-6):429-433.
- McNulty KP. 2005. Permutation proc.d.sas, updated: December 7, 2007. SAS for geometric morphometrics. Available from: <http://anthropology.umn.edu/labs/eal/sas/sasRoutines.html>

- McNulty KP. 2012. Evolutionary development in *Australopithecus africanus*. *Evol Biol* 39:488–498.
- McNulty KP, Begun DR, Kelley J, Manthi FK, Mbua EN. 2015. A systematic revision of *Proconsul* with the description of a new genus of early Miocene hominoid. *J Hum Evol* 84: 42–61.
- Meier, R., 1997. A test and review of the empirical performance of the ontogenetic criterion. *Systematic Biology* 46, 699–721.
- Minugh-Purvis N, McNamara KJ. 2002. Human evolution through developmental change. JHU Press.
- Mitteroecker P, Gunz P, Bernhard M, Schaefer K, Bookstein FL. 2004a. Comparison of cranial ontogenetic trajectories among great apes and humans. *J Hum Evol* 46:679–697.
- Mitteroecker P, Gunz P, Weber GW, Bookstein FL. 2004b. Regional dissociated heterochrony in multivariate analysis. *Annals of Anatomy* 186(5-6):463–470.
- Mitteroecker P, Gunz P, Bookstein FL. 2005. Heterochrony and geometric morphometrics: a comparison of cranial growth in *Pan paniscus* versus *Pan troglodytes*. *Evol Dev* 7:244–258.
- Mitteroecker P, Gunz P. 2009. Advances in Geometric Morphometrics. *Evol Biol* 36:235–247.
- Mitteroecker P, Gunz P, Windhager S, Schaefer K. 2013. A brief review of shape, form, and allometry in geometric morphometrics, with applications to human facial morphology. *Hystrix* 24(1): 59–66.
- Monteiro, L.R., 1999. Multivariate regression models and geometric morphometrics: the search for causal factors in the analysis of shape. *Systematic Biology* 48, 192–199.
- Monteiro, L.R., 2013. Morphometrics and the comparative method: studying the evolution of biological shape. *Hystrix* 24, 25–32.
- Müller GB. 2007. Evo–devo: extending the evolutionary synthesis. *Nature reviews genetics* 8(12):943.
- Neaux D. 2017. Morphological integration of the cranium in *Homo*, *Pan*, and *Hylobates* and the evolution of hominoid facial structures. *Am J Phys Anthropol* 162(4):732–746.
- Nelson, G. 1978. Ontogeny, phylogeny, paleontology, and the biogenetic law. *Systematic Biology* 27, 324–345.

- Nengo I, Tafforeau P, Gilbert CC, Fleagle JG, Miller ER, Feibel C, Fox DL, Feinberg J, Pugh KD, Berruyer C, Mana S. 2017. New infant cranium from the African Miocene sheds light on ape evolution. *Nature*, 548(7666):169.
- Neubauer S, Gunz P, Hublin JJ. 2009. The pattern of endocranial ontogenetic shape changes in humans. *J Anat* 215(3):240-255.
- Neubauer S, Gunz P, Hublin JJ. 2010. Endocranial shape changes during growth in chimpanzees and humans: a morphometric analysis of unique and shared aspects. *J Hum Evol* 59(5):555-566.
- O'Higgins P, Jones N. 1998. Facial growth in *Cercocebus torquatus*: an application of three-dimensional geometric morphometric techniques to the study of morphological variation. *J Anat* 193:251–272.
- O'Higgins P, Chadfield P, Jones N. 2001. Facial growth and the ontogeny of morphological variation within and between the primates *Cebus apella* and *Cercocebus torquatus*. *J Zool* 254:337–357.
- O'Higgins P, Collard M. 2002. Sexual dimorphism and facial growth in papionin monkeys. *J Zool* 257:255–272.
- O'Higgins P, Pan RL. 2004. Facial growth and phylogeny of the African colobines. In: Anapol F., German, R.Z., Jablonski, N. (Eds.). *Shaping Primate Evolution: Form, Function and Behavior*. Cambridge University Press, Cambridge pp. 24–44.
- Penin X, Berge C, Baylac M. 2002. Ontogenetic study of the skull in modern humans and the common chimpanzees: neotenic hypothesis reconsidered with a tridimensional Procrustes analysis. *Am J Phys Anthropol* 118:50–62.
- Perelman, P., Johnson, W.E., Roos, C., Seuánez, H.N., Horvath, J.E., Moreira, M.A., Kessing, B., Pontius, J., Roelke, M., Rumpler, Y., et al. 2011. A molecular phylogeny of living primates. *PLoS Genetics* 7, e1001342.
- Perez SI, Kłaczko J, Rocatti G, Dos Reis SF. 2011. Patterns of cranial shape diversification during the phylogenetic branching process of New World monkeys (Primates: Platyrrhini). *Journal of evolutionary biology* 24(8):1826-1835.
- Pilbeam D, Gould SJ. 1974. Size and scaling in human evolution. *Science* 186(4167):892-901.
- Pilbeam D. 2002. Perspectives on the Miocene Hominoidea. In: Hartwig W (ed.) *The Primate Fossil Record*. p 303-310.

- Ponce de León MSP, Zollikofer CP. 2001. Neanderthal cranial ontogeny and its implications for late hominid diversity. *Nature* 412:534-538.
- Quinn GP, Keough MJ. 2002. *Experimental Design and Data Analysis for Biologists*. Cambridge University Press, New York.
- R Core Team, 2017. *R: A language and environment for statistical computing*. R Foundation for Statistical Computing, Vienna.
- Rae TC. 1997. The early evolution of the hominoid face. In: Begun DR, Ward CV, Rose MD (Eds). *Function, phylogeny, and fossils: Miocene hominoid evolution and adaptations*. Plenum Press, New York. p 59-77.
- Rae TC. 1999. Mosaic evolution in the origin of the Hominoidea. *Folia Primatologica* 70(3): 125-135.
- Raff RA, Wray GA. 1989. Heterochrony: developmental mechanisms and evolutionary results. *J Evol Biol* 2(6):409-434.
- Ravosa MJ, Meyers DM, Glander KE. 1993. Relative growth of the limbs and trunk in sifakas: heterochronic, ecological, and functional considerations. *Am J Phys Anthropol*. 92(4): 499-520.
- Ravosa MJ, Ross CF. 1994. Craniodental allometry and heterochrony in two howler monkeys: *Alouatta seniculus* and *A. palliata*. *Am J Primatol*. 33(4): 277-299.
- Ravosa MJ, Shea BT. 1995. Pattern in craniofacial biology: evidence from the Old World monkeys (Cercopithecidae). *Int. J. Primatol*. 16(1): 801-822.
- Ravosa MJ, Profant LP. 2000. Evolutionary morphology of the skull in Old World monkeys. *Old World Monkeys*:237–268.
- Ravosa MJ, Vinyard CJ. 2002. On the interface between ontogeny and function. In Plavcan JM, Kay RF, Jungers WL, van Schaik (Eds). *Reconstructing Behavior in the Primate Fossil Record*. Springer US. p 73-111.
- Ravosa MJ. 1991. The ontogeny of cranial sexual dimorphism in two Old World monkeys: *Macaca fascicularis* (Cercopithecinae) and *Nasalis larvatus* (Colobinae). *Int. J. Primatol*. 12(4):.403-426.
- Ravosa, M.J., 1992. Allometry and heterochrony in extant and extinct Malagasy primates. *J Hum Evol* 23(2): 197-217.
- Revell, L.J., Harmon, L.J., Collar, D.C., 2008. Phylogenetic signal, evolutionary process, and rate. *Systematic Biology* 57, 591–601.

- Reilly SM, Wiley EO, Meinhardt DJ. 1997. An integrative approach to heterochrony: the distinction between interspecific and intraspecific phenomena. *Biol J Linn Soc* 60:119-143.
- Rice SH. 1997. The analysis of ontogenetic trajectories: when a change in size or shape is not heterochrony. *PNAS* 94(3):907-912.
- Richtsmeier JT, Cheverud JM. 1986. Finite element scaling analysis of human craniofacial growth. *J Craniofac Genet Dev Biol* 6(3):289.
- Richtsmeier JT, Corner BD, Grausz HM., Cheverud JM, Danahey SE. 1993. The role of postnatal growth pattern in the production of facial morphology. *Sys Biol* 42(3):307-330.
- Richtsmeier JT. 2018. A century of development. *Am J Phys Anthropol* 165(4):726-740.
- Rohlf FJ, Marcus LF. 1993. A revolution in morphometrics. *Trends Ecol Evol* 8:129–132.
- Rohlf FJ. 1996. Morphometric spaces, shape components and the effects of linear transformations. In: Marcus LF, Corti M, Loy A, Naylor GJP, Slice DE, editors. *Advances in Morphometrics*. Springer US. p 117-129.
- Rohlf FJ. 1999. Shape statistics: Procrustes superimpositions and tangent spaces. *Journal of Classification* 16(2):197-223.
- Rohlf, F.J., 1998. On applications of geometric morphometrics to studies of ontogeny and phylogeny. *Systematic Biology* 47, 147–158.
- Rohlf, F.J., 2002. Geometric morphometrics and phylogeny. In: N. MacLeod, N. and Forey, P.L. (Eds.), *Morphology, Shape and Phylogeny*. Syst. Ass. Spec. Vol. Ser. 64. Taylor and Francis, London, pp. 175–193.
- Schaefer K, Mitteroecker P, Gunz P, Bernhard M, Bookstein FL. 2004. Craniofacial sexual dimorphism patterns and allometry among extant hominids. *Ann Anat.* 186(5-6): 471-478.
- Schulter, D. 1996. Adaptive radiation along genetic lines of least resistance. *Evolution* 50:1766–1774.
- Schmidt-Nielsen K. 1984. *Scaling: why is animal size so important?* Cambridge university press.
- Schultz AH. 1926. Fetal growth of man and other primates. *Q Rev Biol.* 1(4): 465-521.



- Shea BT. 1981. Relative growth of the limbs and trunk in the African apes. *Am J Phys Anthropol.* 56(2): 179-201.
- Shea BT. 1983. Allometry and heterochrony in the African apes. *Am J Phys Anthropol* 62:275-289.
- Shea, B.T., 1985. Ontogenetic allometry and scaling. In: Jungers, W.L. (Ed.), *Size and Scaling in Primate Biology*. Plenum Press, New York, pp. 175-205.
- Shea BT. 1988. Heterochrony in primates. In: McKinney ML, editor. *Heterochrony in Evolution*. New York: Springer US. p 237-266.
- Shea BT. 1989. Heterochrony in human evolution: The case for neoteny reconsidered. *Am J Phys Anthropol.* 32(S10): 69-101.
- Shea BT. 1992. Ontogenetic scaling of skeletal proportions in the talapoin monkey. *J Hum Evol.* 23(3):283-307.
- Shea BT. 1995. Ontogenetic scaling and size correction in the comparative study of primate adaptations. *Anthropologie* 1-16.
- Sherratt, E., Gower, D.J., Klingenberg, C.P., Wilkinson, M., 2014. Evolution of cranial shape in caecilians (Amphibia: Gymnophiona). *Evolutionary Biology* 41, 528–545.
- Sidlauskas, B., 2008. Continuous and arrested morphological diversification in sister clades of characiform fishes: A phylomorphospace approach. *Evolution* 62, 3135–3156.
- Simons EA, Frost SR. 2014. Cranial shape evolution in the *Theropithecus oswaldi* lineage compared to ontogenetic, allometric, and geographic variation. *American Journal of Physical Anthropology* 153 Supplement, 239.
- Simons EA, Frost SR. 2016. Constructing cranial ontogenetic trajectories: a comparison of growth, development, and chronological age proxies using a known-age sample of *Macaca mulatta*. *American Journal of Physical Anthropology* 161, 296–308.
- Simons EA, Frost SR, Singleton M. 2018. Ontogeny and phylogeny of the cercopithecine cranium: A geometric morphometric approach to comparing shape change trajectories. *J Hum Evol* 124:40-51.
- Singleton M, McNulty KP, Frost SR, Soderberg J, Guthrie EH. 2010. Bringing up baby: developmental simulation of the adult cranial morphology of *Rungwecebus kipunji*. *The Anatomical Record: Advances in Integrative Anatomy and Evolutionary Biology*, 293(3):388-401.

- Singleton, M., Rosenberger, A.L., Robinson, C., O'neill, R., 2011. Allometric and metameric shape variation in *Pan* mandibular molars: a digital morphometric analysis. *Anatomical Record* 294, 322–334.
- Singleton, M., Seitelman, B.C., Gilbert, C.C., Frost, S.R., 2016. Comparative morphometric analysis of a juvenile papionin (Primates : Cercopithecidae) from Kromdraai A. *Annals of the Ditsong National Museum of Natural History* 6, 1–17.
- Singleton M. 2002. Patterns of cranial shape variation in the Papionini (Primates: *Cercopithecinae*). *J Hum Evol* 42:547–578.
- Singleton, M., 2005. Functional shape variation in the cercopithecine masticatory complex. In: Slice, D.E. (Ed.), *Modern Morphometrics in Physical Anthropology*. Kluwer Press, New York, pp. 319–348.
- Singleton M. 2012. Postnatal Cranial Development in Papionin Primates: An Alternative Model for Hominin Evolutionary Development. *Evol Biol* 39:499-520.
- Singleton, M., 2013. Primate Cranial Diversity. *Nature Education and Knowledge* 4, 1.
- Singleton M. 2015. Functional geometric morphometric analysis of masticatory system ontogeny in papionin primates. *Anat Rec.* 298(1): 48-63.
- Slice DE. 1998. Morphueus et al.: software for morphometric research. Department of Ecology and Evolution, State University of New York, Stony Brook, New York.
- Slice DE. 2007. Geometric Morphometrics. *Annu Rev Anthropol* 36:261–281.
- Smith BH. 1989. Dental development as a measure of life history in primates. *Evol* 43(3):683-688.
- Smith KK. 2001. Heterochrony revisited: the evolution of developmental sequences. *Biol J Linn Soc* 73(2):169-186.
- Steiper, M.E. & Seiffert, E.R. 2012. Evidence for a convergent slowdown in primate molecular rates and its implications for the timing of early primate evolution. *Proc. Natl. Acad. Sci.*, doi: 10.1073/pnas.1119506109.
- Strasser, E., Delson, E., 1987. Cladistic analysis of cercopithecoid relationships. *Journal of Human Evolution*. 16, 81–99.
- Strauss RE. 1987. On allometry and relative growth in evolutionary studies. *Systematic Biology* 36(1):72-75.

- Strelin, M.M., Benitez-Vieyra, S., Fornoni, J., Klingenberg, C.P., Cocucci, A., 2018. The evolution of floral ontogenetic allometry in the Andean genus *Caiophora* (*Loasaceae*, subfam. *Loasoideae*). *Evolution & Development* 20, 29–39.
- Szalay FS, Delson E. 1979. *Evolutionary History of the Primates*. Academic Press, New York.
- Tallman M. 2016. Shape Ontogeny of the Distal Femur in the *Hominidae* with Implications for the Evolution of Bipedality. *PloS one* 11(2) p.e0148371.
- Terhune CE, Kimbel WH, Lockwood CA. 2013. Postnatal temporal bone ontogeny in Pan, Gorilla, and Homo, and the implications for temporal bone ontogeny in *Australopithecus afarensis*. *Am J Phys Anthropol.* 151(4): 630-642.
- Thompson D'Arcy W. 1917. *On growth and form*. Cambridge: Cambridge University Press.
- Thompson JL, Krovitz GE, Nelson AJ. (Eds.). 2003. *Patterns of growth and development in the genus Homo* (Vol. 37). Cambridge University Press.
- Turley K, Frost SR. 2014. The ontogeny of talo-crural appositional articular morphology among catarrhine taxa: Adult shape reflects substrate use. *Am J Phys Anthropol* 154(3):447-458.
- Ungar PS, Hlusko LJ. 2016. The evolutionary path of least resistance. *Science.* 353(6294): 29-30.
- Vrba, E.S., 1996. Climate, heterochrony, and human evolution. *J. Anthropol. Res.* 52(1): 1-28.
- Waddington CH. 1942. Canalization of development and the inheritance of acquired characters. *Nature* 150(3811):563.
- Wiley DF. 2006. *Landmark editor*. University of California, Davis, wiley@cs.ucdavis.edu.
- Yoder, A.D., 1992. The applications and limitations of ontogenetic comparisons for phylogeny reconstruction: the case of the strepsirhine internal carotid artery. *Journal of Human Evolution* 23, 183–196.
- Zelditch, M.L., Fink, W.L., Swiderski, D.L., 1995. Morphometrics, homology, and phylogenetics: quantified characters as synapomorphies. *Systematic Biology* 44, 179–189.
- Zelditch ML, Swiderski DL, Sheets HD, Fink WL. 2012. *Geometric morphometrics for biologists: a primer*. Academic Press.

- Zihlman A, Bolter D, Boesch C. 2004. Wild chimpanzee dentition and its implications for assessing life history in immature hominin fossils. PNAS 101(29):10541-10543.
- Zuckerman S. 1926. Growth-changes in the Skull of the Baboon, *Papio porcarivs*. Proceedings of the Zoological Society of London 96: 843-873.
- Zumpano, M.P., Richtsmeier, J.T., 2003. Growth-related shape changes in the fetal craniofacial complex of humans (*Homo sapiens*) and pigtailed macaques (*Macaca nemestrina*): A 3D-CT comparative analysis. American Journal of Physical Anthropology 120, 339–351.